“How to describe protein crystals correctly? -case study of lysozyme crystals-“

Dissertation

zur Erlangung des akademischen Grades
Doktoringenieur (Dr.-Ing.)

vorgelegt dem

Zentrum für Ingenieurswissenschaften
der Martin-Luther Universität Halle-Wittenberg
als organisatorische Grundeinheit für Forschung und Lehre im Range einer Fakultät
(§ 75 Abs. 1 HSG LSA, § 19 Abs. 1 Grundordnung)

von

Dipl. Ernährungswissenschaftlerin
Claudia Müller
Geb. am 12.03.1982 in Anklam

Gutachter:
1. Prof. Dr. Dr. h.c. J. Ulrich
2. Prof. Dr.Ing. G. Schulte

Tag der Verteidigung: 18.04.2012

Acknowledgement

Present research work would not have been possible without the support of many people. I would like to express my gratitude to my supervisor, Prof. Dr. Dr. h.c. J. Ulrich who offered invaluable chances, support and guidance. Deepest gratitude are also due to my second reviewer, Prof. Dr. G. Schulte, to the professional help of Prof. Dr. M. Pietzsch and Prof. Dr. M. Stubbs, as well as to the practical support of Weissbarth, Schütze, Rudolf, Cismak (Frauenhofer, Institut Werkstoffmechanik Halle) and Höser, without their knowledge and assistance this study would not have been successful.

Special thanks to N. Aldabaibeh and to all TVT members e.g. C. Kirchner, T. Stelzer, P. Frohberg, V. Diaz Borbon, L. Helmdach, K. Lee, Y. Liu, D. Pertig, S. Petersen, C. Schmidt, A. Schuster, I. Stolte, A. Wachsmut, J. Iqbal, E. Abohamra, R. Buchfink, K. Chaleepa, C. Yürüdü, E. Römbach, K. Jäger, J. Heinrich, N. Pachulski, S. Dette, I. Trümper, A. Szepes and A. Migge for the caring, sharing valuable thoughts and supporting assistance. All mentioned team members made my time as a PhD student very enjoyable and unforgettable.

I would also like to convey special thanks and gratitude to my best friends Sandra W., Michaela K., Maria C.P., Katrein O., Inken E., Katja R., Britta L., Susanne R., Levi T., Christoph S., Sebastian W., Janine W., Varsha J., Ingeborg F.B., Kesarin C., Younghye K., Sebastian H., Janine & Luke W., Sven & Katrin V., who always been there.

Finally, my particular gratitude refers to my beloved family, for their understanding, endless support through the duration of my studies. I would like to accentuate my parents, my brother and my grandparents, my grand aunt as well as my relatives in Halle for their never-ending encouragement.

Selbstständigkeitserklärung

Ich versichere hiermit ehrenwörtlich, dass ich die vorliegende Arbeit selbstständig und nur unter Benutzung der angegebenen Literatur und Hilfsmittel angefertigt habe. Die aus fremden Quellen direkt oder indirekt übernommenen Stellen sind als solche kenntlich gemacht und werden in der Arbeit aufgeführt.

Die Arbeit hat in gleicher oder ähnlicher Form noch keiner Prüfungsbehörde vorgelegen.

Halle (Saale), 19.04.2012 Unterschrift

Table of content

How to describe protein crystals correctly?

-case study of lysozyme crystals-

1. Introduction

Protein crystallization is mostly used as a technique to obtain large and high in quality crystals suitable for structure determination using X-ray diffraction. Nowadays, protein crystallization also becomes an industrial crystallization technique in order to produce high quantities of protein crystals. Industrial protein crystallization is becoming more popular and it can be a gentle way to improve the purity and storability of proteins and to preserve protein activity while purifying [MCP98]. Numerous studies on crystallization procedures were performed to ensure the quality of the protein crystals which are described in literature, e.g. by Durbin [DUR96], Feher [FEH86], McPherson [MCP90, MCP98] and Pusey [PUS91]. With respect to industrial crystallization, protein crystallization has to be understood differently due to its complexity and its multi-component system. Clear differences and similarities between “classic crystals” and “protein crystals” have to be respected.

Industrial crystallization, in classical understanding, is used to purify substances by phase transfer mainly from the liquid (solution, melt) or gaseous phase into the crystalline state. The known understanding can in principle be used when working with proteins [MYE01]. Kinetics, meaning nucleation, crystal growth and dissolution, and thermodynamics, described by the phase diagram, of industrial crystallization processes are very well studied and “unlimited” literature is available which is not the case, however, in the field of protein crystallization. Protein crystallization in the last years has developed an incredible large and active field of research, not only focusing on kinetics and thermodynamics, molecular interactions as well as the mechanism behind the complex process of macromolecular (protein) crystallization need a better understanding. Understanding the aspects of protein crystallization can finally lead to the prediction of high quality protein crystals.

A searching of literature available for macromolecular and protein crystallization gives only limited data and information about the kinetic and thermodynamic. Investigations and discussions of phase diagrams, nucleation, crystal growth and their mechanisms provide first approaches, explanations and theories [MCP90, MCP98, JON10, LIU10, SHI06, RET02, WEB97, ASH04, GIL02, BLO94], but the state of art is still far away from a complete understanding. Furthermore, special papers concerning the size distribution, the crystals hardness, the seeding and the dissolution of protein crystals are extremely rare or totally missing in literature. These topics open an additional field of interest when integrating and transforming protein crystallization into a standard industrial crystallization process.

Successful protein crystallization demands proper handling and understanding of proteins and protein crystals, hence, knowing what a protein crystal consists of and how it is build. It is the aim to contribute to this rising field of technology and science. Lysozyme from hen egg white serves as model substance. Working with lysozyme brings advantages if compared to most other proteins are e.g. its availability, low price, its ease of crystallization and its useful and assisting literature.

Moreover, in pharmaceutical science, the dissolution of tablet bodies always has been of extremely high importance. A protein or a protein drug, stabilized either by crystallization or lyophilization, has to provide optimal bioavailability, meaning controlled dissolution, to function as a therapeutic agent. Therefore, to control the drug release / protein crystal dissolution to assure bioavailability and activity is an additional challenge. A promising approach for controlled protein (e.g. enzyme) drug release is the use of protein crystals in suspension. One common example is the human insulin that is already available on the market as a crystal containing suspension [HO03, LIL97]. It becomes clear, that bioavailability and therefore the dissolution of protein crystals are crucial important for biopharmaceutical / therapeutic applications.

In most conventional industrial crystallization processes, the dissolution was and still is ignored and underestimated. The dissolution of inorganic crystals such as crystalline sodium chloride, which is a pure and one component crystal, basically depends on the undersaturation of the solvent, e.g. water. In presence of impurities, its dissolution can be influenced and might become more complicated. In contrast, the dissolution of protein crystals is generally much more complicated, because protein crystals are assumed to consist of more than one component, and its dissolution does not only depend on the undersaturation of the solvent. Already the crystallization of proteins is indeed comparable but much more difficult than conventional crystallization, because of its enormous complexity and diversity. The complexity arises among others from the huge variability of the proteins polypeptide chain and its dynamic / flexible character. A dynamic / flexible character means the native conformation can vary. Already small energy changes (e.g. changes of the buffer environment) can cause an extensive number of different conformations. Furthermore, the poly-ionic character of the proteins and the solutions they exist in are of great importance. There are almost unlimited variations of aqueous or physiological environments possible, including a large diversity of applied crystallizing agents. The environment and its composition are highly relevant for the protein crystallization and in the same way for the protein crystal dissolution.

Mentioned importance of controlling the crystallization and dissolution of protein crystals, the lack of related information and observed lysozyme crystal dissolution phenomenon induced extensive studies on different lysozyme crystal morphologies.

2. State of art – proteins

Proteins are macromolecules and show a very high complexity in composition and structure. Detailed information on proteins, their composition and their structure as well as their function and properties can be found for example in the Protein Data Bank [PDBa10, WEI05, BRA99]. The basic knowledge and the most common methods of protein crystallization are described in books such as “Crystallization of biological macromolecules” by McPherson [MCP98] and “Crystallization of nucleic acids and proteins; a practical approach” by Ducruix [DUC92]. The important parts of theory, which are helpful to understand following chapters, will be given and shortly explained by the “state of art”.
Commonly used terms and definitions used in industrial and protein crystallization will be defined first. It is important to define terms such as polymorphisms, hydrates, solvates, complexity as well as purity and mosaicity used in present thesis to create a uniform understanding.

▪ *polymorphism, hydrates, solvates*
In the wide field of protein crystallization, commonly used terms such as polymorphism, hydrates and solvates have to be clearly defined. Grant [GRA99] defines *polymorphism* as: “Polymorphism is often characterized as the ability of a drug substance (chemical compound) to exist in two or more crystalline phases that have different arrangements and/or conformations of the molecules in the crystal lattice”. “Amorphous solids consist of disordered arrangements of molecules and do not possess a distinguishable crystal lattice. *Solvates* are crystalline solid adducts containing either stoichiometric or nonstoichometric amounts of a solvent incorporated within the crystal structure. If the incorporated solvent is water, the solvates are also commonly known as *hydrates*.

▪ *purity*
Conventional (solution) crystallization of inorganic materials (e.g. sodium chloride, potassium or magnesium sulfate etc.) focuses on the purification of raw materials. Unwanted impurities in the crystallization process can be disadvantageous for the crystal outcome e.g. quality (purity), crystal size distribution, crystal shape etc. as well as for the following down-stream processes. Occasionally, additives are used to optimize the crystalline product, but additives are used in very low concentration. In protein crystallization, the term purification by crystallization has to be understood slightly different. In first place, protein crystallization can be used to selectively crystallize the protein of interest out of a protein mixture, which is the same as for industrial crystallization. The difference is that protein crystallization demands the addition of a crystallizing agent (e.g. salts, PEG etc.). In this case, the salt can be understood as an “additive” or as part of the solvent. “Salting-out” takes place because the salt is added in very high concentrations in order to influence the solubility [MCP99]. Another difference is that interactions between the “additive”, the solvent and the protein occur. These interactions result in bonds between the crystallizing agent, solvent and the protein molecule [MCP99]. Therefore, the ”additive” (crystallizing agent) and the solvent are part of the generated protein crystal product. The protein crystal is only *pure* with respect to the unique protein fraction, but it is *not pure* if considering the crystallizing agent and the solvent fraction incorporated.

▪ *mosaicity*

Mosaicity, according to Rossiter [ROS90], is generally understood as: “a construct to explain diffraction effects, and it is not to be taken as a literal description of crystalline character (although it frequently is), we should not expect to see in a real crystal any arrangement of closely aligned mosaic blocks.”. The aspect that mosaicity is related to crystal lattice defects and that crystal examples exist which show high similarities to the theoretical “mosaic block” formations, a “mosaic block” structure theory could seem realistic.

Apart from above, the mosaic structure in crystals is theoretically described by the presence of “mosaic blocks” which are usually not in perfect alignment [ROS90]. The mosaic blocks for many substances are about 10^3 to 10^4 Angström (100 to 1000 nm). The orientation (long-range order) of the unit cells within a crystal represents the average orientation [ROS90]. The orientation leads to several diffraction effects, e.g lower mosaicity indicates better ordered crystals and hence better diffraction.

Mosaic structures have been discussed whether their formation is linked to impurity-induced defects and strains (tensions) in the crystal lattice. Strains caused by impurity incorporation, which were not explicit defined, are assumed to accumulate up to a certain level. If this level is exceeded, strains have to be relieved. The relief occurs through deformation and thus the formation of “mosaic blocks” [CHE98]. The mosaicity can be reduced or avoided if impurity incorporation during crystallization is minimal.

Protein crystals may show a mosaic structure when grown quite large. The onset of mosaicity is suggested to be size dependent [CAR03]. That means, large crystal size leads to higher impurity incorporation during growth, and thus an increase density of defect within the lattice. An example for existing mosaic structure can be given by ferritin and apoferritin crystals if larger than 300 µm. These crystals showed visible boundaries which separated the crystals into two or three etc. The mosaic blocks observed here were found to be about 20 to 100 µm [CAR03].

An estimate of mosaicity of lysozyme crystals has been described in literature, too, but rare. However, one exemplary reference describes the mosaic structures for a Tetragonal lysozyme crystal (larger than 170 µm) and illustrates its dissolution (on page 187, [CAR03]). Demonstrated dissolution is characterized by “fast” dissolution along the block boundaries which leads to a “hairy” morphology [CAR03]. Same reference also shows a lysozyme crystal of smaller size (less than 170 µm) that dissolves slowly and uniform which indicates a lack of block boundaries [CAR03]; unfortunately no dissolution conditions are described. Again a correlation of size and crystal defects is postulated.

2.1 Structure of proteins

In nature, protein molecules (proteins) are the building blocks of living organism and exist in a huge variety. In principle, all proteins have the same basic backbone of 20 different amino acids connected to each other to form a polypeptide chain. In general, proteins are long peptide chains of amino acids in different number and sequence. Each amino acid consists of a central C-alpha-atom that has an amino group, a carboxyl group, and a mutable side chain connected. The amino acids are bind together by a covalent bond that is known as a peptide bond between the amino and the carboxyl group (Figure 2.1.1a and b) [STR07].

a)

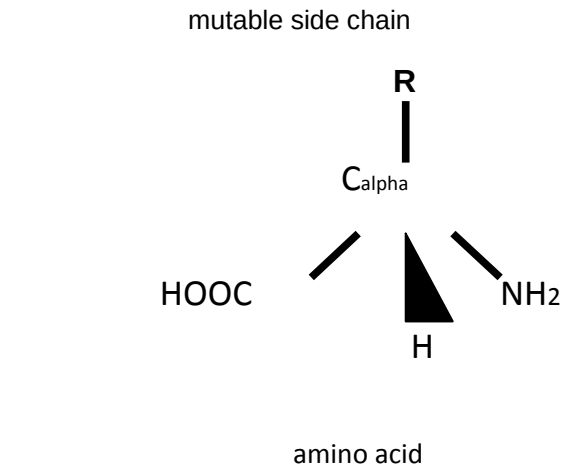

b)

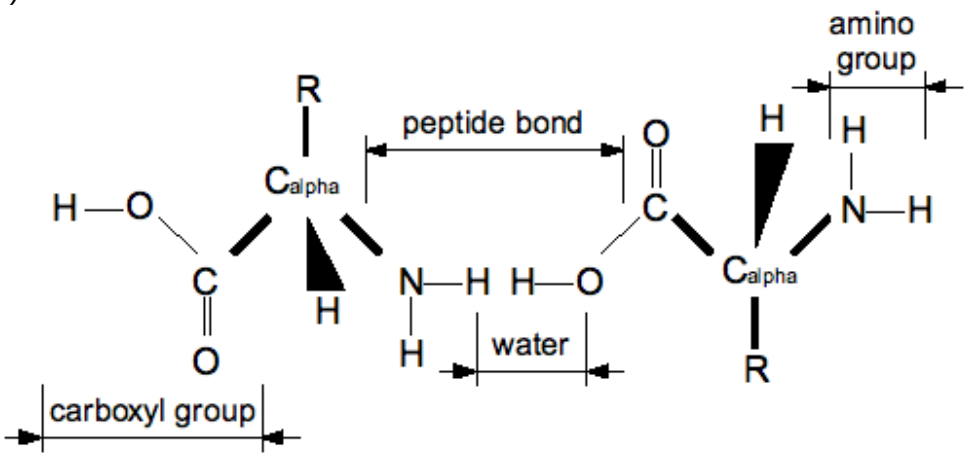

Figure 2.1.1: Built up of proteins.

a) General amino acid.

b) Two amino acids linked by a covalent peptide bond after splitting of a water molecule.

The side chain (residue) of an amino acid determines its properties. There are non-polar and aliphatic amino acids (for example Alanine, Leucine and Valine), aromatic amino acids (Phenylalanine, Tyrosine and Tryptophan), polar and uncharged amino acids (Serine, Cysteine, Proline), positively (Lysine, Arginine and Histidine) and negatively (Aspartate and Glutamate) charged amino acids (Figure 2.1.2) [STR07, KOO08].

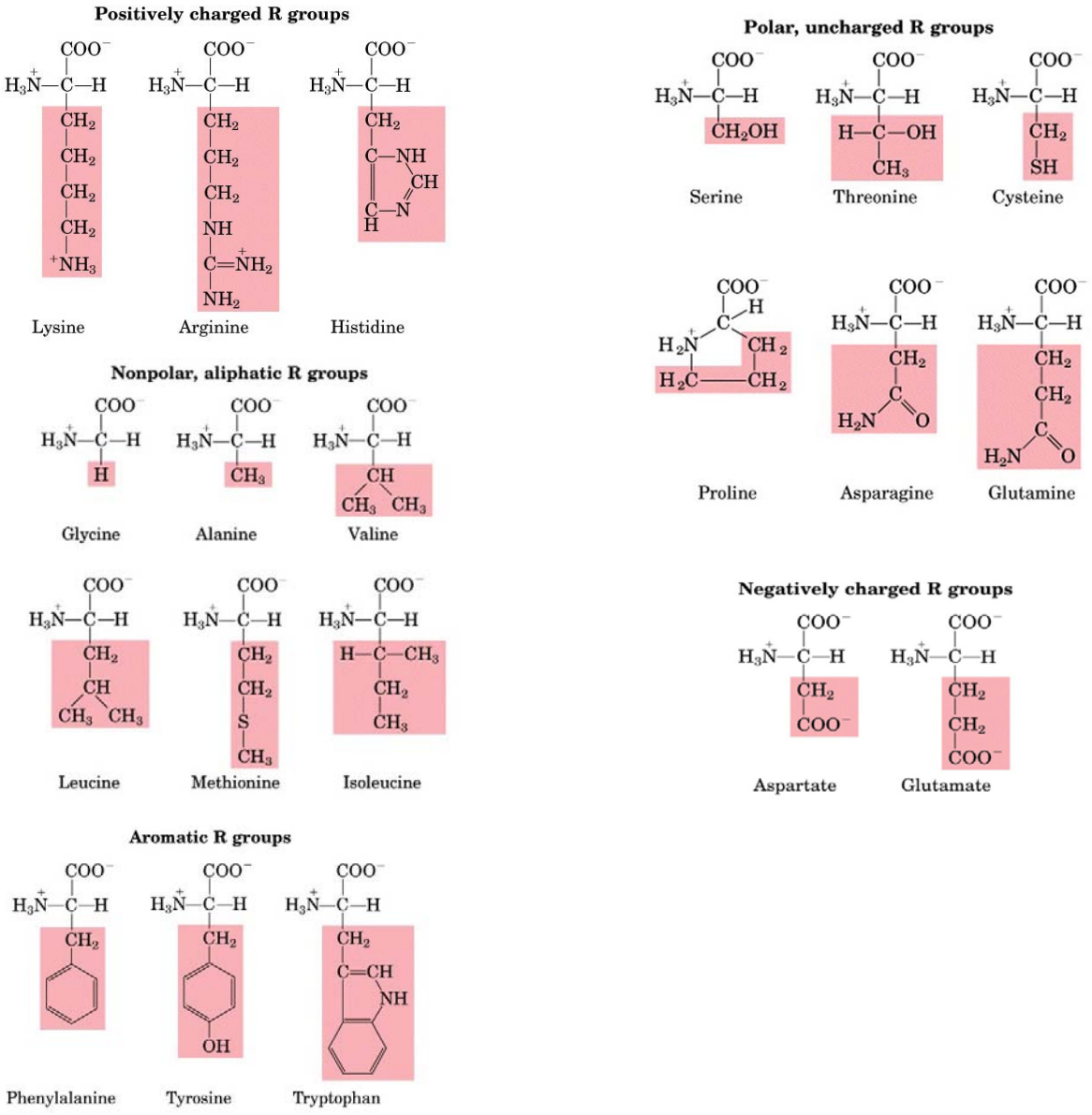

Figure 2.1.2: Overview of 20 amino acids organized by properties of their side chains [KOO98].

To understand the nature of proteins, a short and simple insight of the protein structure will be given. The protein structure is described by the primary, secondary, ternary and quaternary structure [ATK90]. The primary structure is determined by the sequence of amino acids which are the building units of a polypeptide chain. The polypeptide chain is the backbone and gives all main structural information on a protein. The secondary structure refers to regular local sub-structures that are e.g. hydrogen bonds in between the peptides of the polypeptide chain. If all hydrogen bond donors and acceptors of the polypeptide chain are saturated an alpha-helix or a beta-sheet formation occurs. Either the alpha-helix or the beta-sheet formation determines the ternary structure. The ternary structure can be taken as the three-dimensional structure of a single protein molecule. In addition to hydrogen bonds, the hydrophobic interactions and the disulfide bonds are responsible for its stability as well. Therefore, non-polar side chains of the amino acids, which are hydrophobic, are hidden inside of the folded protein (globular). Charged, polar, and neutral side chains are hydrophilic and mainly expose on the surface of the protein. This arrangement of the ternary structure is important to understand the process of protein crystallization. However, several polypeptide chains organize a protein and each polypeptide chain represents a domain or subunit. Complexes of two domains are dimers and of several domains are called multimers. Depending on the properties of the polypeptide chains, the domains are organized in a specific order that leads to the quaternary structure but the quaternary structure is not a must. Many proteins don’t build a quaternary structure so that they function as monomers [BAN06, DAV96].

2.2 Physical and chemical properties of proteins, solubility

The physical and chemical as well as biological properties (e.g. solubility, stability and activity) of a protein molecule arise from its structure meaning its polypeptide chain, their three-dimensional folding or coiling, the number of residues of the amino acids and the linear arrangement of these residues. The protein size, shape, hydration and charge have to be considered as well. Furthermore, the properties can depend on non-protein portions that are more or less strong attached to the polypeptide chain within the protein molecule. Working with proteins can already cause slight changes in the protein molecule structure which may change its properties. The risk of denaturation should be eliminated. Denaturation is an extreme case of structure alternation and can arise from too high temperatures, too high or low pH or too high salt concentrations. To avoid such alternation and to preserve its native state is of great importance [DAV96].

Most proteins are soluble in water, in aqueous solutions of salts, and in some cases even in polar, organic solvents like ethanol. Proteins which are very soluble in water or water-salt solutions are not or just little soluble in organic or water-organic solvent mixtures [BAN06].

The solubility is one of the most important properties of either organic or inorganic substances. The phase diagram which contains the solubility data is the most important tool in order to control crystallization processes. In literature, only few protein phase diagrams are available due to its high complexity. Its complexity is caused by many parameters like temperature, buffer concentration, pH, ionic strength and pressure that affect the solubility [ASH04]. Available solubility data of protein crystals were achieved by different techniques, e.g. the hanging-drop or the sitting-drop method [MCP98]. Another way to determine the solubility of proteins in a more accurate way can be carried out in batch scale with a static column method by Ataka and Asai [ATA88]. The solubility is then determined starting with a supersaturated protein solution. After crystallization occurred and the system reaches an equilibrium state, the protein concentration in the mother liquor is measured. Obtained solubility data are accurate, but very time consuming and last several weeks. Therefore, Pusey et al. [PUS91] developed a similar but faster method, a “micro-apparatus”. This static method can reduce the equilibrium time to a few hours. Consequently, lysozyme was intensive studied. Ewing [EWI94], Judge [JUD99], Pusey [PUS88, PUS91] and Aldabaibeh [ALD09] described the solubility of the Tetragonal and the Orthorhombic lysozyme crystal morphology in buffer solution at various temperatures, pH and sodium chloride concentrations. Among others, Ries Kautt et al. [RIE89, BEN02] worked on the influence of the ionic strength and the pH. Due to the fact that most available solubility data for lysozyme crystals in literature are reported for only limited and specific conditions, more investigations have to be carried out, and achieving data need to be added to the lysozyme phase diagram.
In general, one main factor that controls and leads of protein solubility is the electrostatic surface charge. Proteins consist of amino acids in a specific sequence. These amino acids carry the mentioned charged residues. The charged hydrophilic residues are arranged on the surface of the globular protein molecule because of the protein folding. Hydrophobic residues are facing the inside of the protein. Hydrophobic interactions are important within

the physiological protein – protein interactions, hence for their biological function. They develop with high affinity and very high biological specificity. The hydrophilic surface residues interact with polar molecules and ions of the solvent. The pH of the solvent determines the charge of the residues or functional groups, respectively, of the amino acids and hence the protein charge. To give an example, at neutral pH the glutamic and aspartic acid carry a negative charge whereas arginine and lysine a positive. Depending on the sequence, the number, the density of the charge carrying amino acids and the solvent (pH) a protein can be low or high in net charges. Therefore, total protein net charge is the arithmetic average of all surface charges. At a specific pH, the total net charge will be balanced, thus zero, this means the protein has the lowest solubility. This pH is called isoelectric point (pI). If the pH becomes basic, e.g. the lysine charge will change from positive to neutral. For further understanding, the overall protein net charge is responsible for the interactions with polar e.g. water molecules and electrolytes because they have a dipole nature. Due to this, an electrostatic double layer and hydration layer builds up. This causes electrostatic repulsion and attraction. Highly charged proteins generally tend to remain soluble because the polar and charged residues interact with the water and ions in the solvent. Proteins with little / no net charges or hydrophobic residues prefer to aggregate or crystallize in aqueous solvents. However, there are many parameters that influence the protein solubility whereby temperature, pressure, pH, ionic strength, ionic composition and concentration of the solution show the main impact [DAV96].

The following excurse explains the electrostatic forces between the amino acid – amino acid, the ion (salt) – amino acid and the water – amino acid molecules that play a key role for the solubility, in more detail. In solution, depending on the solvent pH and salt concentration, functional groups (amino acid residues) are either saturated or ionized. These functional groups direct the surface charges and the resulting electrostatic interactions, repulsion or attraction. As a consequence, variations in the width of the electrostatic double-layer (cations and anions) as well as in the hydration layer occur. Talking about repulsion and attraction forces, the DLVO (Derjaguin-Landau-Verwey-Overbeek) theory should be mentioned. This theory is characterized basically by the van der Waals attraction (in solution short-range forces) and the electrostatic double layer repulsion (long-range forces) [PEK08]. Both are always present, but if the repulsion forces between the lysozyme molecules are stronger than the attraction forces, solubility is promoted. The opposite supports the crystallization [ISR11, EVA76].
An increased salt concentration can lower the solubility. The decrease of solubility can be explicit reasoned by reducing the density of the protein surface charges. This limits the electrostatic double-layer [BOS03], it reduces the repulsion forces (electrostatic interactions) are reduced [GUI92, BEN02, RET02, RET07], and as a consequence, the attractive forces (van der Waals forces) and therefore the approach of two protein surfaces are supported [BRI91]. If the electrolyte concentration is high enough, the repulsion force will be dominated by the van der Waals attraction. Simply, dominating van der Waals forces can enable coagulation and therefore nucleation / crystallization or precipitation [PEK08]. DLVO forces have limits in explaining all solubility phenomena [BOS01, NIN99, PEK08]. However, the DLVO theory can be generally applied. At high salt concentrations when Debye-length and the distance between two lysozyme surfaces becomes extremely small, less than 1 nm, the

DLVO forces cannot be taken into account anymore. They are replaced by other strong short-range forces [MCB97]. At this point, forces such as solvation/hydration forces, thermal fluctuation forces etc. become dominant [LEC01, CHR83, BOS01, PEK08].
An increased pH has similar effects on the protein surface and reduces the all-over surface net charge in a comparable way. If the all-over surface net charge is zero, attractive van der Waals forces as well as e.g. hydration/solvation forces dominate and the solubility becomes minimal (pI). This means, the higher the pH of the environment (solvent), the closer to the pI (pI 11 [MYE01]), the lower the solubility of lysozyme crystals [MCP98, GUI92, BEN02, RET02, RET07].
In addition, the hydration layer is important to mention because it exists around the protein molecules as well as on the protein crystal surface. As already mentioned, the charged surface interacts not only with the ions of the solvent but also with the dipolar water molecules. Polar interactions occur and hydrogen bonds build that stabilizes the hydration layer. The hydration layer developed is called “biological” hydration layer. The hydration layer consists of water molecules that are bound directly to the lysozyme surface and “free” ones whereas the two types of water are in equilibrium. A second equilibrium exists between this “biological” hydration layer and the bulk solution and forms an additional layer as well. This layer is important for the protein – protein interaction and therefore for the crystallization process [DER06, VEK07, NAN08, FRE94, SAL85].
As known, an increase in pH and/or salt concentration leads to less surface charges of the protein molecule causing existing hydration forces to change. Due to less surface charge, the hydration layer becomes “thinner”, the repulsive hydration forces become weaker and the solubility is reduced [RET97, VAL05, SAL85].
The natural globular lysozyme molecule in aqueous solution always builds up a hydration and electrostatic double layer because of hydrophilic amino acid residues located at the molecule surface. The same is assumed for lysozyme incorporated in a crystal lattice (crystallized lysozyme), too, because it also constructs various interactions with the solvent. Lysozyme during crystallization forms many intermolecular contacts and finally the crystal lattice. Each contact, called “macrobond”, includes several bonds between charged and polar groups of atoms (so called “patches” or residues of the amino acids) of the lysozyme surface. Water molecules, electrolytes and/or other polar molecules present in the solvent bind often to these groups or patches through different kinds of intermolecular interactions / forces such as hydrogen bonds (including ionic bonds) or van der Waals forces. Therefore, they become incorporated in the crystal lattice as well. The contacts (macrobonds) in the crystal lattice use specific areas of the lysozyme surface and can vary in strength. The strength of the macrobonds depends on the number of involved interactions, the interaction “partners” (amino acids, ions, polar molecules and/or water) and the crystal lattice (morphology).
A macrobond (contact) is the sum of different types of hydrogen bonds and non-hydrogen bonds that finally lead to strong attraction. Hydrogen bonds include interactions between amino acids of different lysozyme molecules, amino acid – water, ion (salt) – amino acid (salt bridges) [MAT03]. Supplementary interactions e.g. water – water (hydrogen bond) and non-hydrogen bonds based on van der Waals forces (vdW) are assumed on the crystal / solvent interface, which means the crystal surface including the surface of the interior crystal pores. From the mentioned bonds, the amino acid – amino acid and the ion (e.g. Cl^-) – amino acid

interactions are the strongest (12.6 kJ/ mol), followed by the water – amino acid (6.3 kJ7mol), water – water (2.9 kJ/mol) and the lowest vdW (1.3 kJ/mol) [MAT03]. Marcobonds exists in all three dimensions, but the arrangement varies depending on the unit cell. The Tetragonal lysozyme crystal morphology has an unit cell of 8 lysozyme molecules and forms 4 kinds of macrobonds (A,B,C,D) whereas the HTO morphology contains half the number of lysozyme molecules per unit cell and forms only three macrobond types (A,B,C); references illustrate the macrobonds [MAT03, OKI99]. It is interesting, that only one chloride ion per lysozyme molecule binds, but it can bind to different amino acid groups, depending on the lysozyme crystal morphology. To give an example, only the C macrobond in Tetragonal lysozyme crystals is associated with a chloride ion. The chloride is bond to an asparagine residue. In HTO lysozyme crystals, the chloride ion binds, too, but to a different amino acid, to the argine which belongs to the A macrobond.

2.3 Crystallization of proteins

Protein crystallization is a very complex and difficult process, but follows the basic principles of crystallization of small molecules in industrial crystallization which is described e.g. by Hoffmann [HOF04], Sangwal [SAN07], Mullin [MUL01], Myerson [MYE01], or Ulrich [ULR03]. The solubility is very important, but limited solubility data are available, mostly due to the huge variety in proteins, in possible solvents and solution conditions. Solubility data are the base for the phase diagram that contains information to allow successful, optimized and time reduced protein crystallization. Optimized protein crystallization can represent a gentle purification method and is able to remove even traces of other proteins or contaminants. Protein crystallization is also used to stabilize the protein structure and to preserve its activity. However, protein storage in high concentrated solutions or by fast water removal can retain protein stability and activity. Therefore special caution is required to avoid denaturation. Common methods to reduce the water are evaporation (and / or air drying) through a membrane to avoid contaminants, freezing followed by ice removal, or lyophilization, meaning drying from a frozen state, whereby the latter is preferred due to no or very little loss of protein activity [DAV96].

The following list will briefly answer the given question *"What makes protein crystallization so difficult?"* and summarize the main characteristics of protein crystallization:

- protein crystallization occurs in a multi-component system [MCP98, DUR96, PUS02]
- limited crystallization conditions due to the risk of the protein activity loss and denaturation / degradation [WIE99, PCP98, BAN06, DAV96]
- high supersaturation required, because of slow nucleation due to the large molecule size with respect to small intermolecular distances [MCP98, WIE99, DUR96]
- large molecule size, complexity and diversity of macromolecules and their chemical groups (residues); slight changes in pH, ionic strength, temperature or in concentration of the crystallizing agent can influence the crystallization [ROS96, DUR96]
- growth kinetics dominated by surface kinetics (asymmetry of the macromolecule) when working in small batch volume and stagnant solution [MCP98]
- strong intermolecular interactions meaning hydrophobic and hydrophilic forces, hydrogen-bonds, salt-bridges, van der Waals forces [ROS96, MCP90, PUS02]
- protein crystal lattice contains large number of protein - protein contacts [PUS02, MAT03]
- high water / solvent content (30 to 90 % to keep the protein in its native conformation) resulting from water molecules bonded to the protein structure (crystal lattice) and "free" bulk water (solvent) molecules incorporated in the protein crystal channels / voids [MCP98, MCP90, WIE99, ROS96]
- limited solubility data listed in the Protein Data Bank [MCP98]

Furthermore, the high costs of the equipment necessary to obtain proteins from biomass and the related high impurity intake have to be considered as well.
An additional consideration that explains the difficulties of protein crystallization is the crystallization entropy. Derewenda and Vekilov [DER06] intensively studied the thermodynamics of protein crystallizing systems and state that the crystallization of dissolved protein molecules is enabled by changes of the Gibb's free-energy, ΔG^0_{cryst} which is described by the Gibb's-Helmholtz equation (2.3.1):

$$\Delta G^0_{cryst} = \Delta H^0_{cryst} - T\Delta S^0_{cryst} \text{ [MUL01].} \qquad (2.3.1)$$

Crystallization is only possible if ΔG^0_{cryst} is negative. Among others, sodium chloride shows a high negative ΔG^0_{cryst} value of -384 KJ/mol [HYP11, CHE11] that cause the crystallization to be "easy" if compared to protein crystallization. The ΔG^0_{cryst} of protein crystallization is just minimal negative, e.g. HTO at pH8.6, 2 wt% sodium chloride, 12 °C results in -21 KJ/mol calculated by Aldabaihbeh [ALD09a], see Table A1: "Variation of the enthalpy and entropy of crystallization for HTO lysozyme". Therefore, already small variations of crystallization conditions, e.g. in temperature, can easily alter ΔG^0_{cryst}. Positive values will thermodynamically make crystallization impossible [DER06].

Most of the protein crystallization methods were developed out of "trial and error" experiments. Therefore, crystallization parameters such as temperature, pH-value, protein concentration, type and concentration of crystallizing agent had to be investigated and analyzed to determine their influence on the crystallization process. Among others, detailed information on the history, techniques, and difficulties of the protein crystallization are summarized and illustrated by e.g. McPherson [MCP91, MCP98], Durchix [DUC92] and Wiencek [WIE99].
In case of protein crystallization as well as of solution or melt crystallization, supersaturation or undercooling is the driving force. Supersaturation can be reached by different methods such as changes in temperature, concentration (e.g. by dialysis, ultracentrifugation) and pH or pressure whereas pressure changes are not common for protein crystallization [GIL02, WIE99]. Unfortunately, the methods just mentioned are often not able to create a high enough supersaturation. Adding a crystallizing agent, e.g. salts, polyethylene glycol etc. which changes the solubility of the desired protein, called salting-in or salting-out, can induce higher chances of successful protein crystallization. Using low salt concentration leads to an increase in solubility, called salting-in. To crystallize e.g. lysozyme, higher salt concentrations are required to lower the solubility again, salting-out, of the dissolved protein. The decrease in solubility simply comes from the water competing interactions of the protein molecules and the salt ions. Both, the electrolytes (salt ions) as well as the protein molecules need to be hydrated on their respective surface [JON05]. A lack of water causes the protein molecules to be partially dehydrated. As a result, other protein molecules fill in the dehydrated surface, protein-protein interactions increase and crystal contacts start to form [WIE99, CHA12, JON05, MYE01]. The effectiveness of electrolytes, in respect to cation or anion and the type of salt ions, were investigated and documented by Hofmeister [HOF88]. He developed the "Hofmeister Series" which points out that the effectiveness of salt anions

also depend on the proteins isoelectric point, pI. Proteins with an acidic pI follow the anion Hofmeister series. Proteins with a basic pI follow the reverse order [HOF88, CHA12]. If required high superstation is reached, crystallization or precipitation occurs [WIE99]. The important step to obtain good quality, well-ordered protein crystals is to avoid precipitation because precipitated proteins form unspecific aggregates. Precipitation can occur if supersaturation is increased to fast. Therefore, the supersaturation has to be increased controlled in order to control the nucleation and the crystal growth. To do so, a phase diagram is helpful. Figure 2.3.1 gives an overview on a general protein phase diagram which illustrates the important information of protein crystallization. After controlled merging of the solution containing the crystallizing agent, $c_{crystallizing\ agent}$, into the protein solution, $c_{protein}$, supersaturation should gradually reach the labile zone of the system so that nucleation can occur. After nucleation that means after the formation of stable nuclei which follows the Gibbs's free energy model [MUL01], see Figure 2.3.2, the crystals will continue to grow until leaving the metastable zone and reaching the equilibrium state.

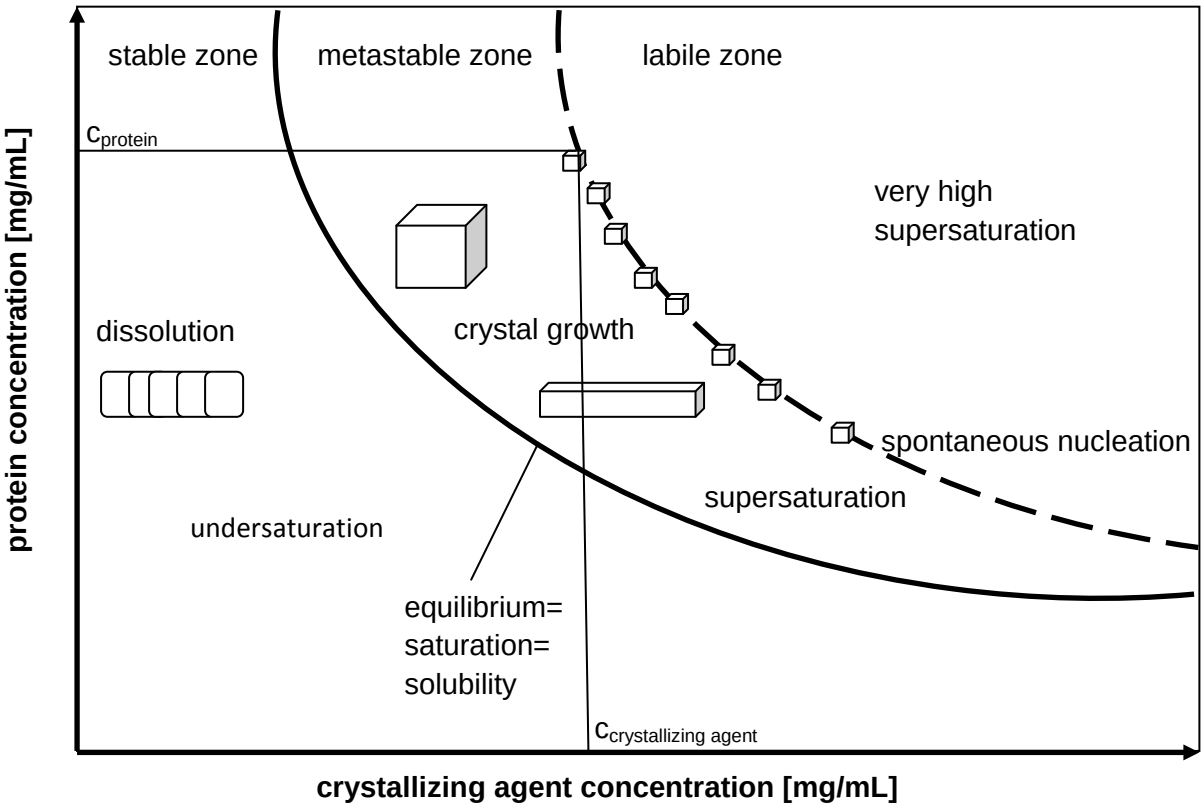

Figure 2.3.1: Phase diagram of protein crystallization.

The phase diagram is divided in the undersaturation and the supersaturation region. The equilibrium line, also called solubility line, separates both regions. The supersaturation is split in the metastable zone for crystal growth and the labile zone.

In the past decay, a more detailed the phase diagram, the generic phase diagram of proteins, becomes established. The generic phase diagram was introduced by Muschol and Rosenberger [MUS97] which additionally describes a zone of fast liquid – liquid phase separation. In this zone, protein crystals occur very fast, but of poor quality. Furthermore, a gel formation zone is introduced which seems to be very suitable for the crystal growth process. Myerson [MYE01] shortly summarized the basics of such generic phase diagram.

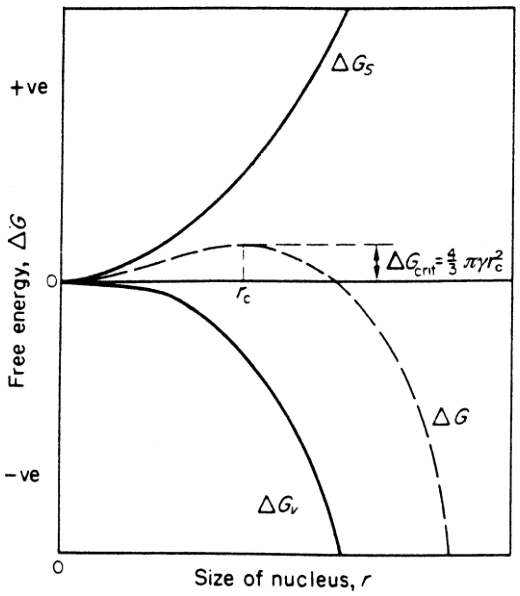

Figure 2.3.2: Gibb's fee energy model [MUL01].

Protein crystals, when grown for structure investigations by e.g. X-ray diffraction, are produced at low supersaturation to have a low nucleation rate, hence, to forms high quality crystals, same principle than for "classic" crystals. For batch protein crystallization in industrial applications, very high supersaturation is required [LU02]. Therefore, during batch crystallization the nucleation and its nucleation rate are hard to control. Precipitation easily takes place and the outcome shows marginal crystal quality. A suggestion for an explanation was given by Lu [LU02] who extensively studied the crystallization and its influencing parameters. Lu [LU02] explained, crystallization strongly depends on many parameters e.g. the buffer solution and its pH, the temperature, stirring or seeding, if used, etc. Therefore, resulting crystal formation, meaning nucleation and crystal growth, and crystal quality, meaning physical, chemical and mechanical properties, cannot be predicted and causes any batch crystallization to be different [DAV96, LU02]. Approaches to predict and control the protein crystallization lead to the introduction of the second osmotic viral coefficient parameter, B_{22}. This parameter was first established by Zimm and McQuarrie [ZIM46, MCQ76, WAN06]. B_{22} demonstrates a mathematical connection between the osmotic pressure and the protein-protein interactions. Crystallization conditions, which stabilize the protein in solution so that no crystallization can occur, show a large positive B_{22} value. In contrast, large negative B_{22} values are common for solution conditions producing amorphous precipitates [WIE99]. Further detailed description for B_{22} and its calculations are given e.g. by Wanka [WAN06, WIE99].

Another promising method to obtain protein crystals that are of high and reproducible quality was first performed by Ryu and optimized by Diaz-Borbon [RYU09, DIA10]. They developed a novel freeze out protein crystallization technology which was successful proven for

Tetragonal lysozyme crystals without enzymatic activity loss. With Diaz-Borbon's own words: "The key of the novel method is to control the concentration of a protein solution by use of freezing out the solvent (melt crystallization techinque), reaching the supersaturation and controlling crystal growth as a suspension crystallization process." [DIA10].

2.4 Nucleation and growth mechanisms

Crystallization starts with nucleation. Its control and the control of crystal growth are important to predict crystal quality. In general, nucleation is base for the protein crystal outcome with respect to the number of crystals, crystal size, crystal quality, meaning perfection or imperfection. Literature on nucleation and the growth of protein crystals is e.g. [MCP98, DUR86, FEH86, ALD46, WEB97, ASH04, DUR96, DRE98, ATA93, CHE03, VEK04, WIE99]. In the following section, models of nucleation and crystal growth will shortly be introduced.

One of the existing nucleation models for protein crystals is the “self-associated-based model”. It describes the formation of self-assembled aggregates in the solution [PUS02, ATA90, DUR86]. In addition, Chernov [CHE03] briefly defines the nucleation process as a result of a random aggregation of single molecules (monomers) or oligomers in supersaturated solution.
The self-assembled aggregates are the building blocks of a defined crystal lattice to obtain stable nuclei. Such building blocks are n-mers of the protein molecules. In case of Tetragonal lysozyme crystals, the building blocks are first dimers [PUS02], then tetramers and/or octamers [FOR94, NAD95]. Attachment and detachment of building blocks to n-mers occurs until a critical size is reached and a stable nucleus is formed.

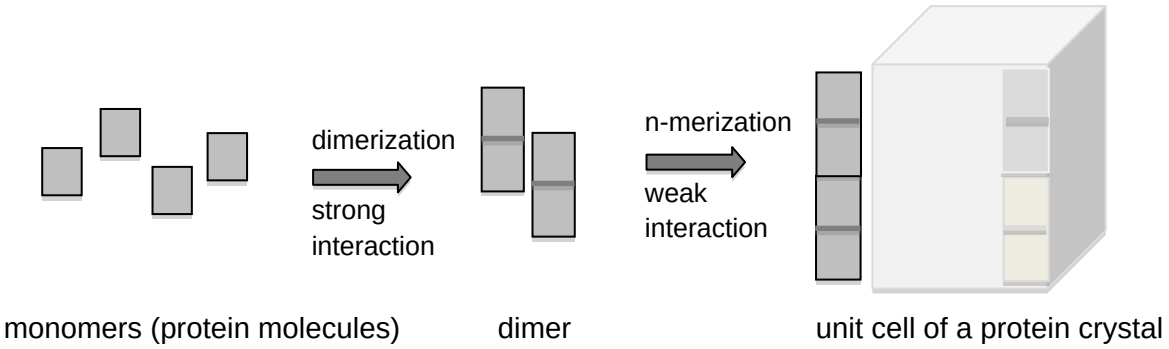

Figure 2.4.1: Self-associated reaction of lysozyme molecules in solution to form a Tetragonal lysozyme crystal.

Once a stable nucleus is formed, the detachment of building blocks minimizes. At the same time, the attachment of growth units is promoted due to the Gibbs-Thomson relation [MUL01]. Afterwards, crystal growth occurs by diffusive transport of building blocks (growth units) to the nuclei surfaces, followed by their attachment. To imagine the nucleation process according to the “self-associated-based model” see Figure 2.4.1.

One unit cell of a Tetragonal lysozyme crystal contains 8 lysozyme molecules [MAL11, MAT03, VAN01, FOR94, NAD95, PUS02] which could be determined by the height of the

growth steps. Orthorhombic lysozyme crystals consider 4 lysozyme molecules within a unit cell [MAL11, MAT03]. At the beginning of the nucleation process, a dimerization steps occurs that means linking of two protein monomers (one monomer equals one protein molecule) to a dimer; continuing the linking process will lead to tetramers and n-mers; the formation of dimers, tetra-mers and octa-mers occur fast due to strong interaction (electrostatic repulsion, salt bridges, van der Waals). The n-merization continues until a stable unit cell and finally a stable nucleus is formed. Afterwards, the attachment of the formed growth units to the surface of the growing protein nucleus and crystal occurs much slower then compared to the unit cell formation during the n-merization. Reasons are expected to relate to reduced (repulsive) interactions [PUS02]. Hence, the attachment of the growth unit to the crystal becomes the growth rate determining step.

The nucleation depends on the interaction of the protein molecules with the solvent including the crystallizing agent. For example, the ions of the crystallizing agent can bind to the surface of the protein molecule if the protein is dissolved in a solution unlike its isoelectric point (pI). The ions attached cause a reduction in the number of charged residues of the protein molecule which leads to less protein-solvent interaction. At the same time, the protein-protein interaction will be supported and promotes the aggregation in solution.

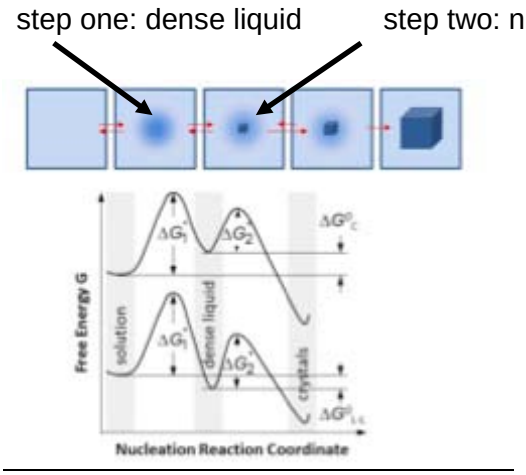

Figure 2.4.2: The macroscopic two-step mechanism of nucleation of crystals by Vekilov [VEK04].

Vekilov [VEK04] energetically describes the nucleation as a two-step mechanism. Basically, while supersaturation increases, step one describes the formation of dense liquid in which a cluster is generated. Step two is characterized by ordering of the cluster and its protein molecules that lead to nucleation and crystal formation (see Figure 2.4.2) [VEK04]. Below the drawing, Vekilov et al. [VEK04] introduces a model to describe the two step nucleation process. The standard free energy needed to form a dense liquid is given as $\Delta G^0_{L\text{-}L}$, whereas the free-energy for the cluster formation is ΔG^0_C . He explains that a mesoscopic cluster,

which could allow nucleation to take place, can form when $\Delta G^0_{L\text{-}L}$ of the dense liquid reaches a positive value, therefore it becomes ΔG^0_C and the free-energy required to form a nuclei will be accordingly smaller. In contrast, if $\Delta G^0_{L\text{-}L}$ remains negative, the dense liquid also remains in its stable state. To that effect, the barrier for cluster as well as nucleus formation is too high and no nucleation can occur. For better imagination of the two step nucleation mechanism, a brief description can be seen in Figure 2.4.2.

After nucleation, further supersaturation is the driving force for the crystals to continue their growth until the equilibrium between solution and crystal is reached. The mechanism of the growth process has been of great interests already in early 19th century. Starting from that time, several growth theories for industrial crystallization, meaning solution or melt crystallization, were developed and published, but none was able to explain all growth phenomena in full. First published theory of the crystal growth was the “surface energy theory” developed by Gibbs [MUL01]. Noyes-Whitney presented the “diffusion theory”. Scientists like Kossel, Volmer or Frank worked on the “adsorption layer theory” [MUL01, SAN07]. Later in the mid 20th century, Borton, Cabrera and Frank introduced the “BCF-theory” [BUR51, MUL01]. Their theory was further defined by Eerden, Bennema and Cherepanara [OHA73, MYE01] and became well known and widely used. Furthermore, the theory of the “growth rate dispersion”, GRD, was established (see e.g. [MYE01, ULR89]) and it was demonstrated that a size-dependent growth does not exist.

To describe the growth mechanism more detailed Mullin [MUL01] developed a 7-step model which demonstrates the complexity during crystallization of inorganic compounds. Here, the heat flow at phase transfer was neglected. All steps of the 7-step model listed below occur simultaneously:

- (1) bulk diffusion of hydrated ions through the diffusion boundary layer
- (2) bulk diffusion of hydrated ions through the adsorption layer
- (3) partial or total dehydration of ions
- (4) surface diffusion of hydrated or dehydrated ions
- (5) integration of the ions into the lattice
- (6) counter diffusion of released water through the adsorption layer to the bulk solution
- (7) counter diffusion of released water through the boundary layer to the bulk solution [MUL01].

Due to simplification, the multi-step process was reduced to a two-step or a three-step process and became widely accepted. The older two-step model limits the growth process to a) the transportation process of the solute to the crystal surface and b) the surface integration process of the growth units on the rough crystal surface. The more new three-step model takes the heat of phase transfer in consideration [GAR71, GAR81, KRU93, ULR94, MUL01].

The 7-step model by Mullin [MUL01] or the simplified models of Garside [GAR71] and Kruse [KRU93] can be basically applied to the protein crystal growth but the multi-component character of the protein crystals complicates the description of the growth process enormously. The complexity in the protein growth process also becomes clear when considering that the protein macromolecule has to diffuse through the multi-component bulk solution and through the boundary layer. The diffusion easily is effected by the protein-ion interaction, meaning ions of the crystallizing agent and the buffer, by the protein-protein interaction and/or the protein-solution interaction (see chapter 2.2 solubility).

The two widely used and most common growth mechanism models for protein crystals are “birth and spread“ (screw dislocation) and the “two-D-nucleation” (layer growth), described in literature [DUR86, CHE03, ROS96, MCP98, MYE01]. Both models are either limited by transportation processes of the solute (protein growth units) to the crystal surface or by the attachment step of the growth units on the rough crystal surface, surface integration. A clear description is given by Durbin and Feher [DUR86]. Chernov [CHE03] expressed: “Normal crystal growth will occur on the so-called rough, disordered, crystal-solution interface which will be generated by two-D-nucleation.”. His statement describes crystal growth from only this one perspective. Discussing crystal perfection / imperfection leads to the other growth mechanism, “screw dislocation”, which bases on defects in the crystal lattice. The screw-dislocation mechanism is also known from the BCF theory. Furthermore, the defects of the crystals lattice are e.g. stacking faults, dislocations or point-defects that can be generated by incorporated impurities, vacancies, amorphous protein or their own agglomerates [MCP98]. These lattice or surface defects function similar as kink sites. Growth units adsorbed on the crystal surface diffuse to the point of defect and start the screw “step” formation [DUR96, MUL01, MYE01].
The “layer by layer” growth provides three attachment possibilities such as on a flat surface, on step or on kink sites. The mentioned incorporation sites are ordered according their energy requirements. Thus, the kink site is the most favorable one [MUL01, MYE01]. The building blocks are 2-D nuclei which have to overcome to critical size to be stable. The nuclei can be generated at the crystal surface directly, but also in the bulk solution from where they have to diffuse to the crystal surface.
The growth of Tetragonal lysozyme crystals was already well studied by Nadarajah et al. [NAD96, NAD97]. It occurs in two steps as described earlier. First, aggregated protein growth units form in the crystallization buffer. Within the aggregated growth units, very strong intermolecular bonds exist. Lysozyme crystals grow by surface attachment of those aggregated protein growth units, kink sites are favoured. The aggregated protein growth units are generally tetramers, octamers or n-mers [NAD96, NAD97, CUI06]. It depends on the crystallization conditions and the crystal face where the growth units attach to. Michinomae et al. [MIC99] described the growth mechanism different but similar. In his view point, during the crystallization process protein molecules will associate to form first short protein molecule “threads” followed by the formation of larger spherical structures. These threads can be taken as growth units. His described growth process did not achieve high popularity [MIC99].

2.5 Dissolution

Dissolution can be defined by molecule or ion transfer processes from a crystal / solid into an adjacent bulk solution. Three main steps, the surface disintegration, the diffusion step and the heat transfer control the dissolution that will be explained later when dissolution mechanisms are described. The dissolution rate, one important parameter for bioavailability, considers the unit time and the surface area that is needed for a certain amount of dissolved substance to diffuse into the bulk solution.

The field of dissolution is an important field of research, especially for pharmacy, medicine, nutrition-food, geology, geophysics and similar research groups. In industry, the dissolution as one of the basic and starting process steps is known, but its importance was and is often underestimated [FAB96]. In past decays, the field of dissolution received more attention due to the pharmaceutical, nutrition and fertilizer industry. Therefore, the bioavailability of e.g. API's (active pharmaceutical ingredient), aromatics, sugars, dietary supplements or fertilizers, which is related and based on dissolution, increased its meaning. Up to now, it is still a major challenge to control the bioavailability, to understand the dissolution mechanisms completely and to apply the knowledge to organic substances, e.g. proteins. The known basic models to describe the dissolution mechanisms in the pharmaceuticals are:

1) the diffusion layer model with respect to the Fick's law [THO04, PHI05, DOK06],

2) the interfacial barrier model [DOK06, PHA11].

In early 19 century, Noyes and Whitney [DOK06] published first correlation between time and dissolving substance of a solid particle. They established an equation which is the basis of today's diffusion layer model of dissolution (see Figure 2.5.1). The diffusion layer model describes a stagnant liquid layer (stagnant film) on the crystal surface. Resulting reaction between the solid – liquid interface causes immediately local steady saturated solution conditions (very fast). The liquid of the bulk solution passes that stagnant liquid layer with a certain velocity. The arising dissolution takes place only by diffusion processes of the solid molecules / ions from the stagnant liquid layer into the bulk solution (much slower). This diffusion process determines the dissolution rate (dM / dt) (see equation 2.5.1) [THO04 PHA11]:

$$dM / dt = DA (c_s – c_b) / h \quad (2.5.1)$$

The diffusion occurs according to Fick's law [PHI05]:

$$J= -D_f \, dc / dx. \quad (2.5.2)$$

Summarizing Fick's law, at time t, when the solid molecules diffused into the bulk solution, it is assumed that the concentration gradient (dc / dx) decreases until no gradient exists anymore (see equation 2.5.2).

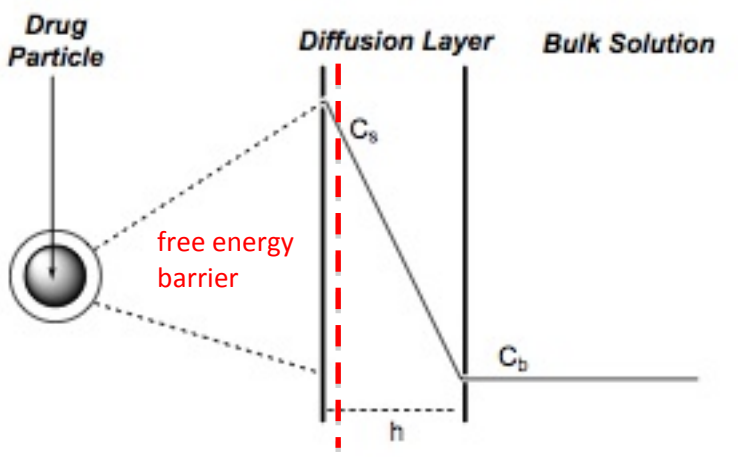

Figure 2.5.1: Dissolution scheme according to the diffusion layer model [THO04, PHA11].

The dissolution according to model 2) the interfacial barrier model is basically the same as the layer diffusion model. Additionally, a high activation free energy barrier is taken into account (see red dashed line of Figure 2.5.1). This energy barrier causes the solid – liquid interface disintegration kinetic to be delayed.
Furthermore, research was carried out to determine the solvent structure and their influence on the dissolution. The dissolution-limiting factor, the influence of impurities on the crystal lattice during growth and dissolution or the dissolution rate dispersion also became of interest and received some attention [FAB96, VAL24, IVE60, IVE63, AND87, FRA58, LAC74].
So far in research, the dissolution behavior of protein crystals, if not used in pharmaceutical applications, seem to play no major role, missing literature gives evidence. Interesting observations of dissolving lysozyme crystals could show otherwise and enhance the relevance of the dissolution. In discussions with biologists or biochemists, the observed dissolution behavior was known and explained simply by existing mosaic structure, but the dissolution mechanism, its correlation to the protein crystal composition and structure is apparently ignored.
Taking a closer look to Figure 2.3.1, on the left side of the phase diagram the dissolution region is located. This region is defined by undersaturation, which is the driving force for crystals to dissolve. The basic principles of organic and inorganic dissolution are comparable as well [FAB96].
Tuladhar et al. [TUL83] describes a dominating influence of the solid-liquid interface meaning the moistening or wettability of the crystal surface during dissolution. Therefore, moistening depends on the polymorphic structure of the compound and/or the presence of additives. Buckton [BUC90] in particular pointed out that the dissolution is a complex process which can be limited by wettability of the crystal surface, solubility of the substance and the additive as well as the disintegration into small units. For this complex process, he differentiates that existing crystal surface, due to surface exposed functional groups of the

compound molecules, influences the wettability. Moreover, the molecular structure and the binding energies within the crystal strongly influence the dissolution of the crystals. Numerous studies proved the importance and the large impact of the surface disintegration which also becomes clear when reviewing e.g. equation 2.5.1. Other parameters which influence the dissolution kinetics e.g. surface-active additives that can promote or inhibit dissolution, agglomeration or even the ration of crystalline / amorphous fractions within a crystal were also discussed [DOK06, VAl24, IVE60, IVE63, FRA58, LAC74, HEI75, HÖR01].

2.6 Enzymes, model substance lysozyme

Enzymes are proteins that can be generally understood as biocatalysts. They share common properties with chemical catalyst e.g. the acceleration of chemical reaction without influencing the reaction equilibrium constant, and no consumption or de novo synthesis of the enzyme during the reaction. Differences exist as well. To mention a few, active enzymes are always proteins (one exception: RNS-molecules which show enzymatic activity), highly specific to one reaction and show, in most cases, strong substrate specificity for only one substrate [DAV96]. During the reaction, the expected product will be generated without any side products. The main characteristic of enzymes is their substrate specific enzymatic activity which is limited to a specific temperature and pH range. However, if activity is present and detectable, the protein is in its native state. The native state represents the natural conformation that assures the catalytic function and allows the protein to crystallize. Therefore, the activity of an enzyme can be taken as an indicator for purity and crystallinity. So far, no denatured protein has been crystallized [NEU53, DAV96].
Additional information and explanations on the enzyme classification, enzymatic mechanisms and kinetics are given e.g. by Davidson [DAV96] and Koolman [KOO98].

Lysozyme from hen egg white, an enzyme also known as Muramidase, is chosen as a model substance to investigate the nature of protein crystals and to advice further protein crystal classification.
The history of lysozyme and its discovery is described in literature, see [WEI05, FLE22, WOR10]. Lysozyme is not only present in the hen egg white, but in milk, in mushrooms or in plant fluids. It is also a component of human body fluids such as salvia, tears fluid, blood plasma and plays an important role for the immune defense in the human body [HEI99]. The function of the lysozyme is important for living organism because it fights the ever-present danger of bacterial infection. Additional information can be found e.g. in [LYS10, WOR10, PDB10a, PDB11b-d].

The native and active hen egg white lysozyme molecule consists of 129 amino acids (Figure 2.6.1c) and has a molecular weight of approximately 14.6 kDa [MAL11, SCH89, BRO96]. The amino acid sequences of other types of lysozyme are homologous, but differ in 4 to 20 amino acids. Lysozyme belongs to the globular proteins. Due to hydrophobic amino acids, the lysozyme achieves an ellipsoidal shape. The allover net charge is dependent on the pH of the solvent, e.g. at pH4.6 lysozyme carries 10 to 12 positive charges [ROS96]. Lysozyme is also a “zwitterionic” protein which has positive and negative charges. However, lysozyme becomes bipolar, a dipole character exists [APG08]. The isoelectric point, pI, of lysozyme is in the range of 11 to 11.5, depending on literature [BER05, MYE01, BRO96]. The surface net charges are responsible for the two main protein – protein interactions:

1) the long-range repulsion (electrostatic forces)

2) the short-range (van der Waals forces) [APG08].

Following Figures 2.6.1.1a to 2.6.1.1e demonstrate the lysozyme molecule in different structure models. Taking a closer look to Figure 2.6.1.1e, primary and secondary structure of the lysozyme chain within a Tetragonal lysozyme crystal is shown. The black dots above the capital letters that stand for amino acids point out where the ions of sodium chloride can bind. In the following, the capital letters are explained [NCB11, STR07]:

- Y = Tyrosine, S = Serine, C = Cysteine, N = Asparagine, R = Arginine

a)

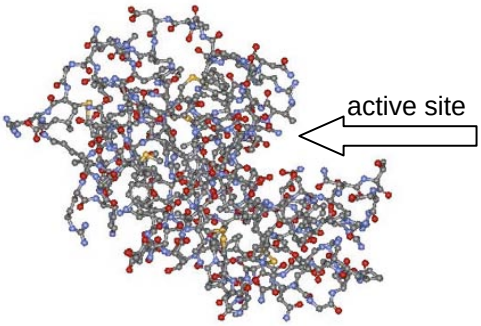

b)

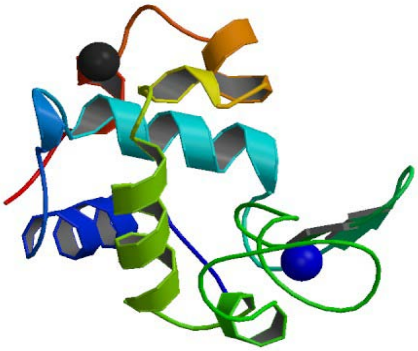

c)

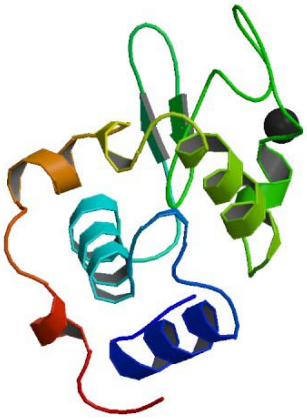

d)

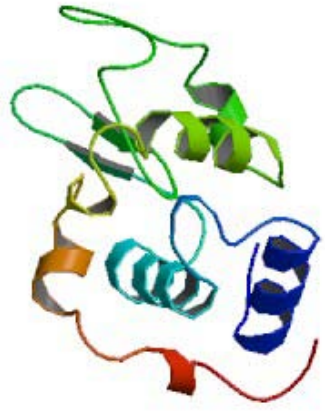

e)

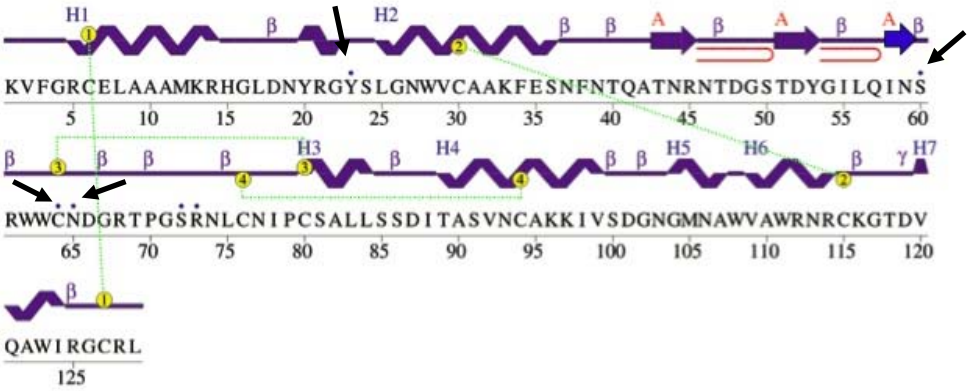

Figure 2.6.1: Lysozyme structure models.

a) Structure of lysozyme in ball-and-stick stereo picture [LYS10].

All protein atoms are shown as balls and the connecting bonds as sticks. The carbon atoms are grey, nitrogen atoms are blue, oxygen atoms are red and the sulphur atoms are yellow.

b) Structure of Tetragonal lysozyme crystallized with NaCl at pH4.3 [PDB10a].

c) Structure of Orthorhombic lysozyme crystallized at high temperature [PDB11b].

d) Structure of Orthorhombic lysozyme crystallized at low temperature [PDB11c].

e) Primary and secondary structure of Tetragonal 193L lysozyme chain A [PDB11d]. Primary structure with its amino acid sequence is shown as capital letters, secondary structure is represented by the symbols above the amino acid sequence, four disulfide bonds are shown green, small black dots (pointed out by black arrows) mark the amino acids where the sodium or the chloride ions can bind [WEI05].

Many studies were performed on lysozyme and lysozyme crystals. Numerous solubility studies build base for a phase diagram and phase transformation which shows the existence of different solvates (in literature often called polymorphs) [BER05, PUS91, PUS88, HOW88, ATA88, GUI92, FOR99, SAZ96, EWI94, ALD09, ANN08].
Among others, Ries-Kautt et al. [RIE89] described the solubility of lysozyme which is in reverse order of the Hofmeister series due to the fact that lysozyme belongs to the basic proteins with a pI of 11 - 11.5 [RIE89, BER05, SAK68, LIM98, VAN01]. Cacioppo et al. [CAC91] summarized the solubility behavior of lysozyme crystals dependent on the salt concentrations in the solvent. They demonstrated that at low salt concentration the solubility decreases with increasing pH.

The crystallization of lysozyme is well described in literature (see chapter 2.3). Therefore, basic information of the production condition to obtain reproducible lysozyme crystals exists. Up to now, six different lysozyme morphologies are known, such as the Tetragonal, the Monoclinic, the Triclinic, two differently produced Orthorhombic and the Needle morphology [LEG02, PET07, JUD99, EWI94, ALD09].
Here the focus is on the Tetragonal, the high temperature Orthorhombic (short HTO) and the low temperature Orthorhombic (short LTO) that are produced by batch crystallization.
Crystallographic studies on the Tetragonal, HTO and LTO lysozyme crystals produced under identical conditions as described in this work were carried out by Aldabaibeh [ALD09a]. He [ALD09a] collected data which were obtained by a one beamline 14-BM-C at BioCARS, Advanced Photon Source, Argonne National Laboratory, Argonne IL USA. The space groups and the lattice parameters of the lysozyme crystals investigated could be calculated by the data processing software XGEN [ALD09a]. Crystallographic data are summarized in the Table 2.6.1.

Table 2.6.1: Crystallographic data for the Tetragonal, HTO and LTO lysozyme crystal morphologies obtained from single crystal XRD [ALD09a].

Crystal, pH	**Space group**	**a (Å)**	**b (Å)**	**c (Å)**
Tetragonal, pH5	$P4_32_12$	77.7	77.7	37.1
HTO, pH5	$P2_12_12_1$	29.9	55.8	72.3
LTO, pH9	$P2_12_12_1$	30.4	57.5	67.6
LTO, pH10	$P2_12_12_1$	30.5	57.5	67.7

2.7 Motivation and objectives

Originally, before protein structure analyses became of interest, protein crystallization was already used for purification purposes. First purification studies were carried out on jack bean urease, [SUM26], and on ovalbumin from chicken egg white [JUD95]. The yield and efficiency was very high and protein crystallization became established. With time, the meaning of crystallizing proteins changed. The new interest why studying the protein crystallization in more detail was then to investigate the structure of proteins, trying to understand and explain their biological function. This understanding gives crucial background and enables pharmacist and/or medical scientists to develop special drugs or API's, in general biopharmaceuticals, for specific diseases. To give examples, biopharmaceutical API's can fight various types of viruses, cancer, leukemia, or metabolism dysfunctions (lactose intolerance, diabetes mellitus) or allergies. However, the medicament design became very specialized to protein causing diseases. Basically, the API (e.g. proteins, mostly enzymes or hormones) binds to a receptor / target protein which is responsible for the disease via "key and lock principle" and limits or inhibits its function so that the disease pathway will be interrupted [MYE01].

Being aware of the role of proteins, their function and the necessity to their crystallization, a wide field of crystallization challenges became established [DER06]. On the one hand side, crystallographer intensively worked on protein crystallization procedures to obtain high quality and suitable size single crystals. It is the first and basic step for X-ray diffraction and therefore protein structure analysis. As mentioned in chapter 2.3, even up to now, obtaining adequate protein crystals is mainly done due to "trial and error". Still some fundamentals are missing. Anyhow, extensively protein structure studies were carried out. Current available protein structure data is collected and can be reviewed in the Protein Data Bank, short PDB, (PDB: http://wwwbmcd.nist.gov:8080/bmcd.html). On the other hand side, protein crystallization gained importance and is essential for the production of therapeutic macromolecules and/or industrial enzymes. It brings advantages if compared to other purification methods, e.g. chromatography which is very expensive. Protein crystallization is easier to scale-up, reduces downstream processes and, if done under proper conditions, is gentle to the protein structure, lowers the risk of unfolding and the loss of activity. In general, protein crystallization is very attractive, even when some protein loss still has to be taken into account.

Detailed protein (or biopharmaceutical macromolecule) crystallization conditions are rare, hard to get and if they exist mostly patented-registered. Previous section indicates already, that the main reason why proteins (enzymes) gain so great attention, especially for the pharmaceutical industry, is mostly due to their therapeutic properties. To preserve the therapeutic (biological) function of proteins, stabilizing and converting them into an easy handling state is also a major challenge. Most common methods to stabilize proteins for long-term storage are drying and lyophilization whereas crystallization is a promising, but still not totally accepted method. Drying proteins at elevated temperatures always carries the risk of degradation, denaturation and activity loss which is not given for crystallization. Therefore, crystallization may replace the drying in future.

With respect to the protein crystallization, still fundamentals about controlling the nucleation, crystal growth and the protein crystal properties are missing or incomplete for detailed

understanding. The lack of understanding mainly comes from the complexity and diversity of protein crystals due to their multi-component character which is often neglected. Limited available solubility data and incomplete phase diagrams make it hard and difficult to define efficient crystallization conditions to control the process, to minimize “trial and error” experiments and therefore to lower costs.
The main objective and aim of the work is to contribute the understanding in the field of protein crystallization by partly filling and answering several “gaps” of knowledge and questions which are introduced in the chapter “state of art”. Among others, these “gaps” / questions refer to:

- A clear definition of what protein crystals are. Here, the hypothesis that protein crystal are multi-component crystals, which means they consist of at least the protein, crystal lattice water, buffer solution and the crystallizing agent, is posted. The multi-component character has to be proven by different analytical methods. Consequences e.g. for a correct and complete protein crystal classification and definition should derived from that.
- Adding missing data to the complex and incomplete protein phase diagrams which improves the control of the protein crystallization process, and thus the protein crystal product (properties, quality), e.g. diffraction quality, storability, purity, activity etc.
- The neglected or even ignored dissolution of protein crystals, its mechanism and impact factors.

The investigations presented are carried out on the model protein lysozyme, thus on three of the six known lysozyme crystal morphologies (Tetragonal, high temperature Orthorhombic and low temperature Orthorhombic). Several “simple” analytics on lysozyme crystals produced by batch crystallization, a time efficient method for solubility measurements and the dissolution phenomenon of lysozyme crystals asked for main attention. The huge complexity and diversity of protein crystallization becomes clear.

3. Materials and methods

3.1 Materials

Studies on lysozyme crystals are carried out using chemicals and equipment listed below. Equipment, analytical devices and experimental set-up will be explained more deeply in chapter 3.2.
Hen egg white lysozyme from Fluka is stabilized by converting it into a lyophilized powder. According to Fluka company, the lyophilized lysozyme powder has a minimum protein content of 90 % and a specific activity of 75759 U/mg lysozyme; traces of buffer salts like acetate and sodium chloride have to be considered.

Chemicals

Lysozyme	Fluka (Sigma Aldrich Chemie), 75759 U/mg, M=14600 g/mol (kDa)
Micrococcus luteus (lysodeikticus)	Sigma, ATCC4698, lyophilized cells
Di sodium hydrogen phosphate	Roth, Na_2HPO_4, 99 % p.a., M=141.96 g/mol
Sodium di hydrogen phosphate monohydrate	Roth, NaH_2PO_4,*H_2O , 98 % p.a., M=137.99 g/mol
Sodium acetate tri hydrate	Roth, $C_2H_3NaO_2$*$3H_2O$, 99.5 % p.a., M=136.08 g/mol
Acetate acid	Roth, $C_2H_4O_2$, 100 % p.a. Rotipuran, M=60.05 g/mol
Glycine	Merck, $C_2H_5NO_2$, 99 % zur Analyse, M=75.07 g/mol
Sodium hydroxide	Roth, NaOH, 99 % p.a., M=40.01 g/mol
Sodium chloride	Fluka, NaCl, 99.5 % p.a., M=58.44 g/mol
Potassium chloride	Roth, KCl, 99.5 % p.a., M=74.56 g/mol
Mono potassium di hydrate phosphate	Roth, KH_2PO_4, 95.5 % p.a., M=136.086 g/mol

Di potassium mono hydrate phosphate	Roth, K_2HPO_4, 95.5 % p.a., M=174.2 g/mol
Calcium chloride	Merck, $CaCl_2*2H_2O$, zur Analyse, M=147.02 g/mol
Coomassie blue	Roth, Brillant blue R250, $C_{45}H_{44}N_3NaO_7S_2$, M=825.99 g/mol
Methylene blue	Roth, für Mikroskopie, $C_{16}H_{18}ClN_5S$, M=319.9 g/mol
Phenolphthalein	Germed, VEB Feinchemie Sebnitz, $C_{20}H_{14}O_4$, p.a., M=318.30 g/mol
Silver nitrate	Roth, $AgNO_3$, 99.9 % p.a., M=169.87 g/mol

Equipment

Analytical weight	Satorius BA210S Basic
	Mettler Toledo AX205 Delta Range
pH-meter	WTW microprocessor pH-meter pH539
	WTW pH-meter pH532
Thermostat	Julabo FP50; Julabo F12; Julabo 12
Peristaltic pump	Ismatec Reglo
Light microscope	Olympus BH2
Digital microscope	Keyence VHX 500F
REM	Raster-Electron-Microscope by REM Jeol SM 7401 F
Device for analysis of elements	Leco CHNS–932 and O–Analysator VTF–900
EDX	Energy-Dispersive X-ray Spectroscopy by REM Jeol SM 7401 F with the EDX System genesis of EDAX
XRPD	X'Pert Pro PANanalytical GmbH/ the Netherlands

Raman	Bruker Raman-spectrometer RFT 100/S (Bruker Optik Ettlingen) with a NdYac-laser of 1064nm
DSC	Netzsch DSC 204, Netzsch TASC 414/4 controller
TGA	Netzsch TG – DSC/DTA (STA) +Netzsch STA 409 cell
Karl-Fischer Titration	Mettler DL35 Karl-Fischer
Photometer	Analysis Jena Zeiz
Spectrophotometer	Varian Cary – UV Visible

3.2 Experimental methods

3.2.1 Frame conditions for the crystallization of lysozyme

Lysozyme is a protein that can be easily crystallized if compared to other proteins. Therefore, it is often used as a model substance in fundamental protein crystallization research. Parameters which show the strongest impact on crystallization, on solubility and morphology of lysozyme crystals are the pH of the buffer solution, the temperature, the protein concentration, the concentration and type of the crystallization agent (for example salt), the ionic strength and the supersaturation [NAD96, VEK96, MCP98]. By changing crystallization conditions, one can produce various lysozyme crystal morphologies. Six different lysozyme crystal morphologies (Monoclinic, Triclinic, Tetragonal, High Temperature Orthorhombic, Low Temperature Orthorhombic and Needle) are known and more or less investigated in details [ALD09, EWI94, JUD99, LEG02, PET07].
Following Table 3.2.1.1 gives a short overview on the lysozyme crystallization conditions, how to produce various lysozyme crystal morphologies. In this work, the Tetragonal, high temperature Orthorhombic (short HTO) and low temperature orthorhombic (short LTO) morphologies are of main interest and investigated in detail.
Additionally, a screening using different crystallization agents is carried out. Therefore, the crystallization conditions of lysozyme with sodium chloride are transferred to different salts. Among others, potassium and calcium chloride di hydrate, Tables 3.2.1.2 and 3.2.1.4, as well as di sodium carbonate and barium di chloride, Table 3.2.1.3, are chosen and replaced sodium chloride. Besides varied salt, the crystallization conditions remain the same as described before for Tetragonal and LTO lysozyme crystals.

Table 3.2.1.1: Production conditions of Tetragonal, High Temperature Orthorhombic and Low Temperature Orthorhombic lysozyme crystals using NaCl.

Tetragonal	**HighTemperature Orthorhombic (HTO)**	**LowTemperature Orthorhombic (LTO)**
acetate buffer 0.1 M	acetate buffer 0.1 M	glycine buffer 0.05 M
pH5; 4 ˚C	pH5; 4 ˚C	pH9.6; 20 °C
100 mg lys*/mL (5 mL)	230 mg lys*/mL (5 mL)	100 mg lys*/mL (5 mL)
8 wt% NaCl (5 mL)	12 wt% NaCl (5 mL)	8 wt% NaCl (5 mL)
final crystallization conditions in the total volume of 10 mL		
50 mg lys*/mL	115 mg lys*/mL	50 mg lys*/mL
+ 4 wt% NaCl	+ 6 wt% NaCl	+ 4 wt% NaCl

lys* = lysozyme

Table 3.2.1.2: Production conditions of Tetragonal and low temperature Orthorhombic lysozyme crystals using KCl and $CaCl_2*2H_2O$.

Tetragonal $_{KCl}$	**Tetragonal $_{CaCl2*2H2O}$**	**Orthorhombic $_{KCl}$**	**Orthorhombic $_{CaCl2*2H2O}$**
acetate buffer	acetate buffer	glycine buffer	glycine buffer
0.1 M	0.1 M	0.05 M	0.05 M
pH5; 4 °C	pH5; 4 °C	pH9.6; 20 °C	pH9.6; 20 °C
50 mg lys*/mL	50 mg lys/*mL	50 mg lys*/mL	50 mg lys*/mL
4 wt% KCl	4 wt% $CaCl_2$	4 wt% KCl	4 wt% $CaCl_2$

lys* = lysozyme

Table 3.2.1.3: Production conditions of lysozyme Tetragonal crystals using Na_2CO_3 and $BaCl_2$ and varied salt concentration.

Tetragonal $_{Na2CO3}$	**Tetragonal $_{Na2CO3}$**	**Tetragonal $_{BaCl2}$**	**Tetragonal $_{BaCl2}$**
acetate buffer	acetate buffer	acetate buffer	acetate buffer
0.1 M	0.1 M	0.1 M	0.1 M
pH5; 4 ˚C	pH5; 4 ˚C	pH5; 4 ˚C	pH5; 4 ˚C
50 mg lys*/mL	50 mg lys*/mL	50 mg lys/*mL	50 mg lys*/mL
4 wt% Na_2CO3	2 wt% Na_2CO3	4 wt% $BaCl_2$	6 wt% $BaCl_2$

lys* = lysozyme

Table 3.2.1.4: Production conditions of high temperature Orthorhombic lysozyme crystals using $CaCl_2*2H_2O$ and $CaCl_2*2H_2O$.

Orthorhombic $_{KCl}$	**Orthorhombic $_{CaCl2*2H2O}$**
acetate buffer	acetate buffer
0.1 M	0.1 M
pH5; 37 ˚C	pH5; 37 ˚C
50 mg lys*/mL	50 mg lys/*mL
4 wt% KCl	4 wt% $CaCl_2*2H_2O$

3.2.2 Analytics for lysozyme crystals

- *Light / Digital microscope*
- *Enzymatic activity test by Shugar*
- *DSC*
- *TGA*
- *SEM*
- *Conductivity*
- *EDX*
- *XRPD*
- *Raman spectroscopy*
- *Infrared spectroscopy*

- *Light / Digital microscope*

Present protein crystal morphology studies are carried out using a *digital microscope* of Keyence VHX 500F with an optical magnification range of 100 to 1000 times, Figure 3.2.2.2. For dissolution studies, a traditional *light microscope* (magnification is 50 times) connected with an ALTRA 20- CCD-camera is used, see Figure 3.2.2.1. The AnalySIS-software is used to analyze the images of the samples.

Figure 3.2.2.1: Light microscope Olympus BH2, an Olympus ocular NFK 2.5x LD 125 and an objective of IC 5 (MDPlan5 / 0.1), digital camera ALTRA 20.

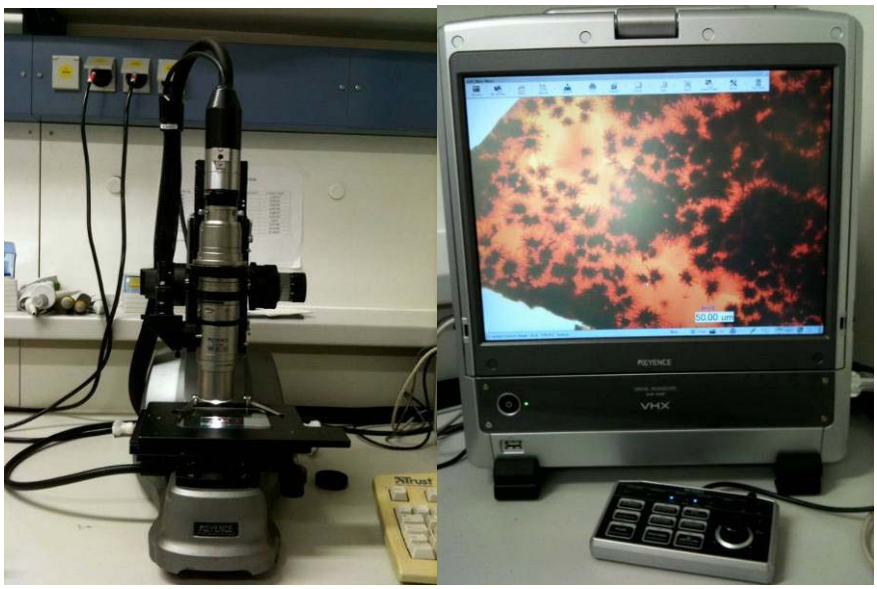

Figure 3.2.2.2: Digital microscope Keyence VHX 500F.

▪ *Enzymatic activity test by Shugar*

The enzymatic activity test is planned and carried out prior to Shugar [SHU52]. Chapter 2.5.1 explains the lyses function of the lysozyme which is the base for the activity test. Lysozyme shows extremely high sensitivity to the Micrococcus luteus which is a gram-positive bacterium. Parameters influencing the activity are the enzyme (protein) and the substrate concentration, the pH, the buffer solution, the temperature and/or added activators or inhibitors [SMO52, GOR71]. The enzymatic activity is given by U/mL (Unit per mL) whereas the specific activity is related to the protein concentration U/mg protein (Units per mg of protein).

Accuracy of enzymatic activity measurements
The solution preparations for the activity test (see appendix A.1) have to be done very precisely, but some pipetting error has to be considered. To some extent, a fault occurs when mixing the lysozyme sample solution into the substrate solution because the enzymatic reaction proceeds immediately. A delay of time until starting the extinction measurements is unpreventable, therefore it needs practical experience to perform the activity test fast enough to obtain reproducible results.

▪ *Thermal analysis by Differential Scanning Calorimetry, DSC*

Thermal analysis is an important analytical tool to study physical or chemical properties of a substance as they may change with temperature. Among others, there are several methods often used such as: Differential thermal analysis (DTA) for temperature differences, Differential scanning calorimetry (DSC) for heat differences, Thermo gravimetric analysis

(TGA) for mass differences, Thermo mechanical analysis (TMA) for dimension changes, Dynamic mechanical analysis (DMA) for mechanical stiffness and damping, or Simultaneous thermal analysis (STA) which refers to the combination of TGA and DSC measurement to the same sample in the same device at the same time [HÖH10].
Thermal analysis studies are carried using a DSC and a STA device and will be shortly introduced for better understanding. Differential scanning calorimetry (DSC) is a common method to determine the amount of heat required to change / increase the temperature of a sample and reference. The heat flow is measured as a function of temperature. The sample and the reference are placed on a holder in a specific DSC oven so that both are maintained at the same conditions throughout the whole measurement. The computer controlled temperature program allows the sample holder and therefore the sample to increase its temperature linearly as a function of time. Differences in the heat flow between the sample and the reference are detectable. However, the DSC can measure the amount of heat released or absorbed by a sample together with the defined profile which gives information about thermal transitions. Expected thermal transition-effects can be e.g. phase transition (crystallization, melting) or glass transition. The heat flow is directed by whether the thermal effect is exothermic or endothermic. To give an example, melting of a substance would give an endothermic signal whereas crystallization gives an exothermic signal. Figure 3.2.2.4 shows possible thermal effects during DSC measurements [HÖH10].

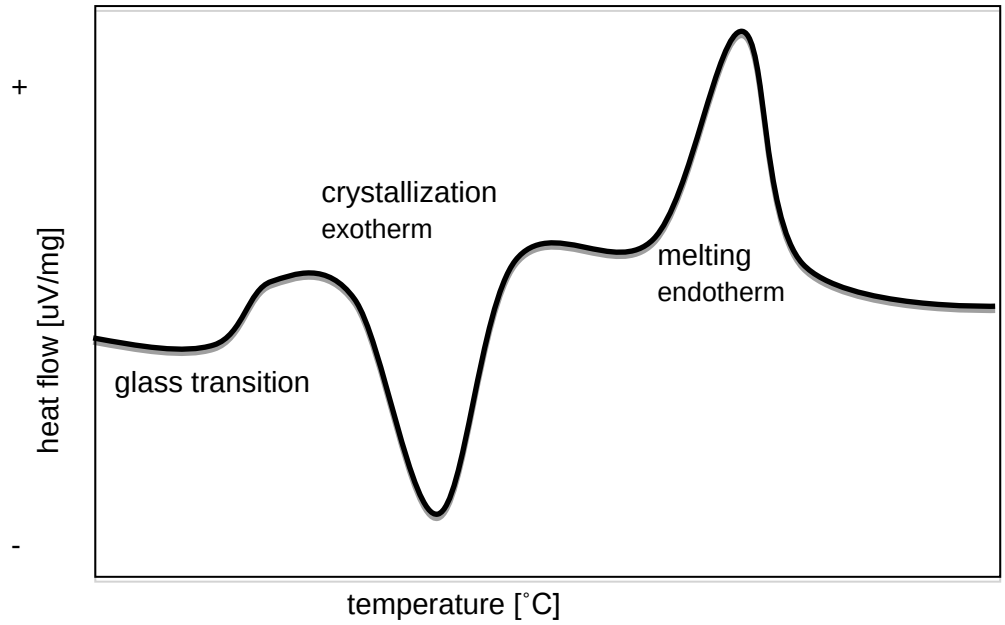

Figure 3.2.2.4: Theoretical DSC curve exemplifying thermal effects.

DSC measurments on crystalline lysozyme performed using Netzsch DSC 204 (see Figure 3.2.2.5) can detect melting, crystallization and/or decomposition (denaturation) as demonstrated in Figure 3.2.2.4. Two series of experiments are carried out. The crystalline

lysozyme, meaning Tetragonal, HTO and LTO, are either taken fresh or dried. Fresh lysozyme crystals are placed on filter paper to remove excess buffer solution before weighing in an aluminum crucible. The drying of lysozyme crystals is done in an oven at 30 ˚C for 3 h. Afterwards, dried crystals are weighed in the crucible for the measurements. The same procedure is carried out for the TGA sample preparation. The weight taken of each lysozyme sample is 10 mg with an accuracy of 0.05 mg, at room temperature. The crucible is covered, sealed and pierced shortly before placing into the DSC oven. The temperature profile is set first to an isothermal phase (3 h at 30 °C), followed by a dynamic phase up to 250 ˚C with a heating rate of 10 K/min. The software program Origin8.5 is used to plot obtained data.

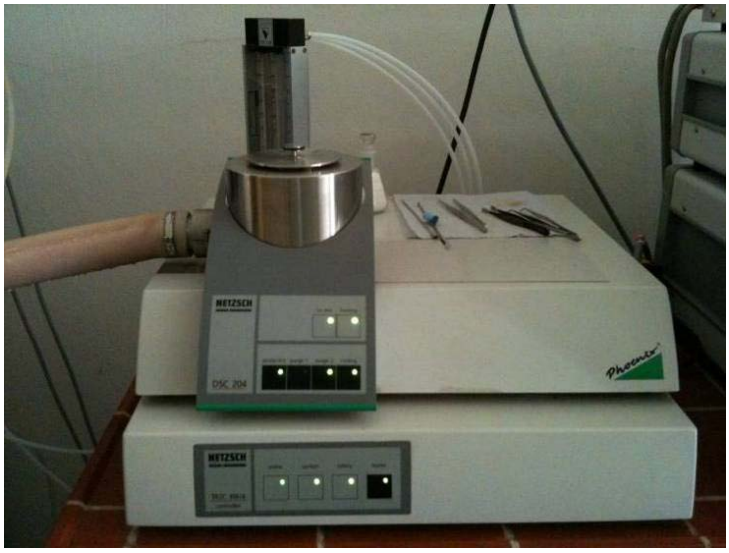

Figure 3.2.2.5: Differential Scanning Calorimeter (DSC) Netzsch DSC 204, Netzsch TASC 414/4 controller.

▪ *Thermalgravimetric analysis, TGA*

Thermalgravimetric analysis, TGA, is commonly used to observe the loss of weight in dependence on temperature, meaning e.g. the loss of water or other evaporable solvents of a substance. In addition, TGA can be used to determine the degradation temperature, hence indirectly the composition (e.g. organic or inorganic components) and/or the decomposition of substances. This device has to be highly precise for the weight, temperature and temperature changes. Therefore, the analyzer of this device is a high-precision balance with a pan in which the sample will be placed. The sensitivity is given for 5 µg [STA11]. The balance with the sample is located in an electrically heated and atmosphere controlled oven that contains a thermocouple to precisely measure the temperature. The atmosphere in the oven is purged with an inert gas to prevent unwanted reactions.

Simultaneous TGA-DTA/DSC by Netzsch, STA, with a Netzsch 409 cell is used for present studies on lysozyme crystals (see Figure 3.2.2.6). The STA instrument combines the detection of the heat flow and the weight changes in a material as a function of temperature and/or time. Two series of experiments are carried out under a controlled nitrogen atmosphere with a flow rate of 30 mL/min. The lysozyme crystals, meaning Tetragonal, HTO and LTO, are either taken fresh or air-dried and treated in the same way as described for DSC investigations (see above section DSC). According to Petrova et al. [PET07], temperature profile is chosen and starts with an isothermal phase of 30, followed by a dynamic phase. During the dynamic phase, the temperature increases up to 250°C with a heating rate of 10 K/min. Results obtained are plotted using the software program Origin8.5.

Figure 3.2.2.6: Coupling system of Netzsch TG–DSC/DTA (STA) with Netzsch STA 409 cell.

▪ *Scanning-Electron-Microscopy, SEM*

A *Scanning-electron-microscope*, SEM, is used to obtain very high-resolution almost 3-D images of the lysozyme crystal surface topography, revealing details less than 5 nm, meaning an optical magnification up to 25000 times. The 3-D appearance of the lysozyme crystal is helpful to understand the surface structure [GOL03]. Especially the edges and broken corners are important because it provides a sight in the inner crystal.

▪ *Conductivity*

Conductivity represents a physical property, is measured by a conductivity meter and describes how an electrolyte solution is able to conduct electricity. The conductivity (anions and cations) given in S/m (Siemens per meter) can be converted into the total dissolved ionic solid. For the conversion, it is assumed that the dissolved ionic solid is sodium chloride. This means that 1 µS/cm is equivalent to 0.6 mg NaCl per kg H_2O [DOW09].
A conductivity meter: Knick Konduktometer 703 is used to detect the presence of ions or changes in the ion concentration of different solutions during the crystallization or during the dissolution process of lysozyme crystals.

Accuracy of conductivity measurements
In general, conductivity measurements are a very precise technique to indirectly determine the ion concentration of electrolyte enriched solutions. In present studies, the conductivity meter was not able to work as precise as given by the manufacturer, < 1.00 µS/cm to 1000 mS/cm. The measuring cell was not in optimum condition, but obtained accuracy is high enough to approve the expected trend. Calculations using the correlation of 1 µS/cm are equivalent to 0.6 mg NaCl per L (kg) H_2O give results within an error of 10 %. This error also included variations in room temperature at which the conductivity is measured.

▪ *Energy-Dispersive-X-Ray Spectroscopy, EDX*

The *Energy-dispersive X-ray spectroscopy*, EDS or EDX, is an analytical device for elemental analysis or chemical characterization which relies on interactions between the electromagnetic radiation and the substance of interest. The electromagnetic radiation is a high-energy beam of charged particles and causes the substance of interest to emit X-rays as a response of being hit by charged particles. X-rays emitted are detected by the energy-dispersive spectrometer. The difference in energy of the emitted X-rays between the pre- and after radiation treated state of the elements in the sample being studied is characteristic. Due to the fact that each element has its own unique atomic structure, the X-rays emitted by EDX clearly identify the elemental composition of the analyzed sample [GOL03].
For the EDX investigations, Tetragonal lysozyme crystals are shortly dried on filter paper to remove attached buffer solution and afterwards carbon steamed. Two samples are taken from the same Tetragonal crystal but from different positions to evaluate its composition which gives information about the homogeneity.

▪ *X-ray Powder Diffraction, XRPD*

Among other, one analytical technique for phase identification of crystalline substances is *X-ray powder diffraction*, short XRPD. The XRPD delivers information about the arrangement of atoms within a crystal and about the unit cell dimension (atomic spacing) that is important for crystal structure studies. The principle of X-ray diffractions relies on interference of

monochromatic X-rays and a crystalline sample. The X-rays generated by a cathode ray tube, filtered to generate monochromatic radiation and finally concentrated will hit the crystalline sample. The crystal layers reflect the X-rays and this can cause interference, which can be described by Bragg's law equation 3.2.2.4.

$n * \lambda = 2d \sin \theta$ [GÖB98, PAN11]. (3.2.2.4)

X-ray powder diffraction is mostly used for the characterization of crystalline or polymorphic materials. In general, for XRPD investigations the sample of interest has to be finely ground and homogenized. XRPD studies on air-dried Tetragonal, HTO and LTO lysozyme crystals are acquired on a XRPD device of X'Pert Pro PANanalytical GmbH/The Netherlands. The fresh or air-dried lysozyme crystals were fine ground and placed on the sample holder. The XRPD device works with CuK_{alpha}-radiation, an X'Celerator detector, in a width range of 3 – 50 ˚ and a step width of 0.0167 ˚ 2theta. The acquisition time is 200 s per step.

Accuracy of XRPD measurements
Sample preparations for XRPD means to grind the crystalline sample, a powder is achieved. The lysozyme crystal powder investigated by XRPD contains randomly oriented particles which demand several measurements to minimize possible errors. The XRPD is carried out only one time for any of the three lysozyme crystal morphologies. An existing error should be estimated but mentioned possible error loses its sight of importance, because in present studies the peak information generated by the sodium chloride is of main interest.

▪ *Raman spectroscopy*

Raman spectroscopy is a contact-free analytical spectroscopic method that uses laser technology to characterize a substance of interest. A Raman spectrometer consists of a monochromatic light source, a sample holder with collection optics, a light dispersing unit and a detector [RAM11, GAR89].
The Raman effect is observed by an interaction of the material and the monochromatic light. Therefore, the molecules of the sample start to vibrate or rotate. The vibrating molecules (or the lattice) will collide with photons and a change in energy may or may not occur. The describe situation can generate three possible outcomes (see Figure 3.2.2.7) which are [RAM11]:

1) Rayleigh scattering will be generated by elastic collision. It means if the molecule hits the photon, no change in energy, neither of the vibrating molecule nor of the photon, occurs.
2) Stokes-lines are inelastic collisions and can be generated if the energy of the molecule after collision with a photon is increase. At the same time, the energy of the scattered photon is decreased for the same amount. Longer wavelength (= Stokes- lines) will be detected.
3) Anti-Stokes-lines are inelastic collisions as well but the energy distribution is the opposite.

In this case, the molecule has to be already excited before the collision with the photon. Therefore, the resulting wavelength (=anti-Stokes-lines) is shorter.

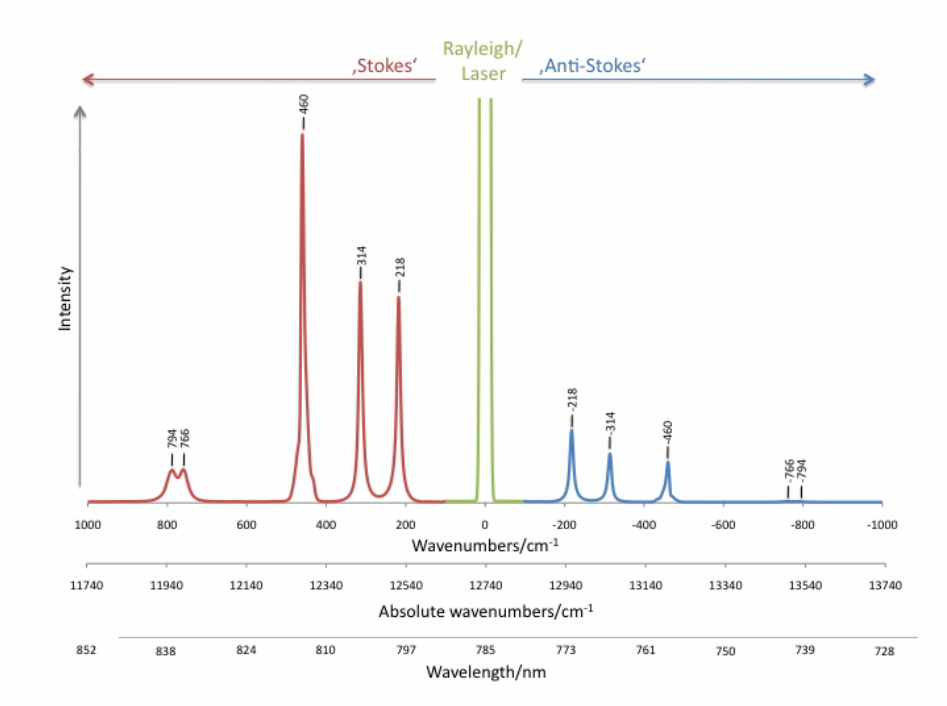

Figure 3.2.2.7: Comparison of the Raman scattering: Stokes-lines, Rayleigh scatter and anti-Stokes-lines [RAM11].

Raman spectroscopy for lysozyme crystals is done using a Bruker Raman-spectrometer RFT 100/S (Bruker Optik Ettlingen) with a NdYac-laser of 1064 nm to obtain the Raman pattern. The HTO and LTO lysozyme crystals are investigated using two different techniques.
For technique one, each lysozyme crystal morphology is produced separately in a centrifuge tube. The crystals are taken out of the buffer solution and air-dried on filter paper and then transferred into a small aluminum pan.
The second technique used lysozyme crystals that are produced inside of glass tube of very small diameter. Before Raman investigation, the buffer solution inside of the glass tube is removed and crystals become air-dried.

▪ *Infrared spectroscopy*

Infrared spectroscopy belongs to the spectroscopic methods that identify and investigate organic and inorganic substances. It uses the infrared region of the light spectrum. The infrared light can be roughly classified into three sub-regions, near- (14000–4000 cm^{-1} / 0.8–

2.5 µm wavelength), mid- (4000–400 cm^{-1} / 2.5–25 µm) and far-infrared (400–10 cm^{-1} / 25–1000 µm). Due to the fact that molecules can absorb specific wavelength (resonant frequencies) a morphology characteristic pattern of their structure is obtained, similar as for Raman spectroscopy. The obtained IR- spectrum of a sample comes from an infrared beam passing through the sample and scanned by a monochromator. Absorption of the IR-wavelength by the sample can occur when the sample contains bonds of same wavelength. Details about the molecular composition of the substance are achieved by analyzing the position, the shape and the intensities of the spectrum peaks.
The IR- method is highly sensitive to covalent bonds, this means samples with a simple IR-spectrum have only a few active bonds and are very pure. Samples containing a complex composition show more absorption peaks (bands) and therefore a more complex spectrum.
The IR- spectrum for HTO and LTO lysozyme crystals is produced by a Bruker FTIR-spectrometer IFS 28. The crystalline sample is placed on a measurement module (Pike Technologies) and measured using the ATR technique on a ZnSe-crystal (1.3 mm). No specific sample preparation is required. The lysozyme crystal is pressed and fixed directly on the ZnSe-crystal.

3.2.3 Solubility and dissolution equipment

3.2.3.1 Solubility

Here, solubility measurements and solubility data should be added to the partially existing lysozyme phase diagram. Therefore, solubility is measured using the optimized technique which allows solubility measurement of lysozyme crystals within a short time. The technique, introduced and described in detail by Weber [WEB08] and Aldabaibeh [ALD09a] is based on a closed system with small liquid volume of total 1mL to maximum 2 mL. PTEF tubes with a diameter of 1.0 mm and a peristaltic pump were applied to ensure the circulation in the system. The peristaltic pump drives the liquid through a packed bed of protein crystals (flow column) and through a flow cuvette which is placed in a UV / Vis spectrophotometer. The extinction was taken at 280 nm. The flow column has a diameter of 6.6 mm, a maximum volume of 1 mL and a filter with a pore size of 2.5 µm to avoid lysozyme crystals passing the column and entering the tube system. For temperature control, the column was kept in the water bath of a thermostat. As a consequence, phase equilibrium is reached much faster in comparison to the static column method, mentioned in chapter 2.2. In favorable cases, equilibrium is achieved within 20 to 40 minutes. Figure 3.2.3.1 gives a schematic overview of the micro-apparatus set up for solubility determination.

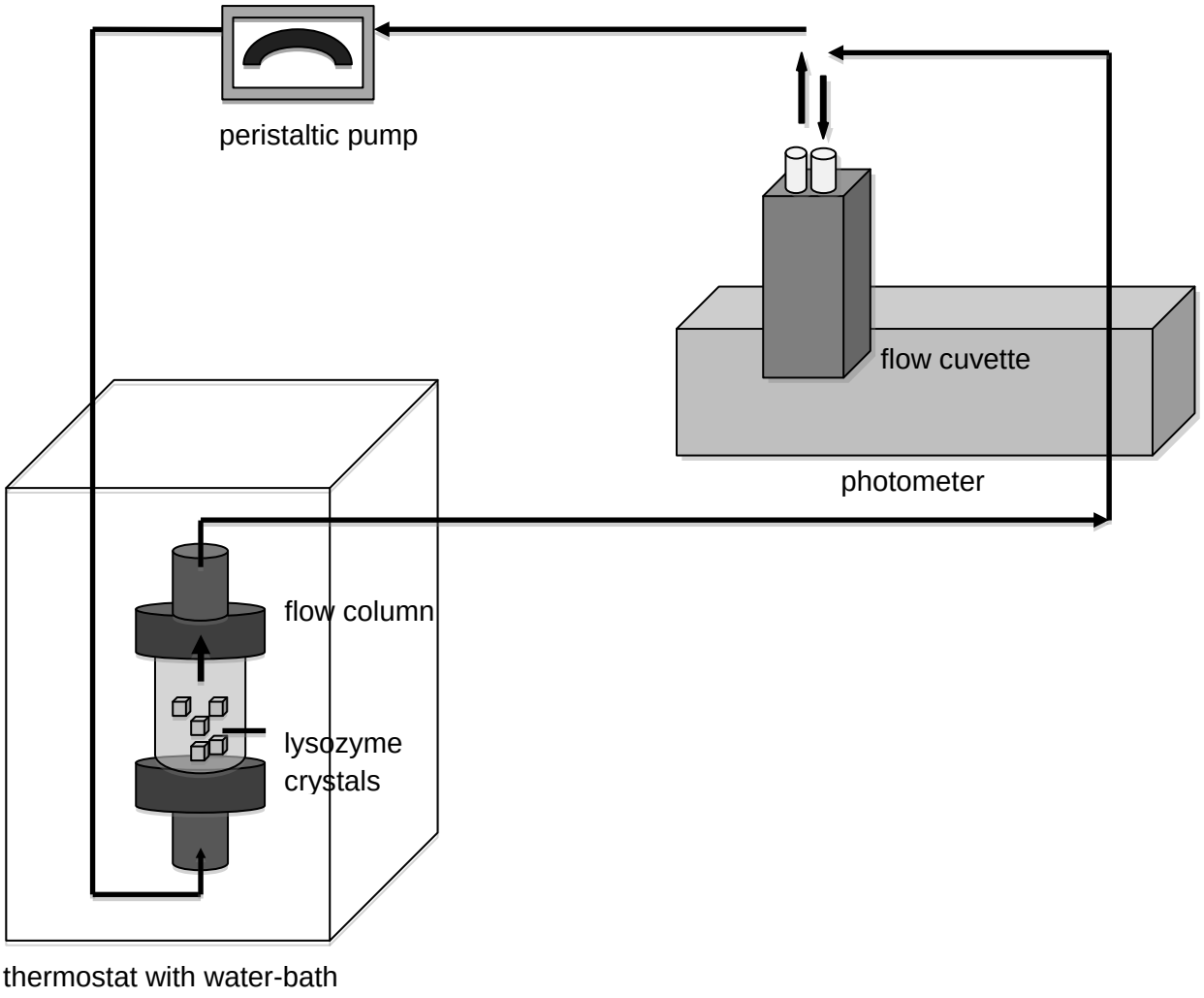

Figure 3.2.3.1: Schematic set-up of the micro-apparatus solubility measurement.

Accuracy of solubility measurements

The spectrophotometer used for present solubility studies has a preciseness of about 0.005 extinction units given by the manufacturer. Measuring the extinction at certain conditions for several times demonstrates the reproducibility. Reproducibility is ensured with an accuracy comparable with the one from the manufacturer. A resulting and expected concentration deviation of 0.1 to 0.2 mg/mL, depending on the cuvette used and conditions investigated, has to be taken into account.

Errors that have to be considered are mainly due to the personal handling of preparing the solutions required e.g. pH (+/- 0.1) or salt concentration (+/- 0. 01 to 0.05 mg), deciding whether the equilibrium of current conditions is reached, some temperature fault of the thermostat which is assumed to be about +/- 0.1 to 0.3 °C, and pipetting errors. All in all, the errors are minor because obtained solubility data for the HTO morphology was compared with previous studies done by Aldabaibeh [ALD09a] and showed good agreement.

3.2.3.2 Dissolution

In Figure 3.2.3.2, shown dissolution experiments are carried out in undersaturated solution, which is placed into a microscope cell. This cell is tempered by a thermostat. A digital camera is installed above the cell. The AnalySIS software was used to observe the dissolution of the lysozyme crystals with time.

Accuracy of dissolution measurements

Dissolution experiments using a microscope cell shown in Figure 3.2.3.2 are carried to observe the dissolution behavior of lysozyme crystals under different dissolution conditions. Main error refers to the microscope cell itself used in present studies. The microscopy cell cover cannot guarantee complete sealing. Different types of covers are tested, but none of them yield in complete satisfaction. Depending on the dissolution conditions, some dissolution observations are long-term experiments, meaning two to ten days, that gives a potential risk of concentration changes within the microscope cell, if not sealed correctly. Due to this important error, dissolution rates cannot be measured precisely enough for meaningful interpretation. Reproducible dissolution rates cannot be assured. In addition, the temperature control of the microscope cell by a thermostat using none-isolated tubes also carries the risk of errors. This risk is neglected because for all experiments the temperature is kept constant at 16 °C. Additionally errors are only due to personal handling such as pipetting the liquid into the microscope cell, separating the lysozyme crystals from each other which often stick together when stored over time, removing of adherent buffer solution by filter paper before placing them in the microscopy cell filled with the solution. The time delay of approximately 10 s between placing the crystal into the solution and starting the observation program has to be included, too.

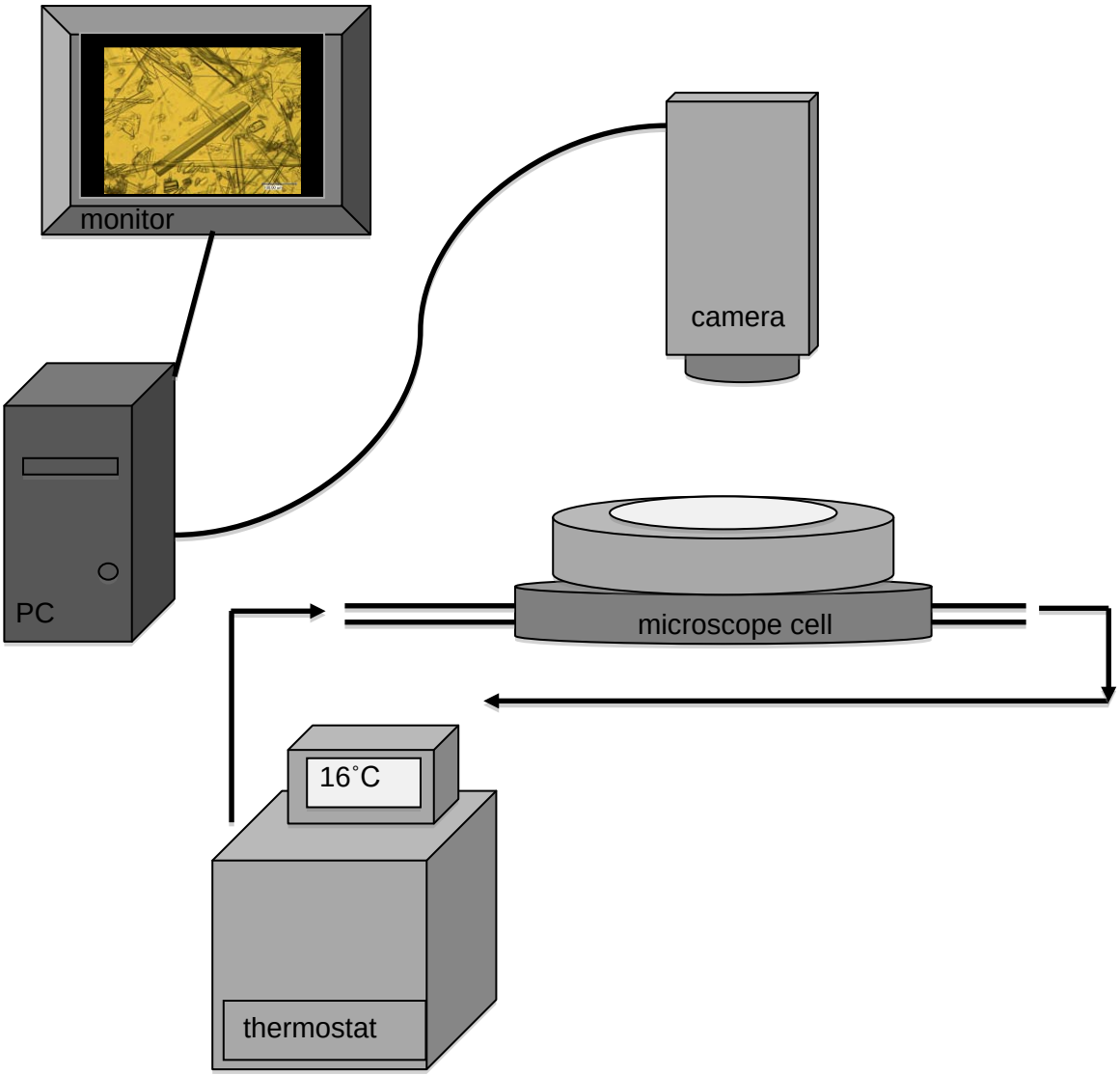

Figure 3.2.3.2: Schematic set-up of the dissolution experiments.

4. Results

The first part of the results demonstrates the successful crystallization of lysozyme using sodium chloride and other salts. The second part studies the Tetragonal, HTO and LTO lysozyme crystals and its crystal characteristics in more detail. Several different analysis methods are used to determine the crystal composition and physical-chemical properties. The third part shows the results of solubility measurements and dissolution experiments. Interesting results of preliminary dissolution observation studies of lysozyme crystals are pictured. This dissolution phenomenon of lysozyme crystals introduced has not been explicit reported.

4.1 Lysozyme crystals

Basis for present lysozyme crystal investigations is the reproducible protein crystallization using lysozyme as a model substance. Previous in house crystallization screening and literature research directed the design of lysozyme crystallization conditions used in present thesis. The lysozyme crystal outcome observed by digital microscope is given in the Tables 4.1.1 to 4.1.6.

Table 4.1.1: Crystallization of lysozyme using NaCl: Tetragonal, High Temperature Orthorhombic and Low Temperature Orthorhombic modification after 24 h.

Tetragonal	High Temperature Orthorhombic (HTO)	Low Temperature Orthorhombic (LTO)
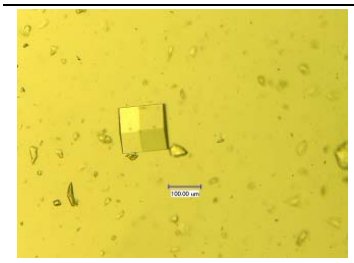	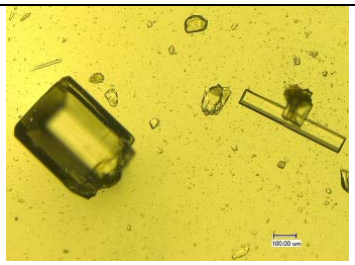	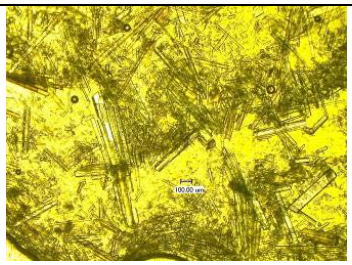

lys* = lysozyme

Among others, successful crystallization screening results can be seen in Tables 4.1.2 to 4.1.6. Shown lysozyme crystals are produced using potassium, calcium or barium di chloride and di sodium carbonate under described conditions for Tetragonal, HTO and LTO crystals.

Executing the same crystallization procedure for the Tetragonal morphology, see first two columns of Tables 4.1.2 and 4.1.3, results in a stable Tetragonal shape, whereas the crystals obtained under conditions where the low temperature Orthorhombic are stable vary. The LTO condition with potassium chloride generates first an unstable mixture of Tetragonal and extremely small crystals of not detectable shape (see Table 4.1.2 third column). After 14 days, all lysozyme crystals transformed into a needle like morphology (see Table 4.1.3 third column). The same LTO conditions but using calcium chloride resulted again in a stable Tetragonal crystal morphology (seeTables 4.1.2 and 4.1.3 fourth column).

Table 4.1.2: Crystallization of lysozyme using KCl and $CaCl_2$*2H_2O under conditions of the Tetragonal and low temperature Orthorhombic modification after 24 h.

Tetragonal $_{KCl}$	**Tetragonal** $_{CaCl2*2H2O}$	**Orthorhombic** $_{KCl}$	**Orthorhombic** $_{CaCl2*2H2O}$
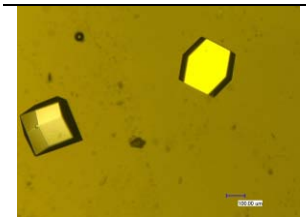	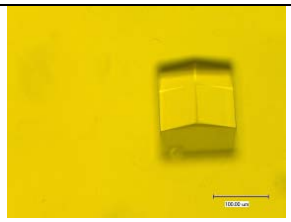	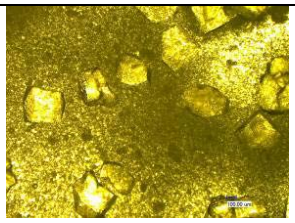	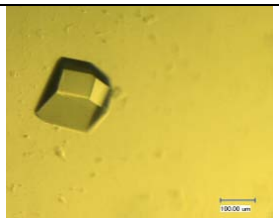

lys* = lysozyme

Table 4.1.3: Crystallization of lysozyme using KCl and $CaCl_2$*2H_2O under conditions of the Tetragonal and low temperature Orthorhombic morphology after 18 d (Tetragonal), 14 d (Orthorhombic).

Tetragonal $_{KCl}$	**Tetragonal** $_{CaCl2*2H2O}$	**Orthorhombic** $_{KCl}$	**Orthorhombic** $_{CaCl2*2H2O}$
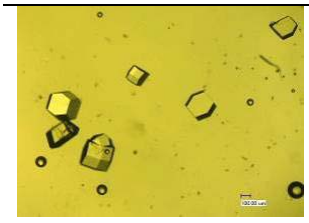	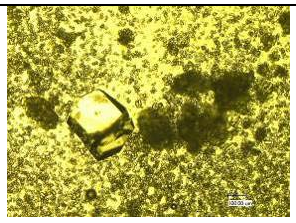	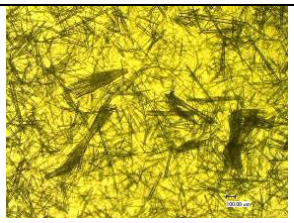	

lys* = lysozyme

Similar crystal outcome is observed for the lysozyme crystallization by di sodium carbonate or barium di chloride. In all crystallization experiments, a stable Tetragonal morphology,

except for 4 wt% Na_2CO_3, is obtained (see Table 4.1.4). Checking the samples after two month, same crystal morphology is recognized.

Cystallization of lysozyme under conditions of the low temperature Orthorhombic morphology with di sodium carbonate is different. Adding di sodium carbonate-buffer solution into the lysozyme-buffer solution results in a gel-like turbid solution (see first column of Table 4.1.5). After 24 h, no crystal could be discovered. Storing the sample at temperatures of 4 °C for several days leads to nucleation. The formation of small crystals is observed after 14 days (see second column of Table 4.1.5). Further storage of the crystallization sample at mentioned conditions results finally in the orthorhombic lysozyme crystal morphology, observed after 42 days (see third column of Table 4.1.5).

Table 4.1.4: Crystallization of lysozyme using Na_2CO_3 and $BaCl_2$ under conditions of the Tetragonal morphology and varied salt concentration after 24 h.

Tetragonal $_{Na2CO3}$	**Tetragonal $_{Na2CO3}$**	**Tetragonal $_{BaCl2}$**	**Tetragonal $_{BaCl2}$**
4 wt% Na_2CO_3	2 wt% Na_2CO_3	4 wt% $BaCl_2$	6 wt% $BaCl_2$
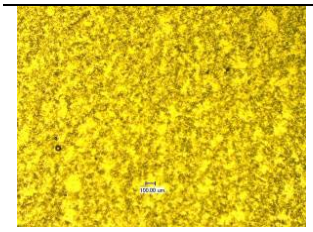	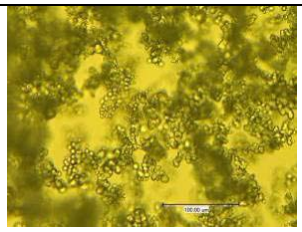	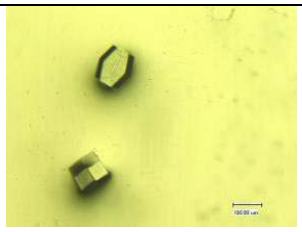	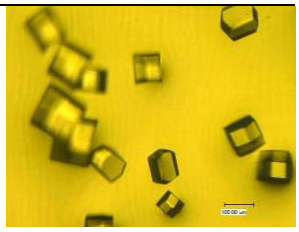

lys* = lysozyme

Table 4.1.5: Crystallization of lysozyme using Na_2CO_3 under conditions of the low temperature Orthorhombic morphology after 24 h (first column), 14 d (second column), 42 d (third column).

Orthorhombic $_{Na2CO3}$	**Orthorhombic $_{Na2CO3}$**	**Orthorhombic $_{Na2CO3}$**
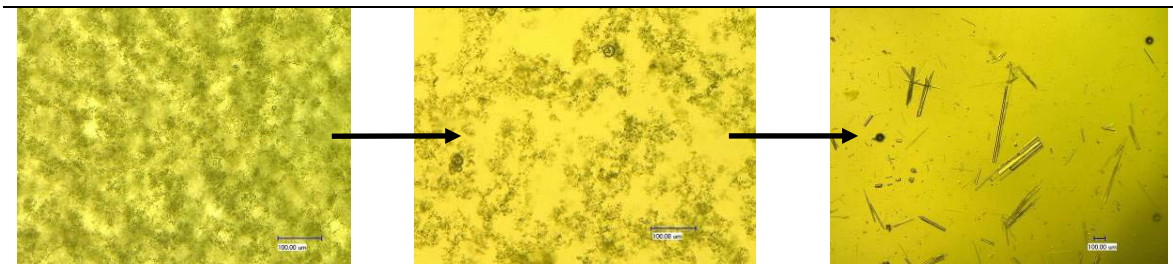		

lys* = lysozyme

Furthermore, the crystallization of lysozyme under conditions of the high temperature Orthorhombic crystals using potassium and calcium di chloride again succeed. Table 4.1.6 clearly shows the orthorhombic morphology.

Lysozyme crystallization using different salts under different conditions, which are successful for the crystallization with sodium chloride, is reproducible whether using potassium, calcium and barium di chloride or di sodium carbonate. The most effective and favored morphology of the lysozyme crystal outcome for studied salts is the Tetragonal morphology.

Table 4.1.6: Crystallization of lysozyme using Na_2CO_3 and $BaCl_2$ under conditions of the high temperature Orthorhombic morphology after 24 h.

Orthorhombic $_{KCl}$	**Orthorhombic $_{CaCl2*2H2O}$**
	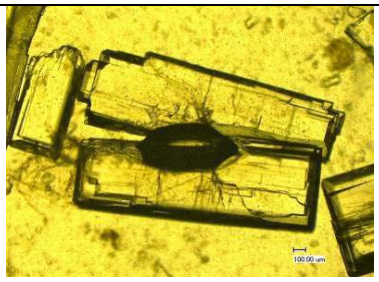

lys* = lysozyme

4.2 Analytics of lysozyme crystals

The results of the analytics done for the lysozyme crystals produced by already described method (chapter 3.2.2) using sodium chloride as crystallizing agent are summarized.

▪ *Enzymatic activity*

The enzymatic activity of the lysozyme after crystallization was determined using the reaction of the lysozyme with the micrococcus luteus bacterium. Before testing the enzymatic activity, according to Shugar [SHU52] (see chapter 3.2.2 and appendix A.1), the protein content, meaning lysozyme concentration within the lysozyme crystals, has to be determined.

Lysozyme concentration

The lysozyme concentration of the Tetragonal, HTO and LTO lysozyme crystals is determined in two steps. First a calibration curve has to be developed (see Figure 4.2.1) by dissolving pure lysozyme of different concentration (1.25, 0.625 and 0.3125 mg/mL) in the

test buffer solution and measuring the extinction at 280 nm. Second step follows by dissolving 1 mg of 24 h air-dried lysozyme crystals in the test buffer solution (see appendix A1), extinction at 280 nm is taken again. The lysozyme concentration can be calculated with the help of the extinction coefficient which is taken from literature 2.64 mL/mg*cm [SOP62], because it is in good agreement with the slope of 2.6464 obtained by the calibration curve (see Figure 4.2.1) and with the Lambert-Beer's law [UAA11, AJE11] (see equation 4.3.1) in next chapter.
While measuring the lysozyme enzymatic activity, the temperature of the spectrophotometer has to be constant at 25 °C. The wavelength used is set to 450 nm. The activity then can be measured indirectly by an extinction decrease with time. To obtain the activity data, the "zero"-extinction also known as blank is determined first. Then, preliminary activity tests concerning different lysozyme concentrations have to be performed to estimate convenient lysozyme concentration. Knowing practical conditions, the actual enzymatic activity test due to the reaction between lysozyme and the Micrococcus luteus can be carried out. Activity calculations using the extinction values achieved follow the equation 4.2.1. The specific enzymatic activities are calculated by the equation 4.2.2.

$$\text{Enzymatic activity (U/mL)} = -(\Delta E \text{ Blank /min} * DF) / (0{,}001 * V_{enzyme}) \quad (4.2.1)$$

$$\text{Specific enzymatic activity (U/mg)} = -(\Delta E \text{ Blank /min} * DF) / (0{,}001 * V_{enzyme} * c_{protein}) \quad (4.2.2)$$

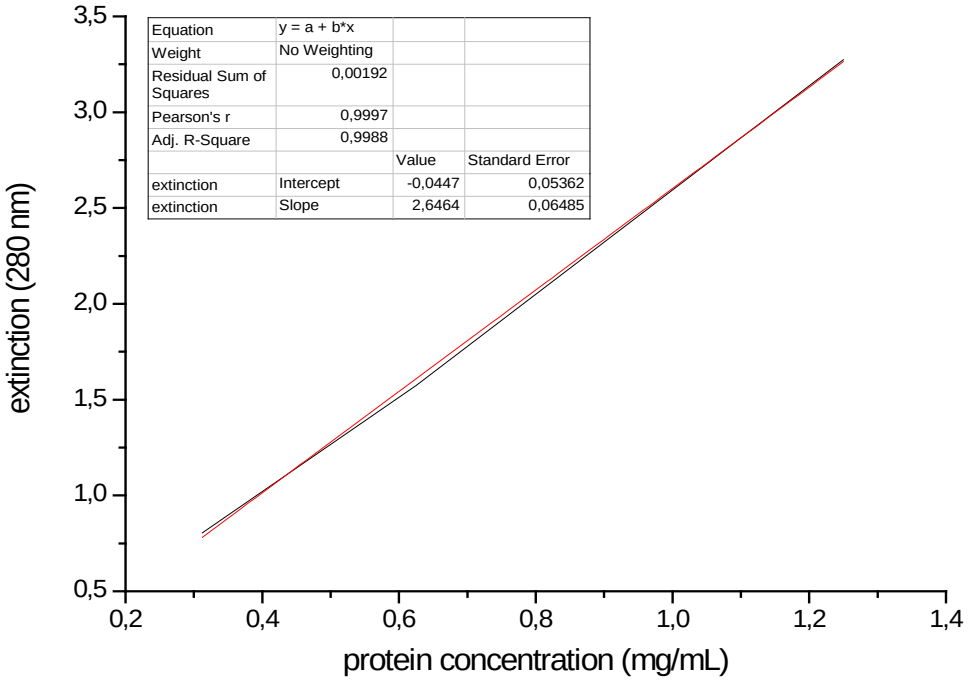

Figure 4.2.1: Calibration curve of protein (pure lysozyme) concentration versus extinction of 280 nm; linear fit visualized by red line, slope is 2.6464.

Figure 4.2.2a displays the average lysozyme concentration of the Tetragonal, HTO and LTO lysozyme crystals that derived from 15 to 20 batches.
Comparing the protein concentration of the lysozyme crystals, differences are detected. Deviations of about 3 wt% have to be considered. Calculating the average, the HTO crystals have the highest protein concentration with 0.842 $mg/mg_{crystal}$*mL, followed by the Tetragonal (0.822 $mg/mg_{crystal}$*mL) and the LTO (0.816 $mg/mg_{crystal}$*mL) crystals.

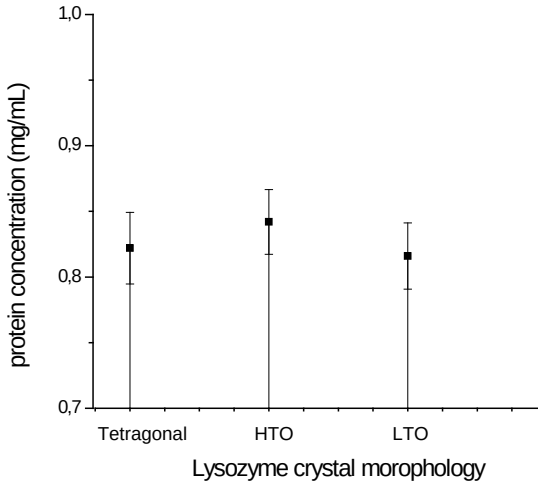

Figure 4.2.2a: Protein (lysozyme) concentration of 1 mg air-dried Tetragonal, HTO and LTO lysozyme crystals.

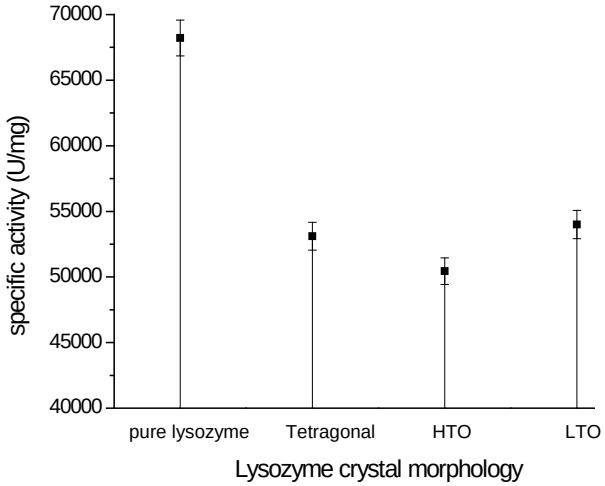

Figure 4.2.2b: Specific activity of the Tetragonal, HTO and LTO lysozyme crystal morphology.

Specific activity
Knowing the protein content of the lysozyme crystals, the specific enzymatic activity that refers to the protein concentration within the lysozyme crystals can be measured and calculated (equation 4.2.1 and 4.2.2). Figure 4.2.2b summarizes the average specific activity data which are obtained from same batches used for protein concentration determination.
The specific enzymatic activity of the pure lyophilized lysozyme, 70000 U/mg +/- 1500 U/mg, matches the given activity by the manufacturer. (Some activity loss occurs due to air exposure.)
The specific activity of the crystallized lysozyme decreases, including a 2 % fault. Comparing the specific activities of the different lysozyme crystal morphologies, the LTO crystals are most active, followed by the Tetragonal and the HTO crystals. In comparison to lyophilized lysozyme before crystallization, the average activity loss for crystallized lysozyme of the LTO morphology is about 23 %, of the Tetragonal is 26 %, and of the HTO is 29 %.

▪ *SEM*

For higher resolution and more detailed images of the lysozyme crystals and their surface, SEM pictures are taken. The lysozyme crystal edges (see in Table 4.2.1) and their crack behavior are of great interest. The SEM pictures obtained for lysozyme crystals show “classic” broken crystal edges which are comparable even with fractured edges of highly crystalline sodium chloride, investigated by Ulrich [ULR81].

Table 4.2.1: SEM images for a detailed picture of the Tetragonal, HTO and LTO lysozyme crystal surface.

Lysozyme crystal sample	**Optical magnification of** **Tetragonal: 500 x** **HTO: 500 x** **LTO: 2500 x**	**Optical magnification of** **Tetragonal: 5000 x** **HTO: 5000 x** **LTO: 5000 x**	**Optical magnification of** **Tetragonal: 10000 x** **HTO: 25000 x** **LTO: 25000 x**
Tetragonal fresh	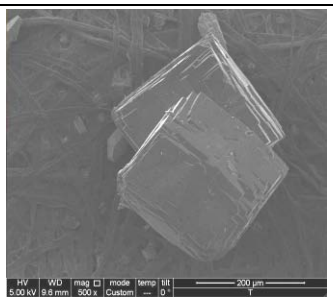	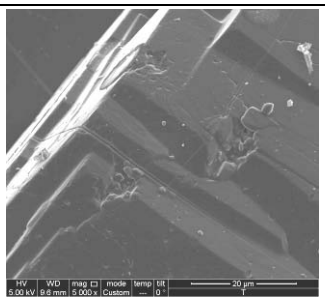	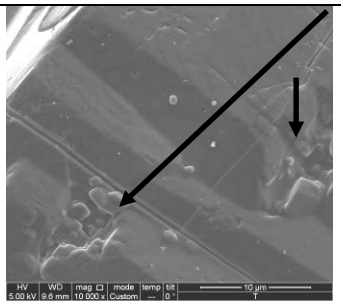
HTO fresh	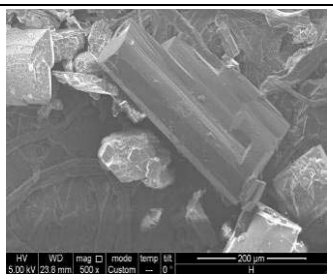	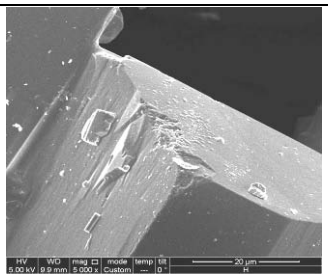	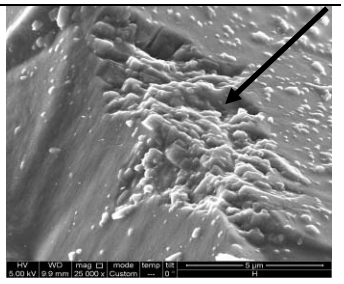
LTO fresh	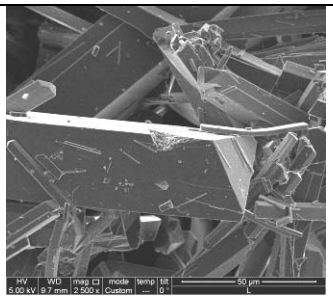	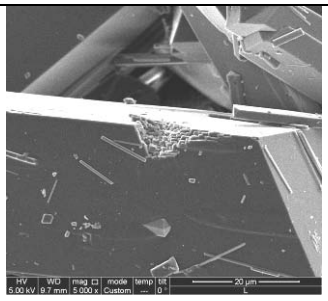	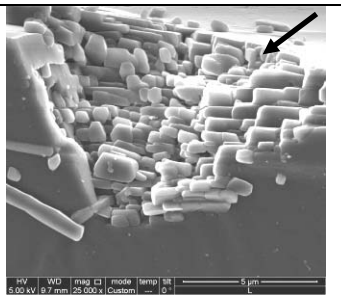

▪ *Dye - experiments*

In general, protein crystals have high water content [MCP98]. The same applies for lysozyme crystals. The water content has to be defined, because two types of water exist in the crystal. It is assumed that there is water fixed in the crystal lattice and “flexible” or “free” water as component of the buffer solution in which lysozyme is crystallized and stored. The buffer including the “free” water is expected to be enclosed in the cavities / crystal pores of the lysozyme crystals.
Dye experiments are carried out to prove the existence of buffer solution (and “free” water) inside of the crystal, and the diffusion processes between the interior and the environment. Therefore, three series of experiments are developed. First series of experiments is carried out with dye colored buffer solution whereby two different dyes become tested. To produce colored lysozyme crystals (see Table 4.2.2) fresh and clear lysozyme crystals are placed into the blue colored buffer solution. After 24 h, the lysozyme crystals are taken out of the blue buffer and studied by microscope. The second series of experiment uses blue colored salt-buffer solution during lysozyme crystallization (see Table 4.2.4). The third type of experiment is set up to bleach / discolor obtained blue lysozyme crystals. Therefore, the methylene blue colored lysozyme crystals are placed into colorless buffer solution and observed by microscope (see Table 4.2.5). Pictures of the lysozyme crystals during the coloring and discoloring experiments document the results.

Table 4.2.2: Dye (Coomassie blue, Methylene blue) solution preparation; pipetting scheme of coloring of lysozyme crystals using different dyes.

Lysozyme crystal modification	**Coomassie blue**	**Methylene blue**
Tetragonal	60 mg/L in acetate buffer pH5	0.4 g/L in acetate buffer pH5
HTO	60 mg/L in acetate buffer pH5	0.4 g/L in acetate buffer pH5
LTO	60 mg/L in glycine buffer pH9.6	0.4 g/L in acetate buffer pH9.6
Pipetting scheme		
Tetragonal crystals +	1 mL buffer solution: 1 mL dye solution	1 mL buffer solution: 1 mL dye solution
HTO crystals +	1 mL : 1 mL	1 mL : 1 mL
LTO crystals +	1 mL : 1 mL	1 mL : 1 mL

In addition to the dye experiments just mentioned, a different method trying to color the LTO lysozyme crystal modification is developed. Therefore, a solution containing phenolphthalein is prepared and added to an acetate buffer solution in which LTO crystals were placed (see Table 4.2.3). Base for this method is a pH dependent indicator (phenolphthalein) reaction because phenolphthalein switches its color from colorless (in acidic pH) into a red / pink if basic pH is present.
As assumed, the basic glycine buffer, used to prepare LTO crystals, is present within the LTO crystal, and if diffusion processes between the crystal inside and the buffer environment occur, the crystal should receive a red color. 24 hours after the transfer of LTO crystals into the phenolphthalein containing buffer solution, the LTO crystals are checked for its red color.

Table 4.2.3: Pipetting scheme of the coloring of LTO lysozyme crystals by indicator reaction of phenolphthalein.

Lysozyme crystal morphology	**Indicator: Phenolphthalein**
LTO	Solution: 0.092 mg phenolphthalein/L distilled H_2O 1 mL acetate buffer solution : 20 µL phenolphthalein solution

Table 4.2.4: Crystallization conditions to produce Tetragonal, HTO and LTO lysozyme crystals in methylene blue colored buffer solution.

Lysozyme crystal morphology	Methylene blue
Tetragonal / HTO crystals	+100 µL methylene blue solution pH5 (see Table 2.2.3) + 0.9 mL pure acetate buffer solution pH5 + 8 wt% NaCl (Tetragonal) / +12 wt% NaCl (HTO) = (Tetragonal / HTO) for each a volume of 1 mL + (Tetragonal / HTO) each 1 mL pure acetate buffer solution pH5 with 100 mg dissolved lysozyme = total volume of 2 mL → Tetragonal at 2-4 ˚C / HTO at 37 ˚C
LTO crystals	+100 µL methylene blue solution pH9.6 (see Table 2.2.3) + 0.9 mL pure glycine buffer solution pH9.6 + 8 wt% NaCl = volume of 1 mL + 1 mL pure glycine buffer solution pH9.6 with 100 mg dissolved lysozyme = total volume of 2 mL → 20 °C (room temperature)

Table 4.2.5: Conditions for the discoloring of methylene blue dyed lysozyme crystals in clear buffer solution.

Lysozyme crystal morphology	Discoloring conditions
Tetragonal / HTO crystals	+ 1 mL pure acetate buffer solution pH5 + 8 wt% (Tetragonal) / 12 wt% (HTO) NaCl → Tetragonal at 2-4 ˚C / HTO at 37 ˚C
LTO crystals	+ 1 mL pure glycine buffer solution pH9.6 + 8 wt% NaCl → 20°C (room temperature)

Do to the sensitivity of protein crystals to their environment, possible influence of the dye on the pH of the buffer solution has to be tested. The effect of coomassie and methylene blue on the pH of the buffer solution is shown in Table 4.2.6. No dramatic changes in pH occur.

Table 4.2.6: Effect of coomassie and methylene blue on the pH of acetate and glycine buffer.

Buffer solution + dye	pH-value
Acetate buffer 0.1 M, pH5 + Coomassie blue	5.1
Acetate buffer 0.1 M, pH5 + Methylene blue	5.1
Glycine buffer 0.05 M, pH9.6 + Coomassie blue	9.8
Glycine buffer 0.05 M, pH9.6 + Methylene blue	9.8

Coloring experiments using coomassie or methylene blue give different results, shown in first part 1) of Table 4.2.7. Dyeing lysozyme crystals using coomassie blue is not successful for all three lysozyme crystal morphologies, whereas using methylene blue causes the Tetragonal and HTO lysozyme crystals to turn blue. Blue LTO crystals could not be obtained.
Coloring experiments carried out by coloring the buffer solution in which the lysozyme crystallization takes place, here only methylene blue is used, generate blue Tetragonal and HTO crystals (see second part 2) of Table 4.2.7), but the LTO crystals behave different.

As demonstrated in Table 4.2.7, using coomassie or methylene blue to dye LTO crystals is not successful. Another effective method using phenolphthalein is introduced in Table 4.2.3.

Phenolphthalein is colorless at low pH values but changes its color to red at basic pH. The LTO crystals after placing them in a acetate-phenolphthalein buffer solution change their colorless look to red (see Table 4.2.8).

Table 4.2.7: Coloring of lysozyme crystal using different dyes, coomassie and methylene blue, pictures taken after 24 h.

1) Buffer solution + dye	**Tetragonal lysozyme**	**HTO lysozyme**	**LTO lysozyme**
+ Coomassie blue	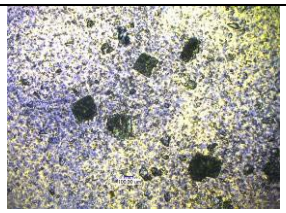	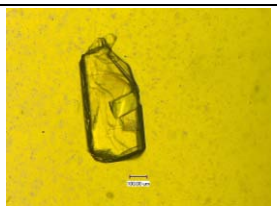	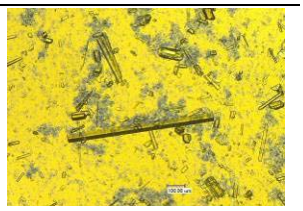
+ Methylene blue	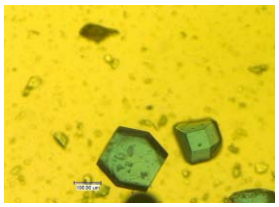	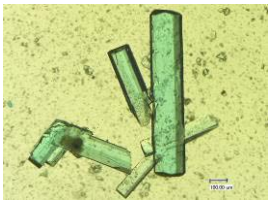	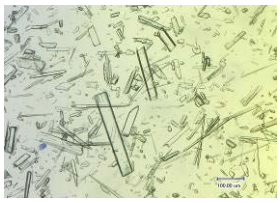
2) Buffer solution + salt + dye → crystallization	**Tetragonal lysozyme**	**HTO lysozyme**	**LTO lysozyme**
+ Methylene blue	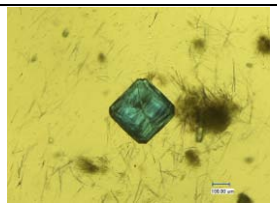		

Table 4.2.8: Coloring of LTO lysozyme crystals by phenolphthalein, pictures taken after 24 h.

Buffer solution + dye	LTO lysozyme crystals	
Dye solution of 0.092 mg Phenolphthalein/L distilled H_2O 1 mL buffer solution : 20 µL dye solution		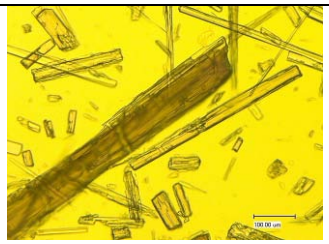

Discoloring experiments with blue Tetragonal (methylene blue), HTO (methylene blue) and red LTO (phenolphthalein) resulted in clear crystals after placeing them into pure crystallization buffer solution. The discoloring process observed is illustrated in Table 4.2.9.
The investigated Tetragonal crystals show very slow discoloring. After 120 min only disoloring of the crystal edge regions is observed, shown in first row of Table 4.2.9. Checking the sample after 24 hours results in complete discolored Tetragonal crystals, not illustrated in the Table 4.2.9. Observations for the HTO crystals are slightly different. The discoloring of the HTO crystals (see second row of Table 4.2.9) is faster. After 70 min the HTO crystals are clearly lighter in blue color. The LTO lysozyme crystals again show a very slow discoloring process, last row of Table 4.2.9. As mentioned for the Tetragonal crystal, after 20 to 24 hours the HTO and LTO crystals turn back to their original colorless look.

Table 4.2.9: Discoloring of methylene blue dyed Tetragonal and HTO lysozyme crystals as well as the phenolphthalein red dyed LTO crystals in clear buffer solution, pictures taken with time.

Lysozyme crystal morphology	Discoloring of lysozyme crystals with time	
Tetragonal crystal 1) start 2) after 120 min	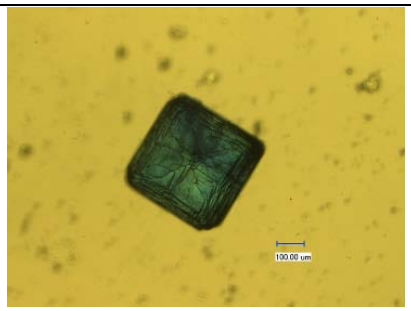	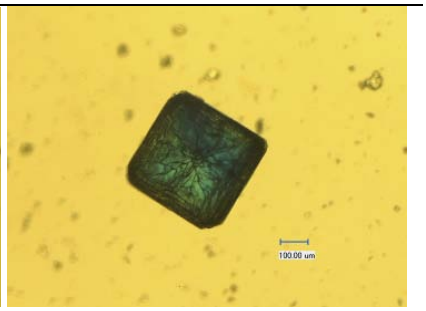
HTO crystal 1) start 2) after 70 min	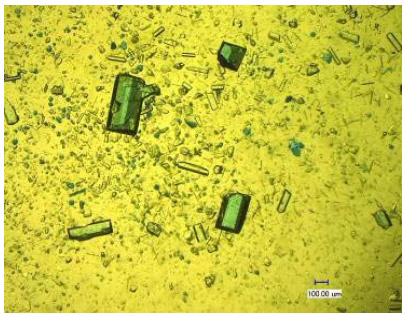	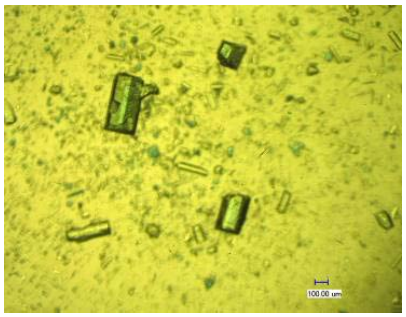
LTO crystal 1) start 2) after 24 h	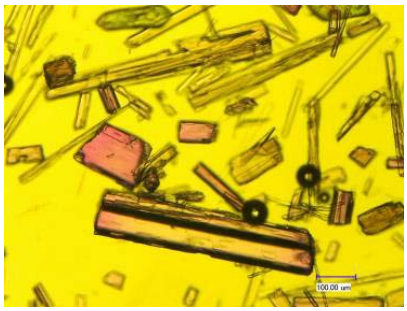	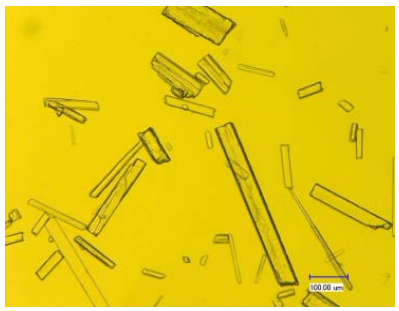

▪ *Thermal analysis by DSC*

Thermal analysis done for fresh and air-dried Tetragonal, HTO and LTO crystals are examined as shown in Figures 4.2.3 and 4.2.4.
DSC data obtained is plotted by DSC [uV/mg] versus time [min], black line. The temperature profile used is shown as the red line. For all measurements, the same trend is observed. First, two small endothermic peaks can be recognized and show heat absorption. They are more clearly for air-dried lysozyme crystals than for the fresh ones (see Figure 4.2.4).

A strong exothermic peak (strong heat release), a decomposition peak respectively, at 251 ± 2 ˚C is observed for fresh and air-dried lysozyme crystals (see Figures 4.2.3, 4.2.4 and Table 4.2.10).

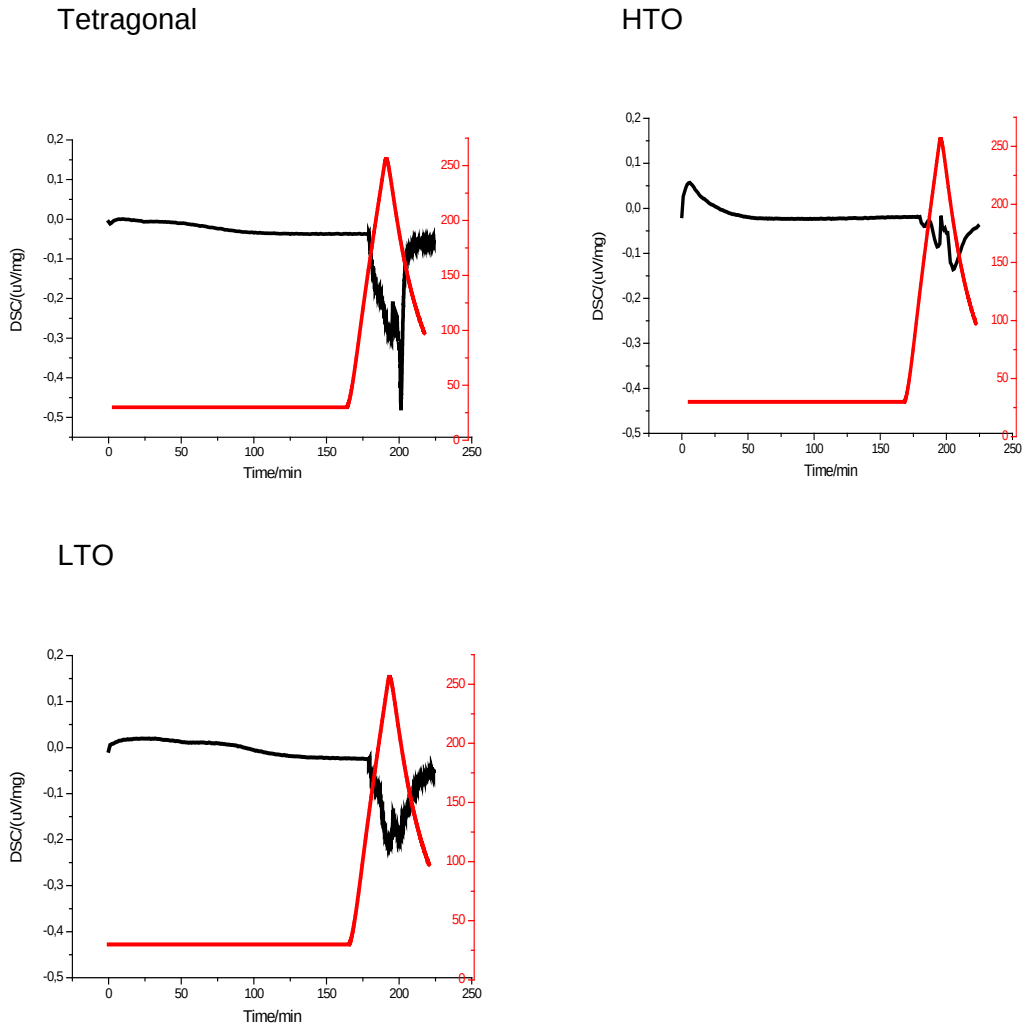

Figure 4.2.3: DSC curves of fresh Tetragonal, HTO and LTO lysozyme crystals; temperature profile starts with an isothermal phase (at 30 ˚C for 3 h), followed by a dynamic phase (10 K/min up to 250 ˚C).

Tetragonal

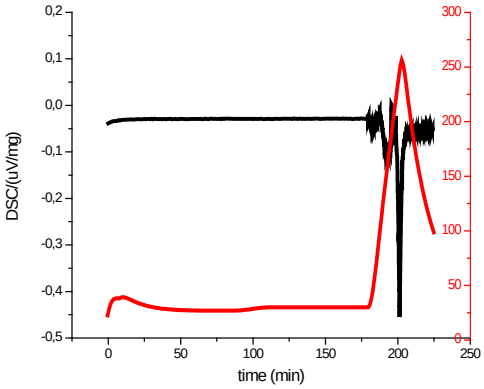

HTO

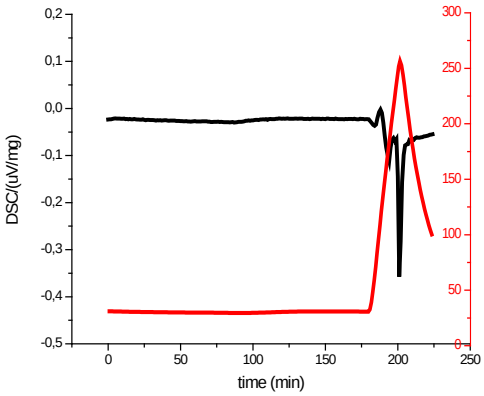

LTO

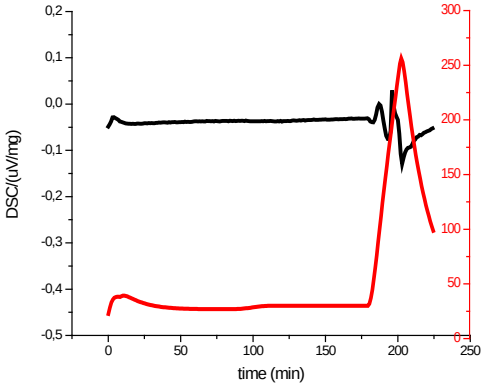

Figure 4.2.4: DSC curves of air-dried Tetragonal, HTO and LTO lysozyme crystals; temperature profile starts with an isothermal phase (at 30˚C for 3 h), followed by a dynamic phase (10 K/min up to 250 ˚C).

Table 4.2.10: Average decomposition temperature of fresh and air-dried Tetragonal, HTO and LTO lysozyme crystals.

Lysozyme crystal morphology	Decomposition temperature [˚C] for fresh lysozyme crystals	Decomposition temperature [˚C] for air-dried lysozyme crystals
Tetragonal	251	251
HTO	253.3	251
LTO	252.6	252.3

▪ *Thermal analysis by TGA*

A common technique to determine thermal effects such as the loss of weight (e.g. the solvent water) and the stability of a compound when exposed to heat is TGA, thermo gravimetric analysis. TGA curves achieved for fresh and air-dried lysozyme crystals are plotted by the black line versus time, Figures 4.2.5 and 4.2.6. Same trend is observed for all samples. The red line displays the temperature profile. The TGA curves of fresh and air-dried lysozyme crystals form three clear steps. The steps are pointed out by the Tetragonal sample. The shown steps refer to the loss of weight during the first isothermal phase and the second dynamic heating phase. The steps of weight loss arise from evaporation during heating and represent the loss of water (buffer / solvent).

In Figure 4.2.5, first step, the isothermal phase, refers to the loss of “loose associated” / “free” water, whereas second steps, the heating phase, to the loss of “bonded” / “fixed” water of the crystal lattice. Further heating with temperatures above ˚200 leads to some additional loss of weight during decomposition.

Figure 4.2.6 demonstrates mentioned three steps of weight loss, too, but obtained only from air-dried lysozyme crystals. Results presented show a smaller weight loss during the starting isothermal phase (first step) than observed for fresh lysozyme crystals. In the following, again a second step and the decomposition appear.

Tetragonal

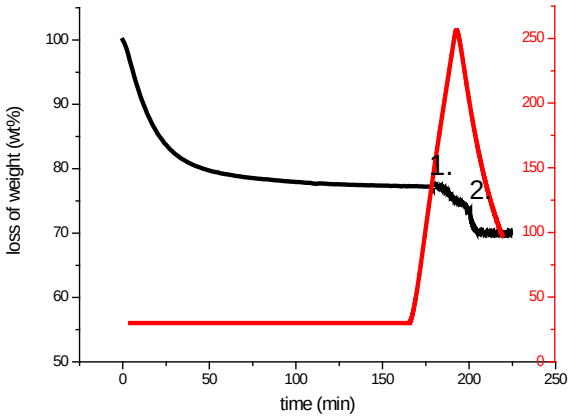

1. step: free water molecules (buffer)

2. step: bonded water molecules (crystal lattice)

→ further heating causes decomposition

HTO

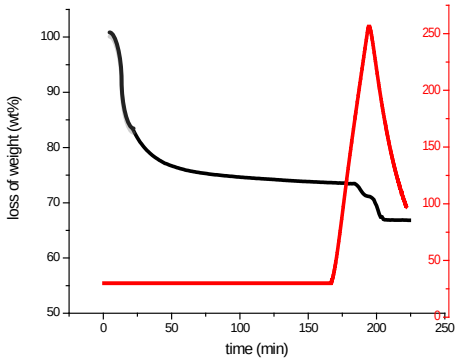

LTO

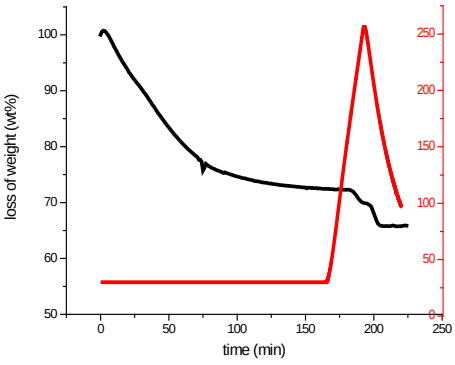

Figure 4.2.5: TGA curves of fresh Tetragonal, HTO and LTO lysozyme crystals; temperature profile starts with an isothermal phase (at 30˚C for 3 h), followed by a dynamic phase (10 K/min up to 250 ˚C).

Tetragonal

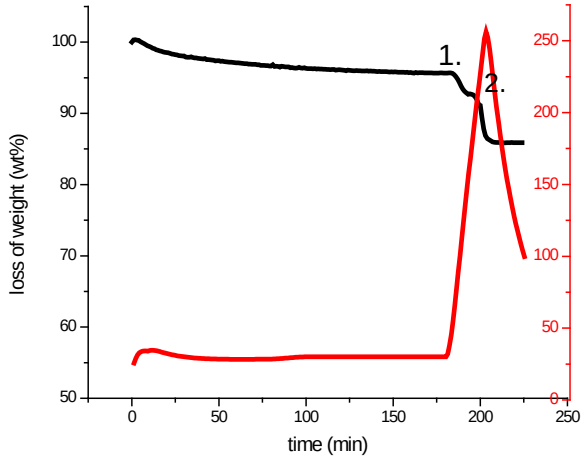

1. step: free water molecules (buffer)

2. step: bonded water molecules (crystal lattice)

→ further heating causes decomposition

HTO

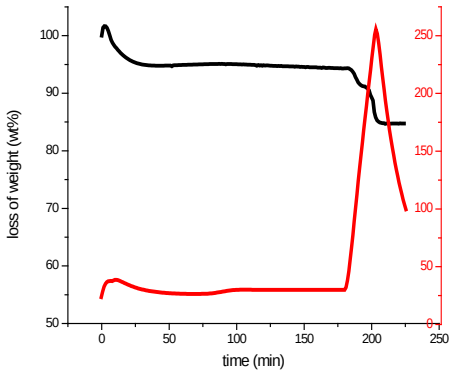

LTO

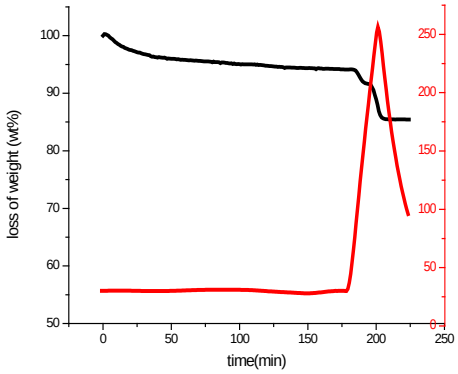

Figure 4.2.6: TGA curves of air-dried Tetragonal, HTO and LTO lysozyme crystals; temperature profile starts with an isothermal phase (at 30 ˚C for 3 h), followed by a dynamic phase (10 K/min up to 250 ˚C).

Summarized data of the loss of weight (loss of water) done for fresh and air-dried lysozyme crystals are illustrated in Figure 4.2.7. Figure 4.2.7 a) shows the total loss of weight which is equal to the total water content. Obviously, the fresh LTO morphology has the highest water content of about 41 %, whereas the fresh Tetragonal (30 %) and HTO morphology (26 %) have a much lower one. In contrast to the differences in the total water contents observed for fresh lysozyme crystals, the bound water content, which is part of the crystal lattice and

determined from air-dried lysozyme, crystals gives minor only differences (see Figure 4.2.7 b). For all three morphologies, the boned water content is in between 6.5 and 7 wt%.

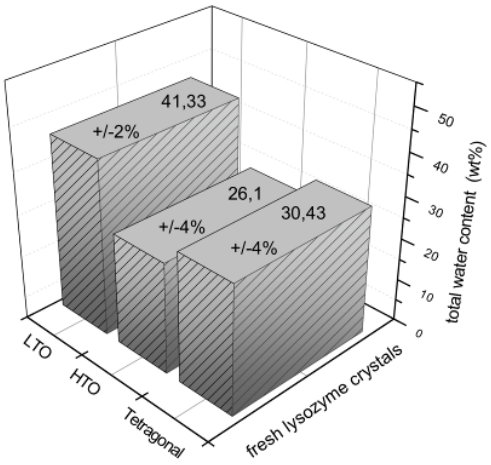

a)

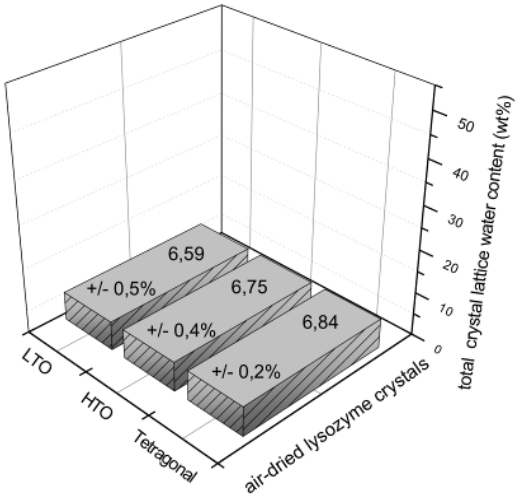

b)

Figure 4.2.7: Determination of the total water content of fresh (a) and air-dried (b) Tetragonal, HTO and LTO lysozyme crystals by the TGA method.

▪ *Chloride detection test, conductivity and pH*

A common method to analyze the chemical composition of substances, e.g. salt, is to determine the type of ions by ion specific detection / reaction tests. Among others, the ion specific reaction is based on precipitation that means very fast solid formation because of extremely low solubility.

Tetragonal, HTO and LTO lysozyme crystals produced using sodium chloride (see section 3.2.1) are tested for chloride ions using silver nitrate. To perform the chloride detection test, fresh lysozyme crystals are washed with sodium chloride free buffer and air-dried for 24 h. Afterwards, 0.16 g of dried lysozyme crystals are dissolved in 20 mL distilled water at room temperature. To initialize the chloride precipitation (see equation 4.2.1), a silver nitrate solution of 0.2 M is prepared and added by 1:1. If chloride ions are component of the lysozyme crystals, the chloride ions will be released in the distilled water during dissolution. The adding of silver nitrate should result in a white solid, silver chloride.

$$(\text{lysozyme})^{+/-} + 2Na^{+} + (CH_3COO)^{-} + Cl^{-} + Ag^{+} + (NO_3)^{-} \rightarrow \underline{AgCl} + (\text{lysozyme})^{+/-} + 2Na^{+} + (CH_3COO)^{-} + (NO_3)^{-} \quad (4.2.1)$$

As mentioned before, the lysozyme is crystallized by sodium chloride. Therefore, sodium chloride is dissolved in the buffer solution (before crystallization) and its conductivity is measured. Then, lysozyme is dissolved separately in the same buffer (without salt, before crystallization) and conductivity is measured as well. Afterwards, the salt-buffer solution becomes transferred into the lysozyme-buffer solution to initialize the crystallization process, the same procedure as described in Table 3.2.1.1. The conductivity of the mixture at morphology specific crystallization conditions and temperatures is taken after 24 h when lysozyme crystals developed. Comparing the conductivity before and after the crystallization process gives information whether the ions of the salt-buffer solution bind and/or are incorporate somehow in the lysozyme crystal after crystallization.

Experimental data of the conductivity measurements, which includes the pH control, are given for the crystallization of the Tetragonal and the LTO morphology generated by sodium, potassium and calcium chloride, and for the HTO morphology obtained from only sodium chloride. Chloride detection tests using silver nitrate and dissolved lysozyme crystals always resulted in a white solid (precipitate).
Table 4.2.7 summarizes first the conductivity and the pH of distilled water, pure lysozyme powder dissolved in distilled water and acidic acetate buffer. Data obtained show that pure lysozyme powder has no significant conductivity in distilled water. It also does not change the pH of distilled water. The pure acidic acetate buffer has a very low conductivity at pH5.
Section 1) of Table 4.2.7 shows the conductivity and pH values of the buffer-salt solutions before lysozyme is added, hence before crystallization of lysozyme. The conductivity varies depending on the buffer, the type of salt and the salt concentration. Adding the crystallizing agent (here the different salts) to the buffer solution did not change the pH of the buffer solutions.

Assuming that the influence of the buffer ions on the conductivity is insignificant, the conductivity of 1 µS/cm can be equivalent to 0.6 mg NaCl per L (kg) H_2O, mentioned in chapter 3.2.2. Sodium chloride concentration could be calculated with an error of less than 12 % using described correlation and conductivity data measured (see 1) in Table 4.2.7). The calculations show a trend which is in good agreement with the production conditions. Two calculation examples are given below:

Assumed correlation: *1 µS/cm = 0.6 mg NaCl /L H_2O*

1 mS/cm equivalent to 0.0006 g NaCl / mL

*X (NaCl in g/mL) equivalent 1 mS/cm * 0.0006 g NaCl /mL*

First example:

- ➔ example for acetic acetate buffer pH5 + 8 % NaCl which means 0.08 g NaCl /mL
- ➔ X = 118 * 0.0006 = 0.0708
- ➔ X = 0.0708 g NaCl /mL calculated shows a comparable trend to the production conditions that uses 0.08 g NaCl /mL; error of 11.5 %.

Second example:

- ➔ example for acetic acetate buffer pH5 + 12 % NaCl which means 0.12 g NaCl /mL
- ➔ X = 186 * 0.0006 = 0.1116
- ➔ X = 0.1116 g NaCl /mL calculated shows a comparable trend to the production conditions that uses 0.12 g NaCl /mL; error of 7 %.

Section 2) of Table 4.2.7 shows the conductivity after lysozyme is added, hence after crystallization is completed. Comparing the conductivities before (first section of Table 4.2.7) and after the lysozyme crystallization, an explicit decrease in conductivity is observed when crystallization finished. Changes in pH are neglectable small.
The last 3) part of Table 4.2.7 summarizes the investigations of the produced lysozyme crystals. The lysozyme crystals are air-dried and dissolved in distilled water. Before carrying out the chloride detection test, the solution pH of dissolved lysozyme crystals is determined. In the case of the lysozyme crystals produced using sodium chloride, the pH value of the distilled water, in which the crystals are dissolved, changed to a value comparable with the original buffer solution. If considering the pH change of distilled water for dissolved lysozyme crystals produced by potassium and calcium chloride, the pH values show similar trend but with a larger fault.
The chloride detection test using silver nitrate is positive for all lysozyme crystals investigated. White precipitate could be observed after transferring the silver nitrate solution into the lysozyme crystal containing solution.

Table 4.2.11: Experimental detection of chloride ions by $AgNO_3$ (0.2M), conductivity (of anions and cations) and pH at room temperature.

Sample	Chloride detection by $AgNO_3$ (0.2M)	Conductivity [$mS*cm^{-1}$]	pH-value
dist. water pure	-	0-1.7	5.75-6
20 mg lysozyme (HEWL) /mL distilled water	-	1.35	5.9-6
Acetic Acetate buffer 0.1 M, pH5	-	4.88	5
1) Before crystallization			
Acetic Acetate buffer 0.1 M, pH5, 8 % NaCl	-	118	5
Acetic Acetate buffer 0.1 M, pH5, 12 % NaCl		186	5
Glycine buffer 0.05 M, pH9.6-10, 8 % NaCl	-	117	9.6
Acetic Acetate buffer 0.1 M, pH5, 8 % KCl	-	117	5
Acetic Acetate buffer 0.1 M, pH5, 8 % $CaCl_{2*}2H_2O$	-	77	5
Glycine buffer 0.05 M, pH9.6-10, 8 % KCl	-	111	9.6
Glycine buffer 0.05 M, pH9.6-10, 8 % $CaCl_{2*}2H_2O$	-	75.3	9.6
2) After crystallization			
Tetragonal (NaCl)+ 100 mg HEWL /mL, after 24 h at 1-4 ˚C	-	65.5	-
HTO (NaCl)+ 100 mg HEWL /mL, after 24 h at 37 ˚C	-	78.1	-
LTO (NaCl)+ 100 mg HEWL /mL, after 24 h at 20-24 ˚C	-	62.7	-
(KCl)+ 100 mg HEWL /mL, after 24 h at 1-4 ˚C	-	59.5	-
($CaCl_{2*}2H_2O$) 100 mg HEWL /mL, after 24 h at 1-4 ˚C	-	42.3	-
(KCl)+ 100 mg HEWL /mL, after 24 h at 20-24 ˚C	-	53.4	-
($CaCl_{2*}2H_2O$)+ 100 mg HEWL /mL, after 24 h at 20-24 ˚C	-	39.1	-

3) Crystalline sample			
Tetragonal (NaCl) washed, air-dried and dissolved in dist. H_2O → 0.16 g/ 20 mL	positive, white precipitate	-	4.9
HTO (NaCl) washed, air-dried and dissolved in dest. H_2O → 0.16 g/ 20 mL	positive, white precipitate	-	5.1
LTO (NaCl) washed, dried and dissolved in dist. H_2O → 0.16 g/ 20 mL	positive, white precipitate	-	8.7
Tetragonal (KCl) washed, air-dried and dissolved in deist. H_2O → 0.16 g/ 20 mL	positive, white precipitate	-	4.4
Tetragonal ($CaCl_{2*}2H_2O$) washed, air-dried and dissolved in dist. H_2O → 0.16 g/ 20 mL	positive, white precipitate	-	4.4
LTO (KCl) washed, air-dried and dissolved in dist. H_2O → 0.16 g/ 20 mL	positive, white precipitate	-	8.1
LTO ($CaCl_{2*}2H_2O$) washed, air-dried and dissolved in dist. H_2O → 0.16 g/ 20 mL	positive, white precipitate	-	7.4

▪ *EDX*

Energy Dispersive X-ray analyses deliver results of detailed lysozyme crystal composition studies (see Figure 4.2.8). Two samples from the same Tetragonal crystal are taken, first of the crystal surface (left) and second of the interior (right) which is shown at the top of Figure 4.2.8. The two EDX patterns of the two samples are illustrating the data which are also summarized in the small tables of elements.
The EDX data obtained show differences in the crystal composition depending on where the sample is taken from. The sodium and the chloride concentration is considerably higher for the crystal interior than for the crystal surface (see tables of elements at the bottom of Figure 4.2.8). Same trend for inhomogeneous sodium and chloride distribution is expected for the HTO and the LTO morphologies.

Tetragonal crystal surface (1. sample)

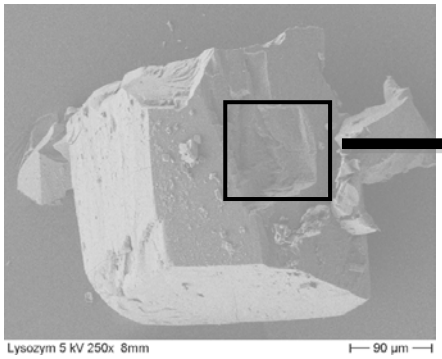

EDAX ZAF QUANTIFICATION STANDARDLESS SEC TABLE : DEFAULT

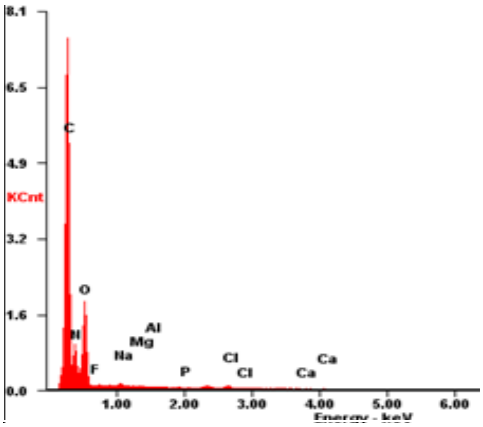

Element	wt%	at wt%
C K	63.90	70.16
N K	15.50	14.59
O K	16.40	13.51
F K	00.07	00.05
NaK	**00.39**	**00.22**
MgK	00.00	00.00
AlK	00.11	00.05
P K	00.00	00.00
S K	01.53	00.63
ClK	**02.00**	**00.74**
CaK	00.11	00.04

Tetragonal crystal interior (2. sample)

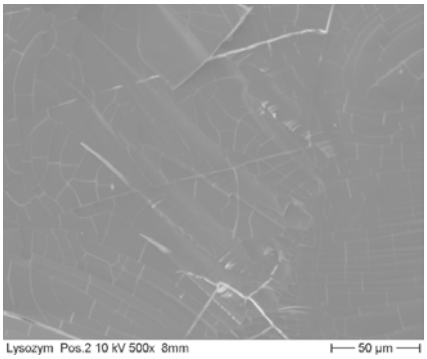

EDAX ZAF QUANTIFICATION STANDARDLESS SEC TABLE : DEFAULT

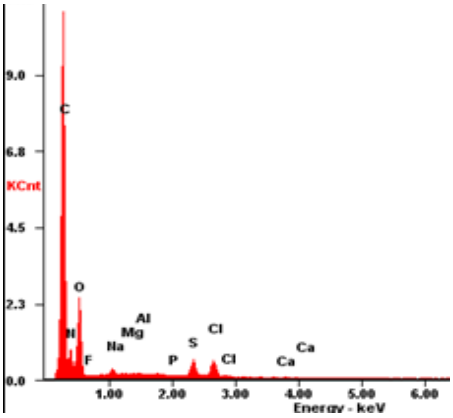

Element	wt%	at wt%
C K	63.53	70.54
N K	14.88	14.17
O K	15.12	12.60
F K	00.09	00.06
NaK	**00.58**	**00.34**
MgK	00.03	00.02
AlK	00.03	00.01
P K	00.02	00.01
S K	02.38	00.99
ClK	**03.28**	**01.23**
CaK	00.06	00.02

Figure 4.2.8: Elemental composition of the Tetragonal crystal surface and interior by EDX.

▪ *X-ray Powder Diffraction*

In present studies, structure information can be obtained from the peaks which are characteristically for the lysozyme. The location and the height / intensity of outstanding peaks give evidence for crystal components and their mass fraction. Generated XRPD pattern for air-dried Tetragonal, HTO and LTO crystals are presented in Figure 4.2.9.
The XRPD patterns of air-dried Tetragonal, HTO and LTO lysozyme crystals are noticable different. All three morphologies show a crystalline fraction which reaches approximately up to 10˚ theta, followed by an amorphous "hill". The lysozyme crystals also show three clear peaks at 27, 31˚ and 46˚. Mentioned peaks are characteristically for sodium chloride (visualized by black lines) that was used as crystallizing agent. The LTO crystal pattern gives the most intensive peaks, whereas the Tetragonal crystals the lowest.

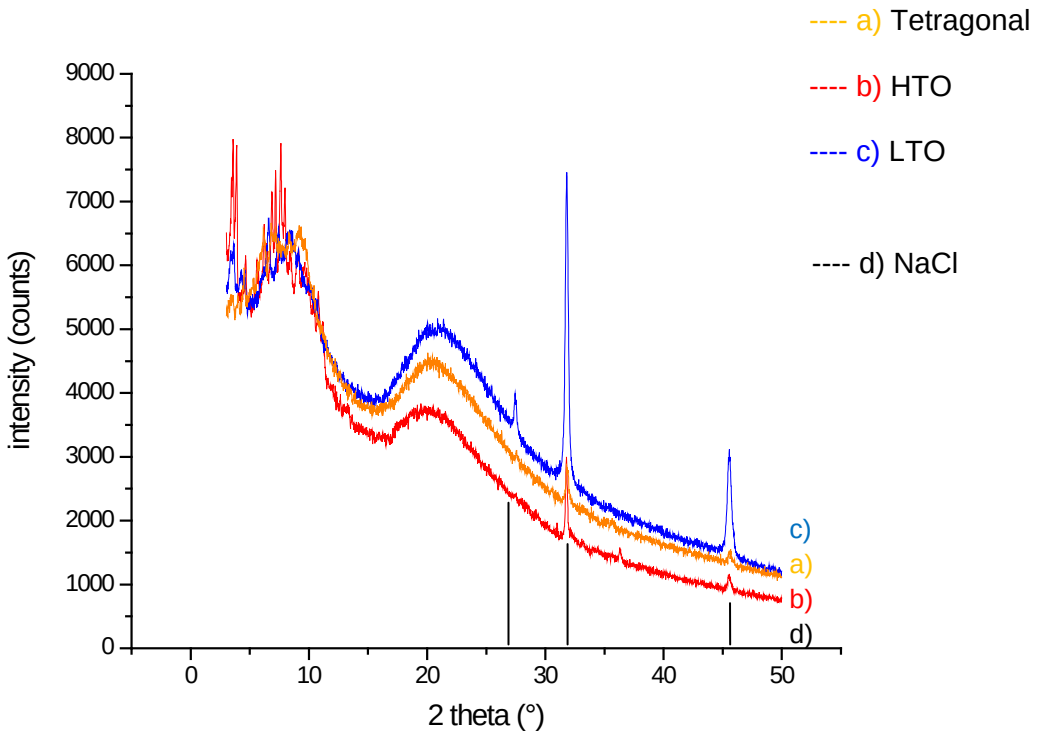

Figure 4.2.9: X-Ray pattern of air-dried lysozyme crystals.

▪ *Raman spectroscopy*

Present Raman-spectroscopy investigations study only the two different orthorhombic lysozyme crystals; the HTO and the LTO orthorhombic morphology (see Figures 4.2.10 to 4.2.11).

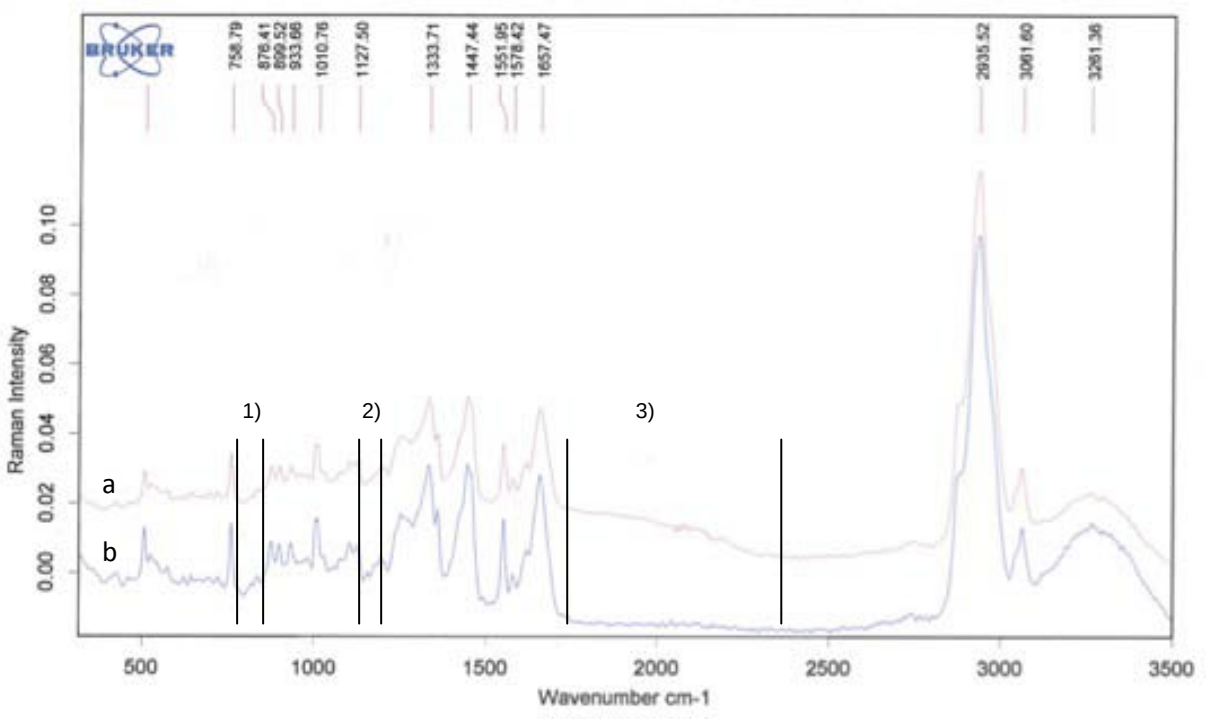

Figure 4.2.10: Raman pattern of fresh HTO (a) and LTO (b) crystals in aluminum pan (sample holder).

The Raman pattern (see Figure 4.2.10) of fresh HTO (a) and LTO (b) crystals displays few minor differences. Three regions named by 1), 2) and 3) show variations only in the peaks intensity. Peak intensities are higher for LTO than for HTO crystals. Figure 4.2.11 shows the Raman patterns of fresh HTO and LTO crystals when freeze-dried. Raman measurements in Figure 4.2.11 focus on the wave number range 400 to 1800 cm^{-1} where most peaks are observed. The Raman pattern of the freeze-dried HTO and LTO crystals again show minor differences, but two clear exceptions occur. Main difference is the extra peak located at wave number 1512 cm^{-1}, pointed out by the black line, which is not noticeable in Figure 4.2.10. The black line for wave number 1154 cm-1 marks a significant change of the peaks intensity than observed in Figure 4.2.10.

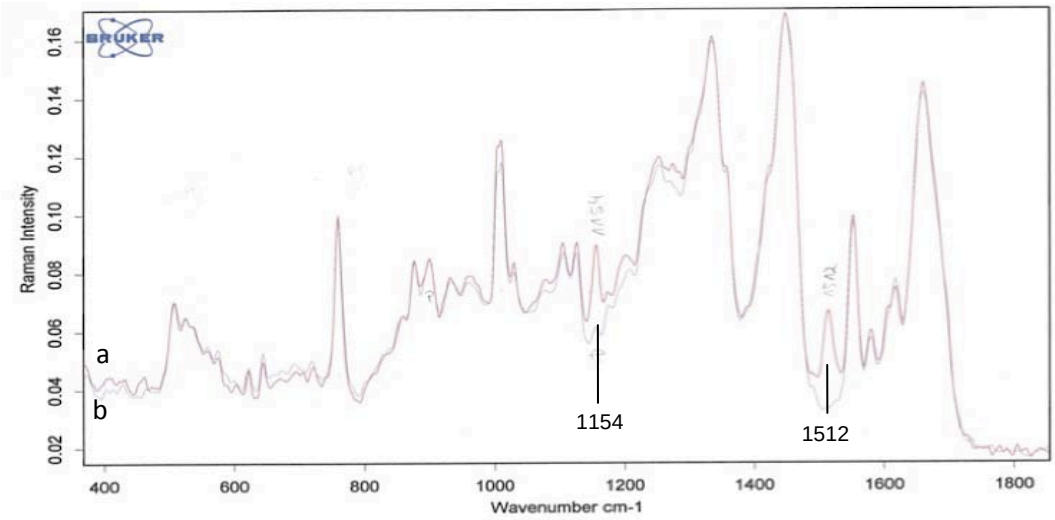

Figure 4.2.11: Raman pattern of freeze-dried HTO (a) and LTO (b) crystals in aluminum pan (sample holder).

▪ *IR spectroscopy*

Additional IR-spectroscopy could also detect differences between the HTO and the LTO morphology (see Figure 4.2.12). IR- spectra are plotted by ATR Units (intensity) versus wave number. Again, the HTO crystal morphology has an extra peak in the range of 1500 to 1520 cm^{-1}, similar as seen in Figure 4.2.11. The strong peak observed between the 3000 cm^{-1} and 3600 cm^{-1} also exists in Figure 4.2.10 but it is shifted towards lower wave numbers 2800 – 3000 cm^{-1}.

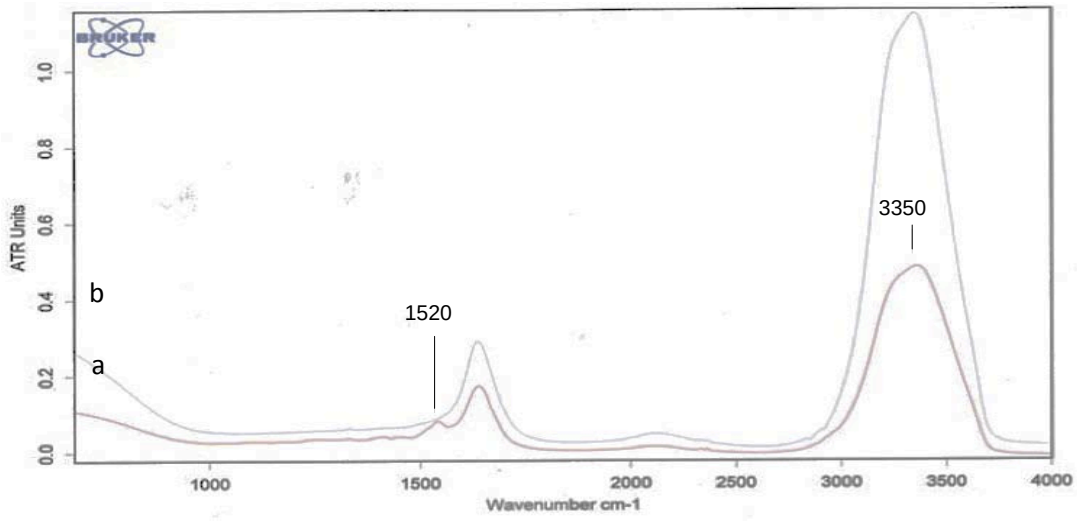

Figure 4.2.12: IR-spectroscopy pattern of fresh HTO (a) and LTO (b) crystals.

4.3 Solubility and dissolution of lysozyme crystals

4.3.1 Solubility

Solubility measurements are carried out under various conditions. Buffer solutions with different pH values and salt concentrations are prepared and placed into the tube system. A peristaltic pump ensures continuous circulation of the buffer solution through the tubes, the column and the flow cuvette. The extinction can be measured continuously using a UV / Vis photometer and recorded by computer.
Before starting the solubility measurement, lysozyme crystals are washed by pumping buffer solution through the column containing the crystals. Washing the crystals removes any adhering mother liquid which possible could change experimental conditions. Conditions for solubility measurements shown in chapter 4 results are marked with (*). Solubility data left out is summarized in the appendix A.2.

- *pH5.7 + *2, 3, 5 and *7 wt% NaCl
- *pH7 + *2, 3, 5 and *7 wt% NaCl
- *pH8 + *2, 3, 5 and *7 wt% NaCl.

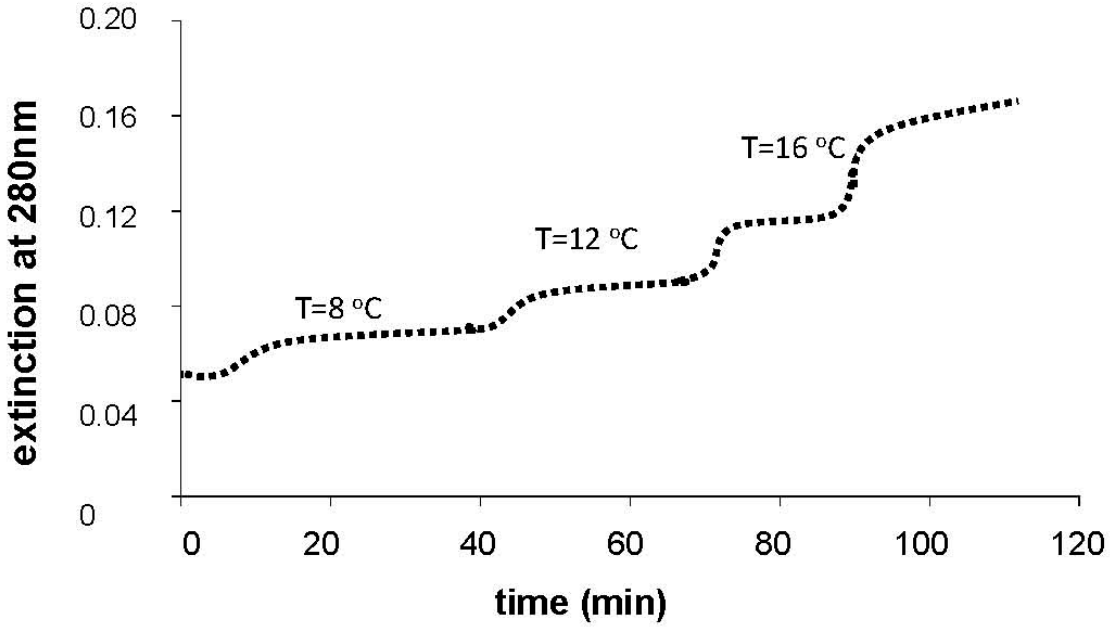

Figure 4.3.1.1: Exemplary solubility curve; extinction increases with increasing temperature.

For all solubility experiments, the measurement starts at low temperature. Temperature increase is arranged mostly in 4 K increments by a temperature controlled water bath. Increasing temperature causes the lysozyme crystals to dissolve. Protein concentration within the tubes changes with time until reaching a constant level, which demonstrates the equilibrium at current conditions. The time required to achieve the equilibrium depends on the present temperature, the size and the amount of crystals placed into the column. Experimental data is monitored as shown exemplary in Figure 4.3.1.1.
Working with proteins in such continuously running system carries the risk of denaturation because of mechanical stress and possible high temperatures. However, a test performed by Aldabaibeh shows that the solubility measurement technique is safe and reproducible results can be obtained [ALD09a].

The solubility measurement occurs via flow cuvette inside a UV / Vis photometer. The photometer is not able to detect protein concentration directly, but it detects the extinction / absorbance of the protein containing liquid. Two flow cuvettes are taken with different path length of either 0.05 or 0.2 cm. Choosing the cuvette depends on the extinction and protein concentration expected. Dissolved proteins are able to absorb UV light at a maximum of 280 nm which is due to amino acids with an aromatic ring such as Tryptophan, Tyrosine, and Phenylalanine (see chapter 2.1). Therefore, extinction of lysozyme solutions is always measured at wavelength 280 nm. The obtained extinction values and the extinction coefficient (2.64 mL/mg*cm [SOP62]) build base for protein concentration calculations according to Lambert-Beer's law (see equation 4.3.1):

$$E = \varepsilon_{\lambda} * c * L \text{ [MYE01, AJE11].} \qquad (4.3.1)$$

For correct protein concentration calculations, a calibration curve has to be prepared. The calibration curve (see Figure 3.2.2.3) gives information about the linear relation between the extinction and protein concentration. Additionally, the linear part of the curve shows the validity of the extinction coefficient. If protein concentration gets to high, the deviation of the extinction coefficient becomes too large and protein concentration calculations loose in accuracy.

Results of the solubility measurements in this chapter are shown for following conditions: sodium acetate buffer of pH5.7 + 2 wt% and 7 wt% NaCl (see Figure 4.3.1.2), sodium phosphate buffer of pH7 + 2 wt% and 7 wt% NaCl (see Figure 4.3.1.3), and pH8 + 2 wt% and 7 wt% NaCl (see Figure 4.3.1.4). Solubility data given for Tetragonal lysozyme crystals were measured in previous studies by Aldabaibeh [ALD09a] and used to complete the clarity and understanding of lysozyme crystal solubility.
In Figures 4.3.1.2 to 4.3.1.4, the effect of temperature as well as the influence of an increasing salt concentration on the solubility of the Tetragonal, the HTO and the LTO lysozyme crystals is illustrated. The solubility of all three morphologies and at all buffer conditions increases with increasing temperature. The effect of temperature is less strong when salt concentration is increased to 7 wt%. Significant changes in the solubility of the lysozyme crystals are observed when salt concentration is increased, comparing the left (2 wt% NaCl) to the right (7 wt%) diagram of e.g. Figure 4.3.1.2. Same trend is observes for

higher pH conditions. Furthermore, comparing Figure 4.3.1.2 with Figures 4.3.1.3 and 4.3.1.4, shows the effect of an increased pH which also results in solubility decrease.
In general, the HTO morphology shows higher solubility values at low temperature than the Tetragonal morphology, whereas the Tetragonal has higher solubilities at higher temperatures. Both solubility curves (of Tetragonal and HTO crystals) cross each other at a certain temperature. The cross point demonstrates a theoretical possible transition or transformation point, which is at pH5.7 + 2 wt% approximately 16 °C, at pH7 + 2 wt% 17 °C and at pH8 + 2 wt% 18 °C. The cross or transition point is shifted to higher temperatures when pH and/or salt concentration is increased. More results on the transformation of lysozyme crystals are illustrated by Aldabaibeh [ALD09a].
The same solubility trend is recognized for the LTO morphology (see Figure 4.3.1.2 to 4.3.1.4). The solubility of the LTO morphology cannot be compared with the Tetragonal and HTO morphology, reasons will be given in the discussion chapter 5.2. LTO solubility shows an outstanding solubility decrease at temperatures between 15 and 16 °C, which again becomes constant with further temperature increase.

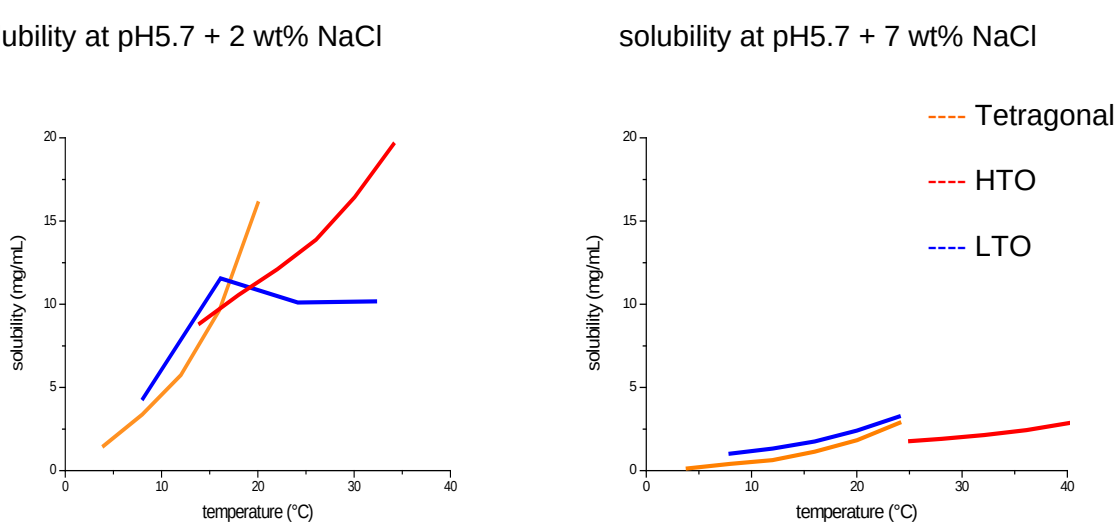

Figure 4.3.1.2: Solubility of lysozyme crystals at pH5.7 + 2 wt% (left) and 7 wt% (right) NaCl.

solubility at pH7 + 2 wt% NaCl

solubility at pH7 + 7 wt% NaCl

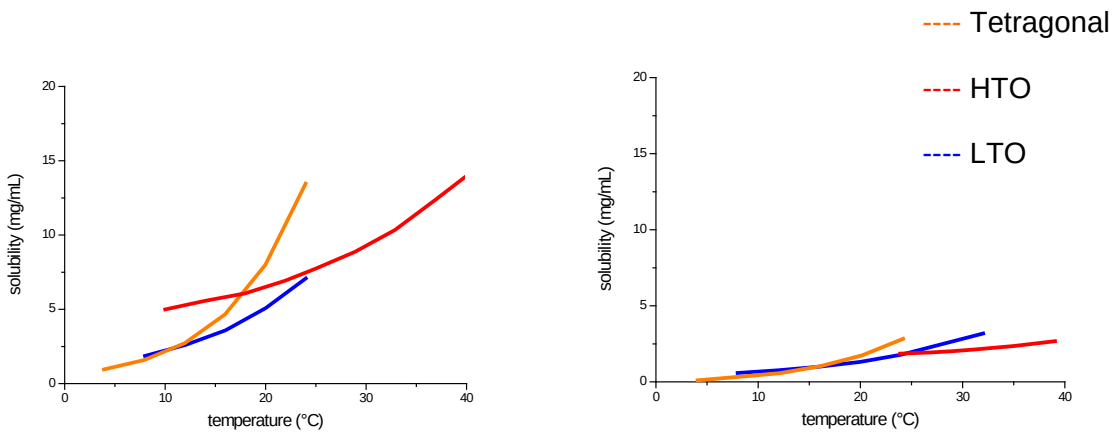

Figure 4.3.1.3: Solubility of lysozyme crystals at pH7 + 2 wt% (left) and 7 wt% (right) NaCl.

solubility at pH8 + 2 wt% NaCl

solubility at pH8 + 7 wt% NaCl

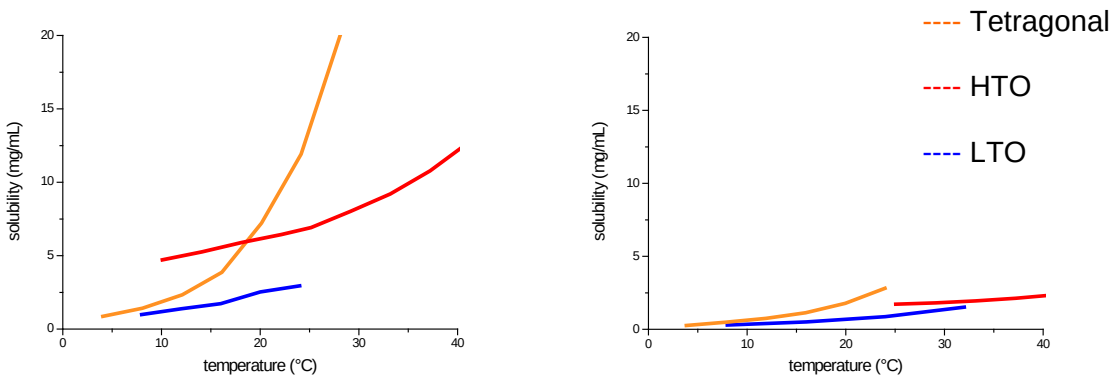

Figure 4.3.1.4: Solubility of lysozyme crystals at pH8 + 2 wt% (left) and 7 wt% (right) NaCl.

4.3.2 Dissolution

The dissolution observed for lysozyme crystals show an unusual dissolution behavior for Tetragonal, HTO and LTO lysozyme crystals. Pictures (see Figure 4.3.2.2 to 4.3.2.9) document the dissolution process over time.
For dissolution observation experiments, solution conditions change, but the temperature remains constant at 16 ˚C. One to three lysozyme crystals of the Tetragonal, HTO and LTO morphology are placed into the covered microscope cell filled with 3 mL solution. Using the software AnalySIS, photo series of dissolving lysozyme crystals are taken for further evaluation. A delay time of about 10 seconds before imaging the dissolution has to be taken into account. The magnification used in all experiments is 50 times. Defining the undersaturation of most shown experiments is not possible because of incomplete solubility data, which represents main disadvantage. Only conditions using buffer solution in the pH range of 5.7 to 8 and a sodium chloride concentration of 2 to 7 wt% solubility is known, see chapter 4.3.1 of solubility measurements. At these conditions the undersaturation can be defined. Resulting from this, dissolution times and rates cannot be compared. However, the lysozyme crystal behavior meaning the appearance of the lysozyme crystals during dissolution and its changes by altering conditions is focus of this chapter.

The dissolution of a sodium chloride crystal, which is illustrated by Figure 4.3.2.1, shows known dissolution behavior of inorganic crystals. The sodium chloride crystal dissolves in distilled water at room temperature. Before dissolution is initiated, the sodium chloride crystal has sharp and detailed edges. A sodium chloride crystal in distilled water which provides highly undersaturation conditions has to dissolve. Dissolution can be observed immediately by a rounding of the crystals edges. This rounding proceeds and the crystal becomes smaller until it completely disappears.

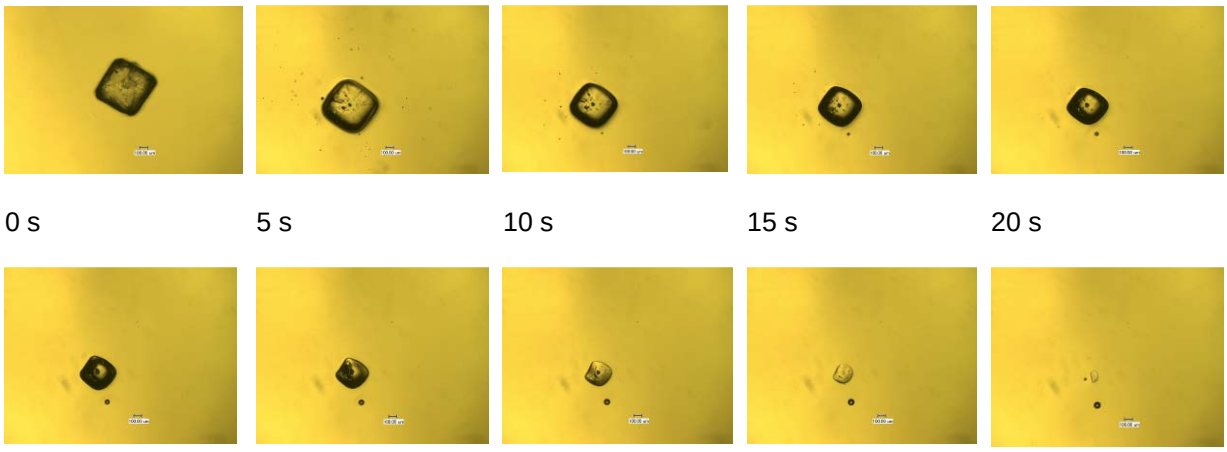

Figure 4.3.2.1: Dissolution behavior of a NaCl crystal at room temperature (20 °C) in distilled water.

Placing Tetragonal, HTO or LTO lysozyme crystals into distilled water, either at room temperature (20 +/- 3 °C) or controlled temperature of 16°C, again highly undersaturation conditions exist, but the crystals dissolve significantly different (Figure 4.3.2.2). The mentioned lysozyme crystals dissolve by falling apart into small irregular particles / crystal fragments. The resulting crystal particles, which look different in shape depending on the lysozyme morphology, dissolve separately. Figure 4.3.2.2 clearly shows how Tetragonal crystals fall apart into very small compact particles which remain the same at any studied dissolution conditions. The HTO crystals fall apart in bigger irregular fragments whereas the LTO crystals in needles.

Changing the dissolution conditions to a buffer solution at pH5.7 and 10 mg dissolved lysozyme at 16 °C (see Figure 4.3.2.3) has no effect on the dissolution patterns. The lysozyme crystals observed still fall apart in a skeleton-like crystal body as just described for conditions in distilled water. Same results are obtained when lysozyme concentration is increased to 50 mg/mL, not shown.

Tetragonal

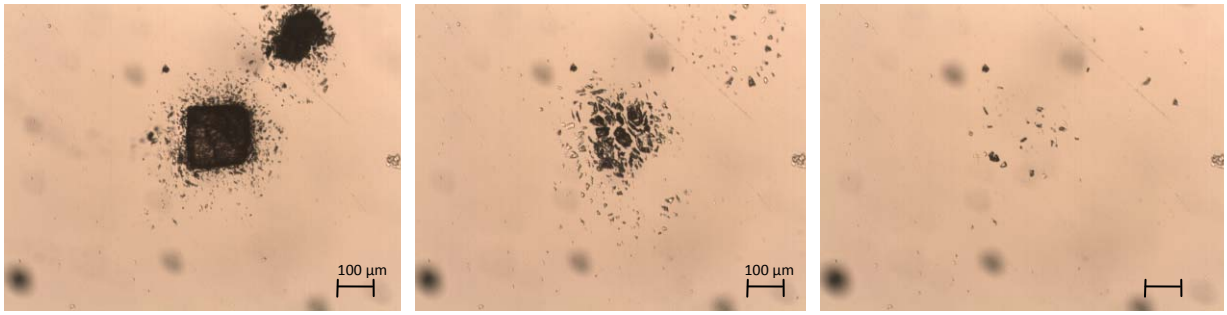

10 s 30 s 60 s

HTO

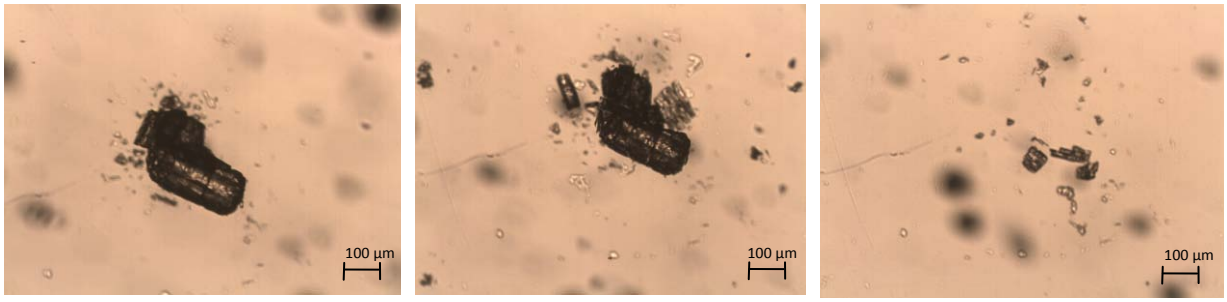

10 s 30 s 20min

LTO

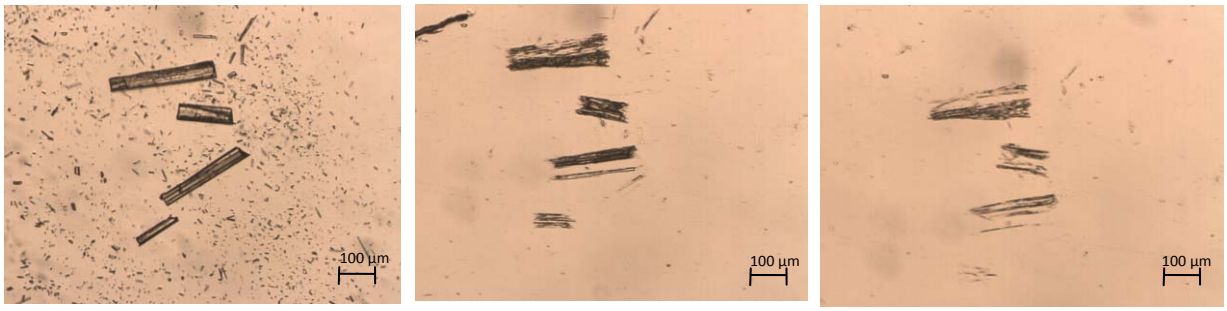

10 s 20 min 120 min

Figure 4.3.2.2: Dissolution behavior of lysozyme crystals at 16 ˚C in distilled water.

Tetragonal

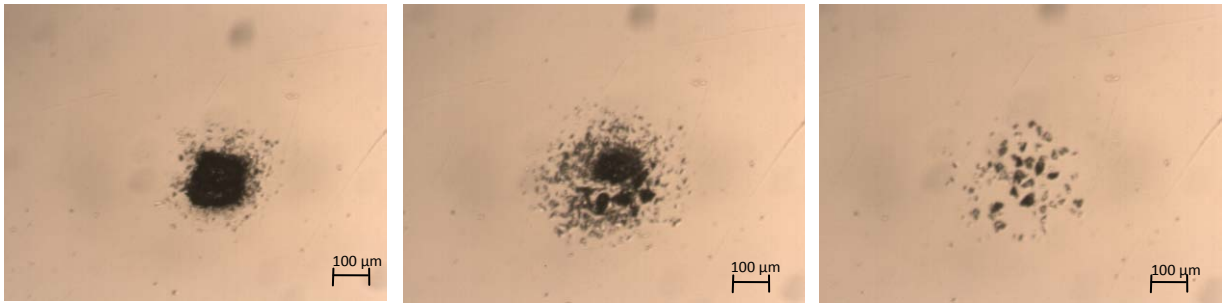

10 s 30 s 60 s

HTO

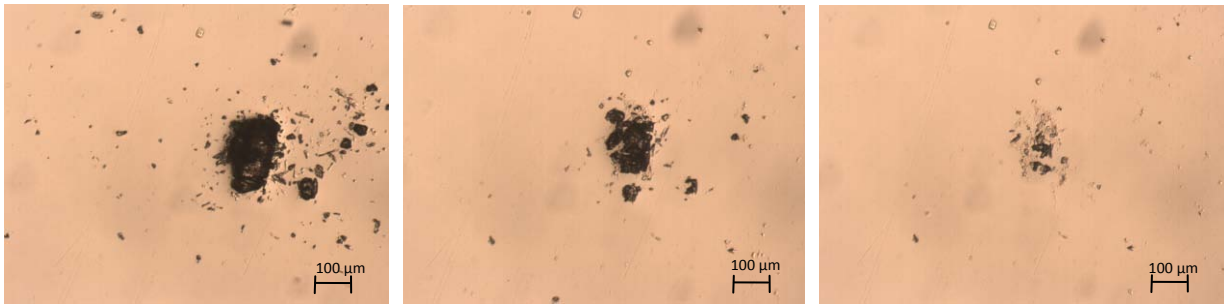

10 s 50 s 120 s

LTO

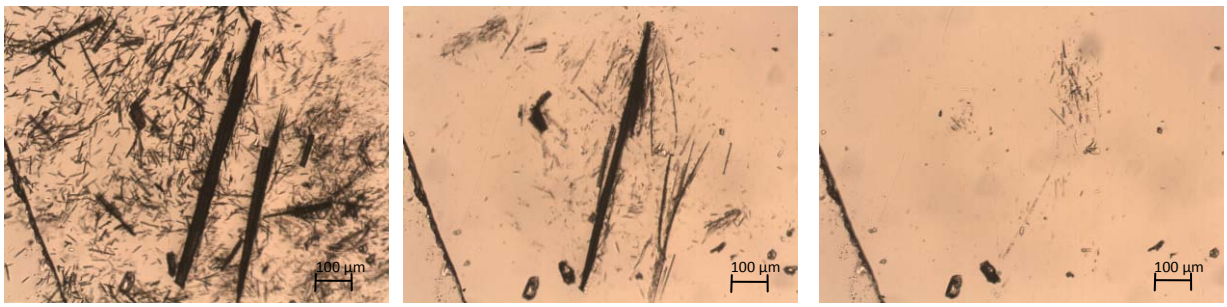

10 s 30 s 60 s

Figure 4.3.2.3: Dissolution behavior of lysozyme crystals in acetate buffer at pH5.7 + 10 mg lysozyme and 16 ˚C.

In the following, dissolution conditions are modified to the same conditions as used for the solubility measurements described above. Figure 4.3.2.4 illustrates the dissolution behavior at pH7 + 2 wt% NaCl and 16 ˚C). First significant difference in the dissolution pattern of the LTO morphology is recognized. The LTO crystals fall apart into a skeleton-like pattern with

many small “bars” arranged next to each other. No needles are noticed anymore. The small crystal “bars” dissolve again separately.

Tetragonal

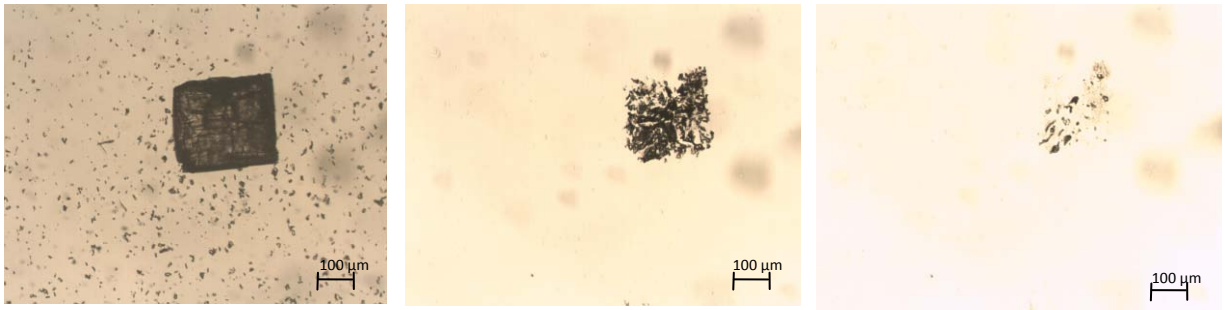

10 s 10 h 18 h

HTO

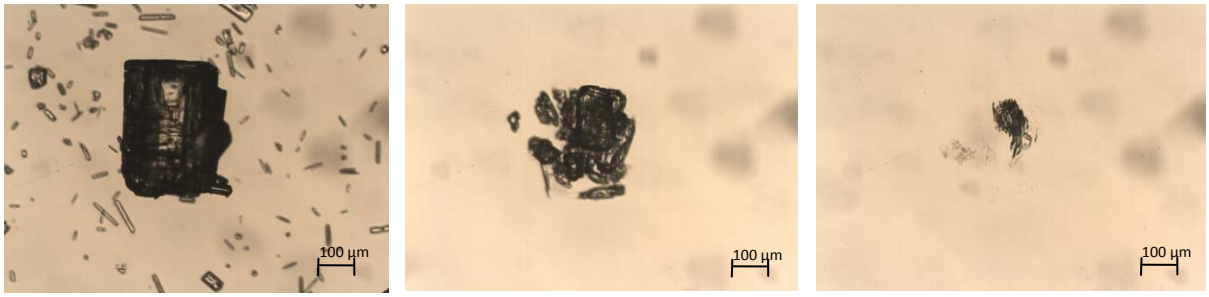

10 s 9 h 21 h

LTO

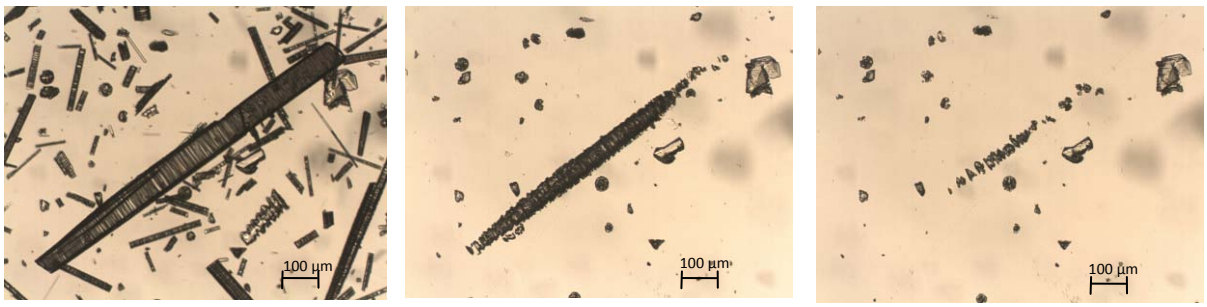

10 s 2 h 18 h

Figure 4.3.2.4: Dissolution behavior of lysozyme crystals in phosphate buffer at pH7 + 2 wt% NaCl and 16 ˚C.

Further increase of pH from 7 to 8 again causes noticeable changes in the dissolution behavior of the LTO lysozyme crystals (Figure 4.3.2.5). Contrary to Figure 4.3.2.4, the LTO crystals seem to dissolve “smooth” and equally. No falling apart is observed anymore but rounding of the crystal edges.

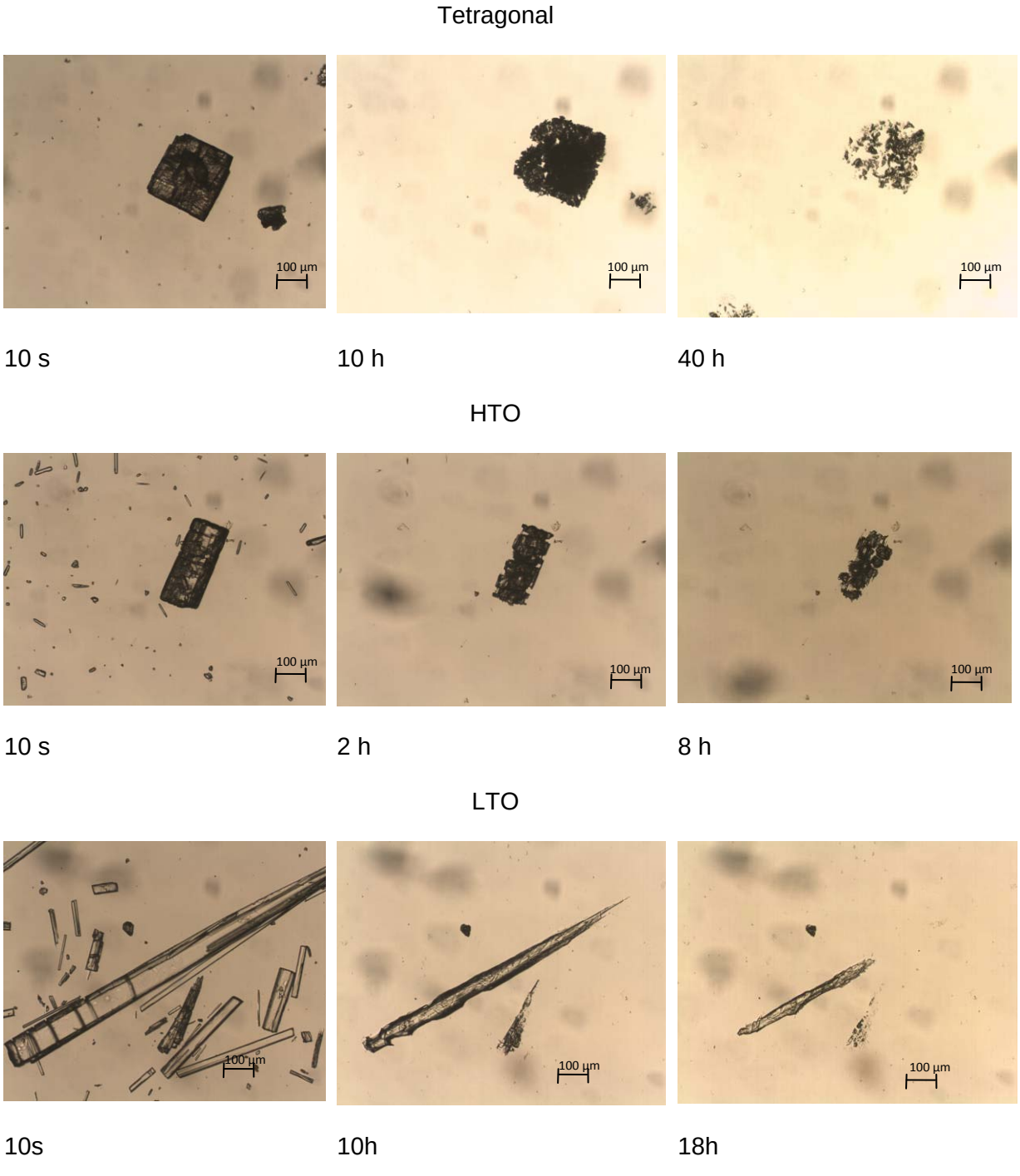

Figure 4.3.2.5: Dissolution behavior of lysozyme crystals in phosphate buffer at pH8 + 2 wt% NaCl and 16 °C.

Tetragonal

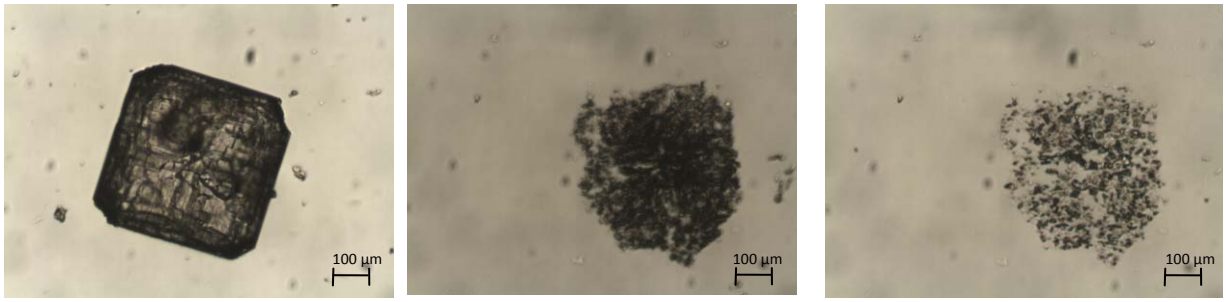

10 min 48 h 84 h

HTO

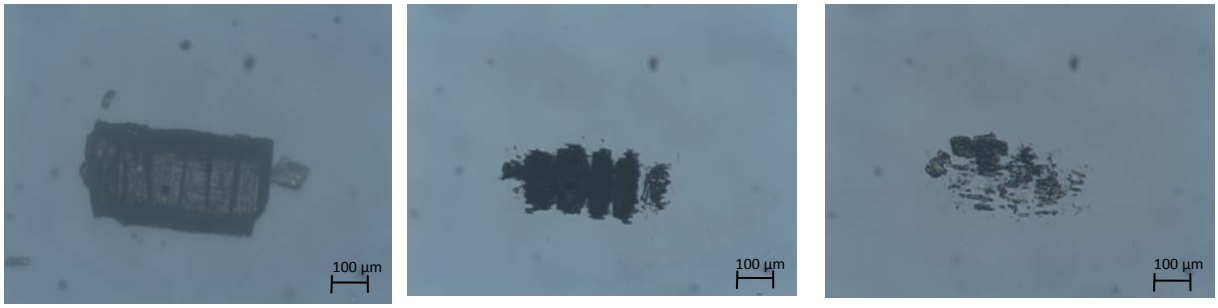

10 min 35 h 92 h

LTO

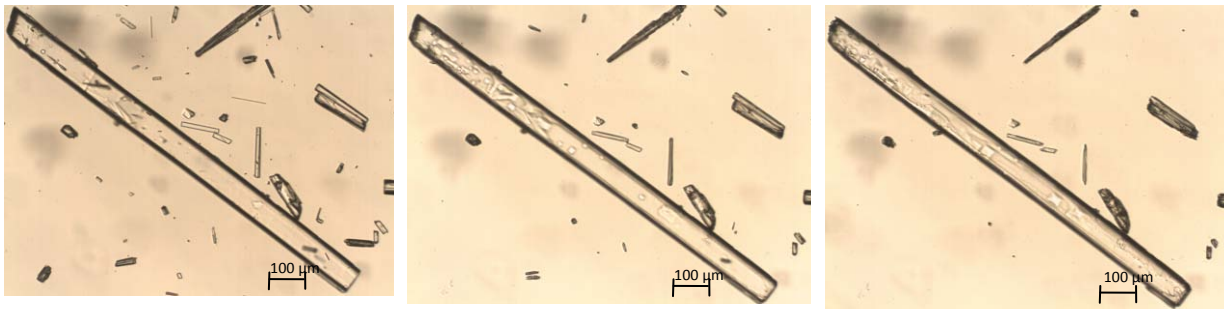

10 min 5 h 15 h

Figure 4.3.2.6: Dissolution behavior of lysozyme crystals in glycine buffer at pH10 + 7 wt% NaCl and 16 ˚C.

More dramatic changes in the dissolution behavior of HTO and LTO crystals are observed in a glycine buffer at pH10 + 7 wt% NaCl. Comparable with the LTO crystals in Figure 4.3.2.4, the HTO crystal shows big “bars” lined up but the “bars” also include small irregular particles. An influence of increased pH and salt concentration becomes very obvious for the LTO and

the HTO morphology. At the very high pH conditions, the LTO crystal does not show any dissolution anymore (see Figure 4.3.2.6).

In the Figures 4.3.2.2 to 4.3.2.6 summarized dissolution behavior of the HTO and LTO crystals give evidence for a significant influence of pH and salt concentration, which seems to be not the case for the Tetragonal crystals.

Screening “spot-tests” studied the possible effects more detailed. Dissolution test in Figure 4.3.2.7 are carried out for all three lysozyme morphologies with pure buffer solutions at a) pH5.7 (first column), b) pH7 (second column) and c) pH10 (third column). In general, the pure buffer at pH5.7 results in the same dissolution appearance as seen before in Figure 4.3.2.4. The allover dissolution behavior of Tetragonal lysozyme crystals remain the same like observed under previous conditions, even at pH10. The HTO morphology shows a different dissolution pattern when exposed to pure buffer with pH10 than at pH10 with 7 wt% NaCl. The formation of big “bars” is not recognizable. Again, the same dissolution behavior of the LTO morphology, which means the “smooth” dissolution behavior, appears at pH8 which is observed in Figure 4.3.2.5, too. At pH10, the LTO dissolution pattern is difficult to evaluate because a few LTO crystal stacked together are observed. Some parts of the crystal bundle seem to be rounded.

a) pH5.7 b) pH8 c) pH10

Tetragonal

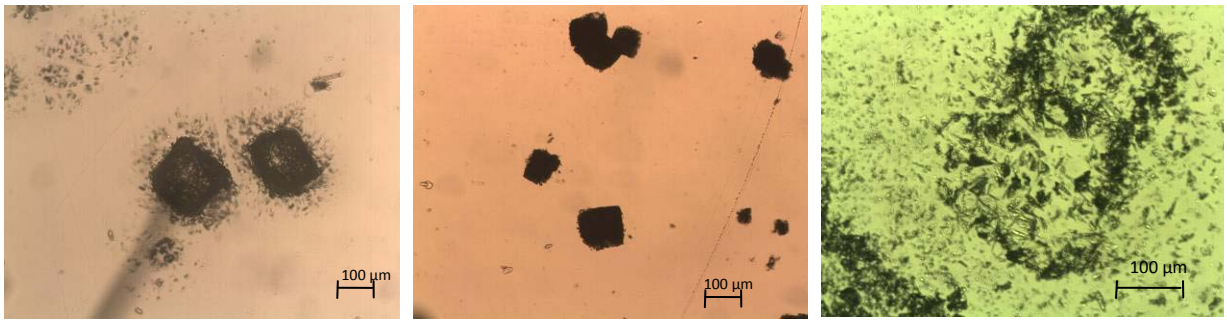

20 s 4 min 4 h

HTO

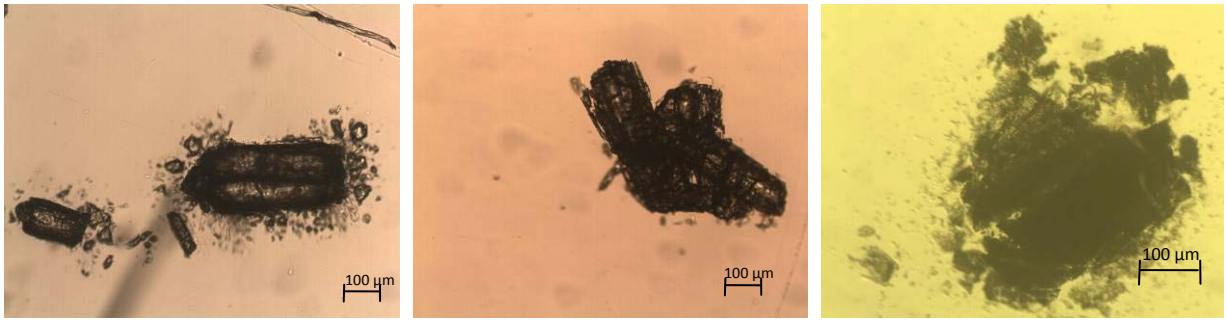

20 s 6 min 8 h

LTO

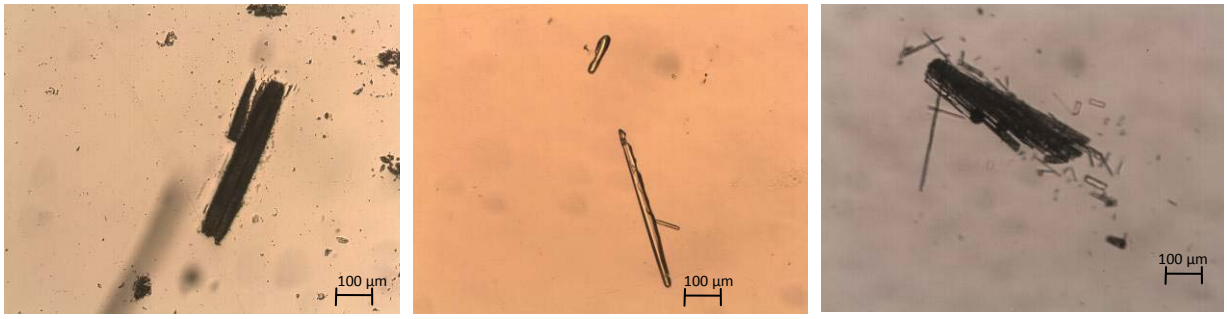

30 s 40 s 1 h

Figure 4.3.2.7: Dissolution behavior of lysozyme crystals in pure buffer at a) pH5.7, b) pH8, c) pH10 and 16 °C.

Additional “spot-tests” regarding the influence of temperature on the LTO morphology during dissolution at constant undersaturation are shown in Figure 4.3.2.8. No effect of temperature, either at 16 or 32 °C, on the dissolution behavior of LTO crystals (the “falling apart”) is observed. They again dissolve as found in pure buffer pH8 and in buffer pH8 + 2 wt% NaCl.

a) LTO: pH8 + 3 wt% NaCl + 0.68 mg/mL lysozyme at 16 °C → S* = 0.5

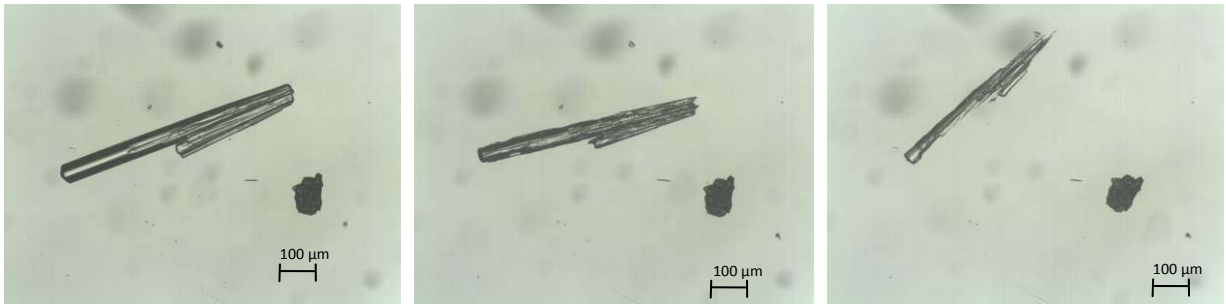

20 s 20 h 40 h

b) LTO: pH8 + 3 wt% NaCl + 2.99 mg/mL lysozyme at 32 °C → S* = 0.5

10 s 3 h 6 h

Figure 4.3.2.8: Effect of temperature on the dissolution behavior of LTO lysozyme crystals in phosphate buffer at pH8 + 3 wt% NaCl + a) 0.68 mg/mL lysozyme at 16 °C and b) 2.99 mg/mL lysozyme at 32 °C; a relative undersaturation of 0.5 exists in both cases.

Figure 4.3.2.9 summarizes the effect of varied controlled undersaturations at pH8 + 3 wt% NaCl on Tetragonal lysozyme crystals. Three undersaturations are adjusted according to previous measured solubilities. The dissolution behavior is observed at constant temperature (16 °C). Undersaturations are a) 0.5 (first row), b) 1 (second row) and c) 1.5 (third row). An increased undersaturation does not affect the dissolution behavior of Tetragonal lysotzyme crystals.

a) Tetragonal: pH8 + 3 wt% NaCl + 0.33 mg/mL lysozyme at 16 °C → S* = 0.5

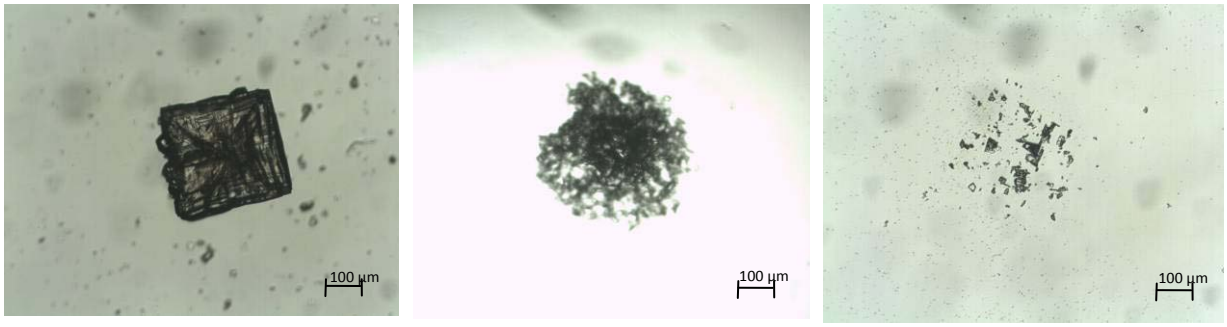

10 s 25 h 50 h

b) Tetragonal: pH8 + 3 wt% NaCl + 1.33 mg/mL lysozyme at 16 °C → S* = 1.5

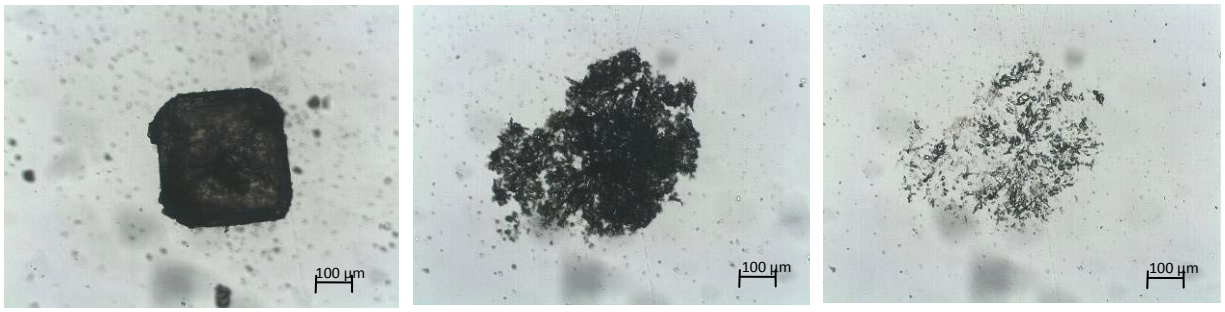

10 s 87 h 275 h

c) Tetragonal: pH8 + 3 wt% NaCl + 1.83 mg/mL lysozyme at 16 °C → S* = 2

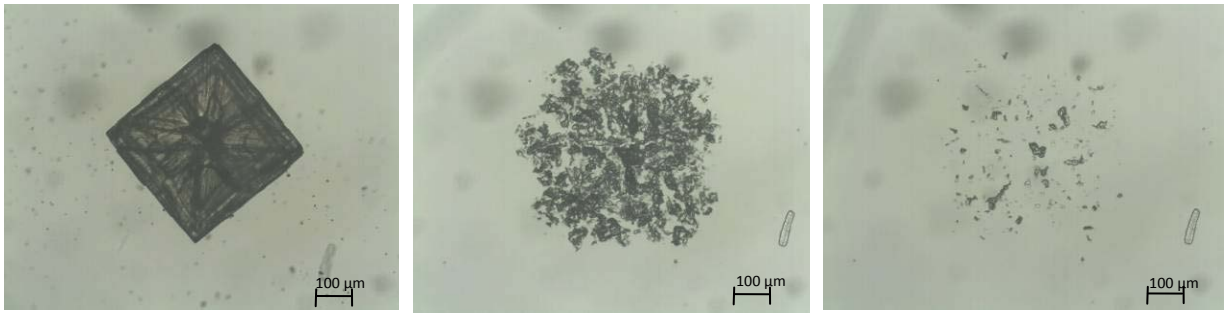

10 s 87 h 150 h

Figure 4.3.2.9: Effect of undersaturation on the dissolution behavior of Tetragonal lysozyme crystals in phosphate buffer at pH8 + 3 wt% NaCl + a) 0.33 mg/mL lysozyme → S* = 0.5; b) 1,33 mg/mL lysozyme → S* = 1,5; c) 1,83 mg/mL lysozyme → S* = 2; constant temperature at 16 °C.

5. Discussion

5.1 Lysozyme crystals

The basic question is how to describe protein crystals correctly. Investigations on the example of lysozyme crystals of different morphologies regarding their structure and properties lead to a more detailed insight.
Starting investigations focus on the detailed and clear description of different lysozyme crystal morphologies. Three lysozyme crystal morphologies that can easily be reproducible generated are used as representatives for protein crystals.
Crystallization of lysozyme is carried out in a batch using sodium chloride as crystallizing agent. Crystal morphologies obtained and used for further analytical studies are named Tetragonal, HTO (high temperature orthorhombic) and LTO (low temperature orthorhombic). In addition, screening test with different salts also resulted in crystalline lysozyme of either Tetragonal or orthorhombic shape. It was found that known crystallization conditions to produce Tetragonal, HTO and LTO lysozyme chloride crystals can only be transferred in some cases to other crystallizing lysozyme – salt systems. The influence of the cations or anions and their ionic strength as well as their valences is consistent with literature, e.g. [BEN02, GUI92, RET02, RET97, MCP99].

The terms polymorphism and solvates, described in chapter 2, have to be discussed in connection with protein crystals, here lysozyme crystals, too. Polymorphism among protein crystals has to consider a multi-component system of minimal four components (protein, crystallizing agent, buffer salt and water), see chapter 5.2. The established four parts of a protein crystal have consequences for the standard definition of polymorphs and solvates with respect to protein crystals.
Due to the fact that Tetragonal and HTO are produced by a different solvent than LTO, in present case a different buffer solution, the resulting chemical composition won't be identical anymore. This becomes even more clear after the removal of the water (e.g. drying the lysozyme crystals), because the salts of the buffer will remain inside the crystal. Consequently, in present work the Tetragonal and the HTO lysozyme crystal morphologies, produced in same actetate pH5 buffer solution could be first understood as polymorphs or solvates whereas the LTO crystals (glycine buffer pH9.6) are chemically different and definetly no polymorph.
Since not only the water content is, however, different within the Tetragonal and the HTO crystals (see Figure 4.2.7) they are also not polymorphs but still solvates. However, the word hydrate is only correct, if the "free" water is the same in the amount and only the bonded water amount is different. This is not the case. Hence the Tetragonal and the HTO crystals are no "classic" solvates anymore.
The existing differences in morphology of the lysozyme crystals, shown in Table 4.1.1, are proven by crystallographic data summarized in Table 2.6.1 obtained from Aldabaibeh [ALD09a]. Aldabaibeh did crystallographic studies on the Tetragonal, HTO and LTO morphologies by single crystals diffraction experiments. The results of Tetragonal and HTO crystals in Table 2.6.1 are in good agreement with recorded crystallographic data by e.g. Vaney [VAN01] and Matsuura [MAT03].

Generally, the Tetragonal, HTO and LTO morphologies show clear differences in the crystal lattice parameters (crystallographic data). The LTO morphologies produced at pH9 and 10 show almost identical lattice data. This leads to the assumption that the LTO crystals produced at pH9.6 also show same crystallographic data. At the same time, this demonstrates that crystallization close to the isoelectric point of lysozyme (pI 11 – 11.5) and the resulting crystal lattice are less sensitive to minor changes in solution pH +/- 1. However, this cannot be generalized. A possible effect of even such small changes on the crystal lattice should not be excluded at current state.

5.2 Analytics of lysozyme crystals

To describe protein (lysozyme) crystals correctly, the assumed main crystal components (the macromolecule, water, buffer+counterion, precipitant [PUS02]) have to be proven. In the following, analytics carried out with the example of lysozyme crystals will demonstrate that the Tetragonal, HTO and LTO morphologies presented consist of four main components such as:

1) the lysozyme (protein),

2) the acetate or glycine buffer solution (water and buffer salt),

3) the water (crystal lattice), and

4) the salt, in present study sodium chloride (crystallizing agent).

Lysozyme crystal components are explicit detected by simple analytics which will be described in the following.

1) The lysozyme (protein)

The protein content of lysozyme crystals is first analyzed by lysozyme concentration determination and lysozyme activity (specific activity). A simple technique for fast protein concentration measurements is carried with a spectrophotometer. This technique bases on the fact that lysozyme (generally proteins) contains aromatic amino acids (phenylalanine, tyrosine, and tryptophan) which absorb ultraviolet light at 280 nm [MCP99]. Salts in the buffer solution are negligible. Protein solutions e.g. lysozyme solutions have an extinction coefficient at E 280 nm, which is described in chapter 3.2.2 and for lysozyme estimated to be 2.64 mL/mg*cm [SOP62, BRO96]. The actual protein concentration of the lysozyme crystals can be calculated with measured extinction at 280 nm, the extinction coefficient and the Lambert-Beer's law [AJE11, MYE01]. The extinction values obtained from the optical enzymatic activity test using the micrococcus luteus as a substrate, see appendix A1, are used to estimate first the activity per volume which is given in Units per mL. Knowing the activity (U/mL) and the lysozyme concentration the specific activity (U/mg) of the lysozyme crystals is calculated, see equation 3.2.1 and 3.2.2, [MCP99].

As shown, crystallization of lysozyme is successful using different salts. Proteins without activity, either in native or crystalline state, are losing their relevance especially when it comes to biopharmaceutical – therapeutic proteins. Enzymatic activity tests for the Tetragonal, HTO and LTO lysozyme crystals showed always some activity loss. This is unpreventable because of the air contact of pure lysozyme powder (before crystallization) and the used batch crystallization methods. Depending on the crystallization conditions, thus the resulting morphology, and methods, the loss of activity can vary. Comparing the specific activities of the three lysozyme crystal morphologies, the LTO morphology shows the highest whereas the HTO crystals show the lowest specific activity. In contrast to own activity studies, Diaz-Borbon [DIA10] could prove a possible minimal specific activity loss when Tetragonal lysozyme crystals are produced by a freeze out protein crystallization technology, see Figure 5.2.1.

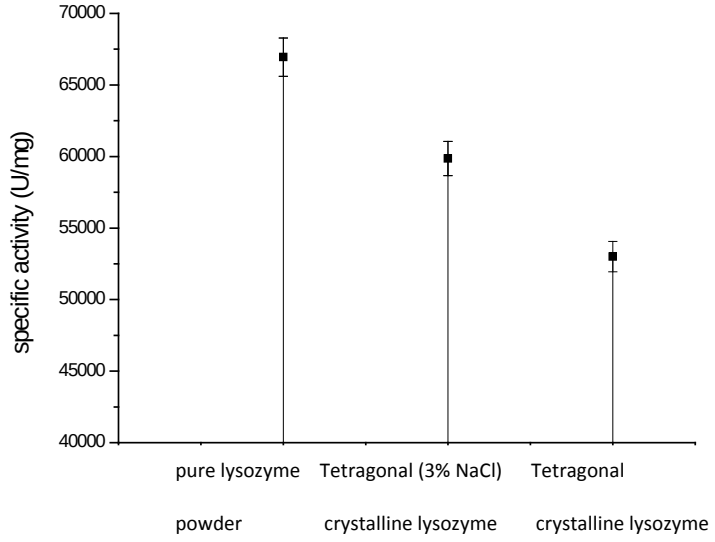

Figure 5.2.1: Specific activity of pure lysozyme powder, Tetragonal lysozyme crystals produced by a freeze out protein crystallization technology using 3 wt% NaCl [DIA10] compared with previous presented Tetragonal lysozyme crystal morphology.

Besides the elaborated influence of the crystallization conditions, the crystallization methodology and the temperature during long-term storage show an impact on the activity, too. HTO crystals are stored in a water bath at constant 37 °C, as used for the crystallization to avoid transformation. In contrast, the LTO (produced at room temperature of 20 °C +/- 3 °C) and the Tetragonal (4 °C) lysozyme crystals are kept in the refrigerator after the crystallization finished. Determined activities, which are higher for Tetragonal and LTO than for HTO crystals, show that the storage at low temperature for a long time is more convenient to preserve the enzymatic activity. Unfortunately, a discrepancy exists for storing

HTO crystals at low temperatures, because the risk of HTO transformation into a low temperature polymorph is high. Therefore, storing HTO at higher temperatures which cause activity loss has to be currently accepted.

2) The acetate or glycine buffer solution (water and buffer salt)

According to literature, protein crystals contain high amounts of water / solvent, starting from 30 up to 90 wt% [MCP98], same refers to lysozyme crystals.

The protein crystals including the lysozyme crystals are very soft which is expected to be the result of high water / solvent content and low binding energies [BER05]. With respect to their softness, it is even more interesting to observe the fracture behavior of lysozyme crystals by scanning electronic microscope (SEM) pictures. The broken crystal edges are of great value. The lysozyme crystals clearly show a fracture behavior which is extremely similar to the fracture behavior of sodium chloride crystals displayed by Ulrich [ULR81] or saccharose crystals by Fabian [FAB93]. From demonstrated fracture behavior high crystallinity could be assumed, but this questions the softness and the high water / high solvent content of the lysozyme crystals. The crystallinity can be determined and evaluated by powder X-ray diffraction which will be discussed later. To show and prove the high water / solvent content, different methods are tested as presented in chapter 4.2.

The solvent content of the lysozyme crystals is expected to come from two different sources. On the one hand, there is the buffer solution which is kept in crystal cavities (also called voids, pores or channels). On the other hand, there exists “fixed” water which is bound directly to the lysozyme molecules and therefore incorporated in the crystal lattice [MCP99] as known from conventional hydrates.

The existence of the “loose” associated water as part of enclosed solvent will be proven. Solvent inside of the crystals are located in crystal cavities or pores generated by the lysozyme molecule arrangement within the crystal lattice. To prove the enclosed solvent, the existing diffusion between the environmental solution and the lysozyme crystal cavities (pores) is visualized with the help of dyes. Similar experiments using bromphenol blue and bromphenol red are described by Nadarajah et al. [LIM98], but used to detect halide ions within the Tetragonal lysozyme crystal. Lysozyme crystals are stored in blue colored buffer solvent for minimal 24h. Expected diffusion of the blue dye inside the lysozyme crystal is supposed to cause a change of the natural colorless look. Using coomassie blue to color Tetragonal and HTO lysozyme crystals fails, whereas using methylene blue succeeds. Comparing both blue dyes, Figure 5.2.2 shows significant differences in the molecular weight, structure and size which give plausible explanation for successful or unsuccessful diffusion and the coloring.

Coomassie blue

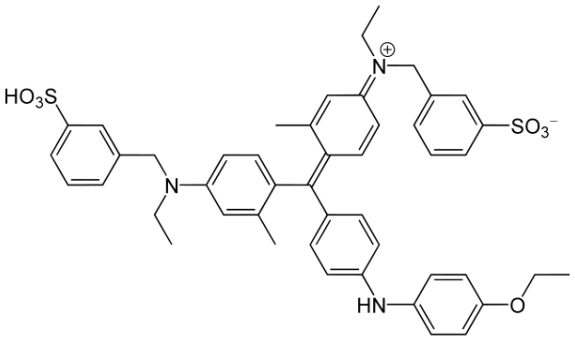

M = 825.97 g/mol

Methylene blue

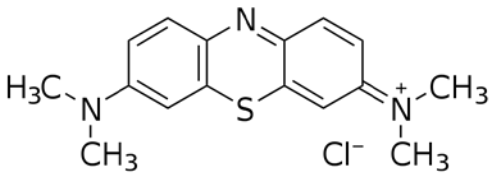

M = 319.85 g/mol

Figure 5.2.2: Molecular structure and weight of Coomassie blue [RÖM12] and Methylene [RÖM12] blue used for coloring lysozyme crystals.

The Coomassie blue molecule is a very large molecule if compared to Methylene blue and has an almost three times larger molecular weight. Hence, the Coomassie blue molecule seems to be too big to diffuse inside and to color the Tetragonal and HTO crystals. Obviously, the lysozyme crystals only can be colored if molecular weight, molecular structure meaning form (shape) and size of the dye are adequate to their pore (cavity) size.
More detailed explanation can be given with the help of simulation studies. Simulation studies on protein crystals, in general, present a crystal pore size (diameter) in the range of approx. 0.3 to 5 nm [MOR95] or 0.3 to 10 nm [MAL07, MAL11]. The molecule size of Coomassie blue is 2.66 x 1.62 nm (length x width) and much larger than Methylene blue which is 1.43 x 0.4 nm (length x width), shown in Figure 5.2.4. Obviously, if Methylene blue is capable of coloring the Tetragonal and HTO lysozyme crystals, their crystal pore size must have at least the size of the Methylene blue molecule. Hence, the pore size of Tetragonal and HTO crystals can be described with a diameter of minimal 0.4 nm and maximal 1.43 nm.
In contrast to Tetragonal and HTO lysozyme crystals, the LTO lysozyme crystals exposed to same Methylene blue dye could not be colored blue. The proof of existing diffusion by coloring of the LTO crystals is carried out differently. Therefore, a pH indicator Phenolphthalein is tested which is colorless in acidic and pink/red in basic conditions. The LTO crystals are produced in a basic glycine buffer causing inclusions of basic solvent. Thus, exposing LTO crystals to a Phenolphthalein enriched solution should result in pink colored crystals. Table 4.2.4 shows pink LTO crystals and delivers proof. Concluding from this, LTO crystals also contain high amounts of solvent likewise Tetragonal and HTO crystals. However, it is questionable why Methylene blues does not and Phenolphthalein does color the LTO lysozyme crystals. Obviously, diffusion and solvent exchange occur in both cases. The molecular weights of both molecules, Phenolphthalein (318,32 g/mol) and

Methylene blue (319.85 g/mol), are very similar and cannot be the reason for this observation.
The reason why LTO crystals could not be colored blue, but pink is explainable, however, by the pore size of LTO crystals, which obviously does not agree with the size and shape of the Methylene blue molecule, but with the size and shape of Phenolphthalein. To be more clear, Figures 5.2.3 and 5.2.4 show a more compact molecular structure of Phenolphthalein, if compared to Methylene blue. The estimated diameters of the Phenolphthalein molecule are 0.97 and 0.83 nm which is shorter than the length (1.43 nm) of Methylene blue. Thus, the pore diameter must be at least 0.83 nm. Furthermore, the pore and the channel shape which leads the solvent to the inside of the lysozyme crystals obviously don't match with the "long"-shape of the Methylene blue molecule. The same simulation studies as mentioned above [MAL07] also described that the pore and channel radius of orthorhombic lysozyme crystals are not constant. The channels show narrow zones due to the lysozyme molecules residues that reach inside the channels. This is the reason why the radius can vary from 0.95 nm to smaller than 0.82 nm [MAL07] and causes the channels to obtain a kind of "zick-zack" shape. Do to the fact that Methylene blue has a small width, diffusion could be expected. With respect to its length, Methylene blue is obviously not flexible enough to fit in the crystal channels, because of such "zick-zack" shape. Therefore, Methylene blue cannot diffuse inside the LTO crystals whereas Phenolphthalein can.

Phenolphthalein

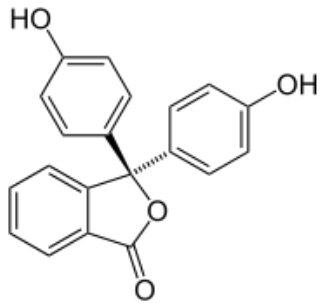

M =318.32 g/mol

Figure 5.2.3: Molecular structure and weight of Phenolphthalein used for coloring LTO lysozyme crystals [RÖM12].

Coomassie blue

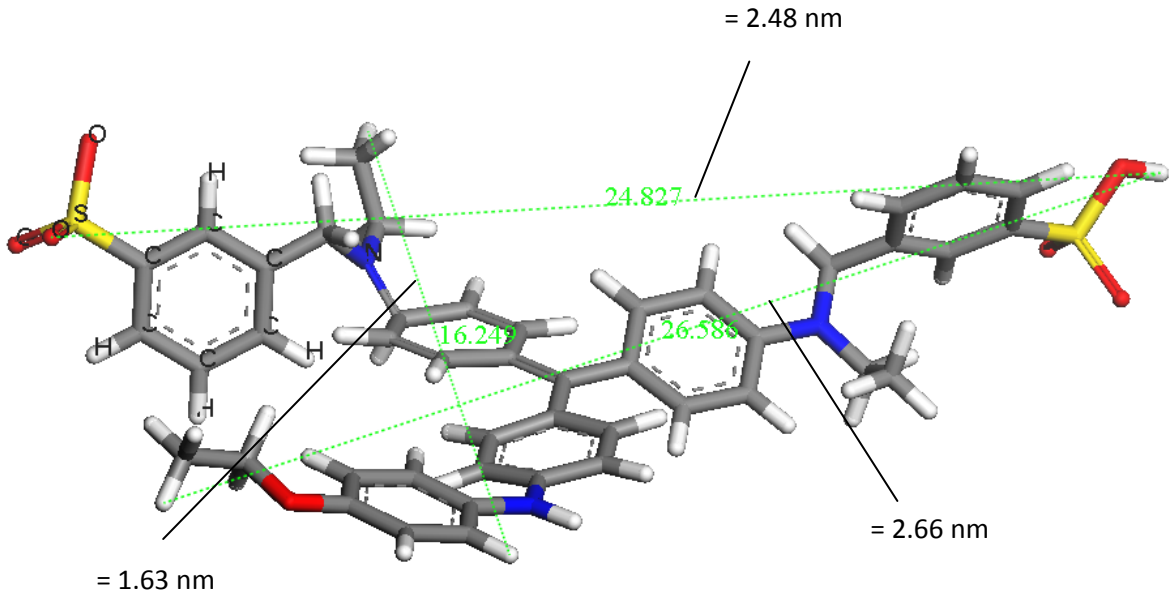

Methylene blue

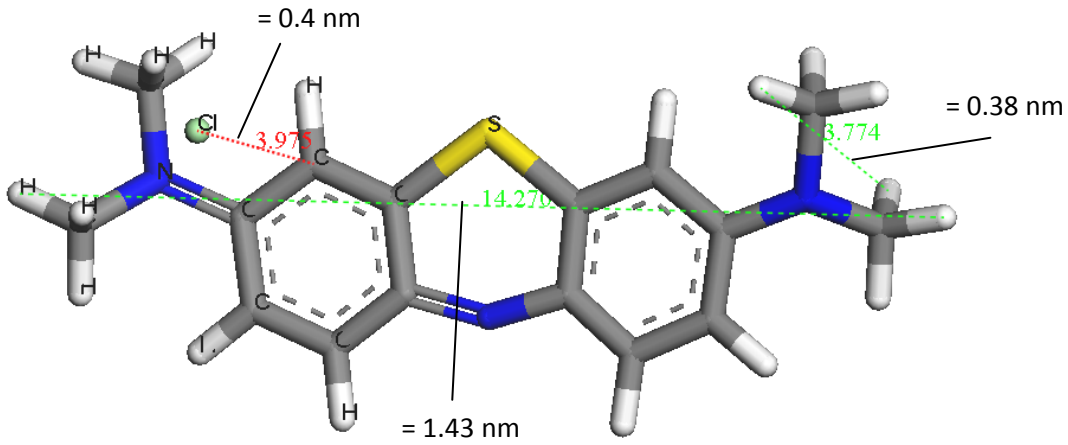

Phenolphthalein

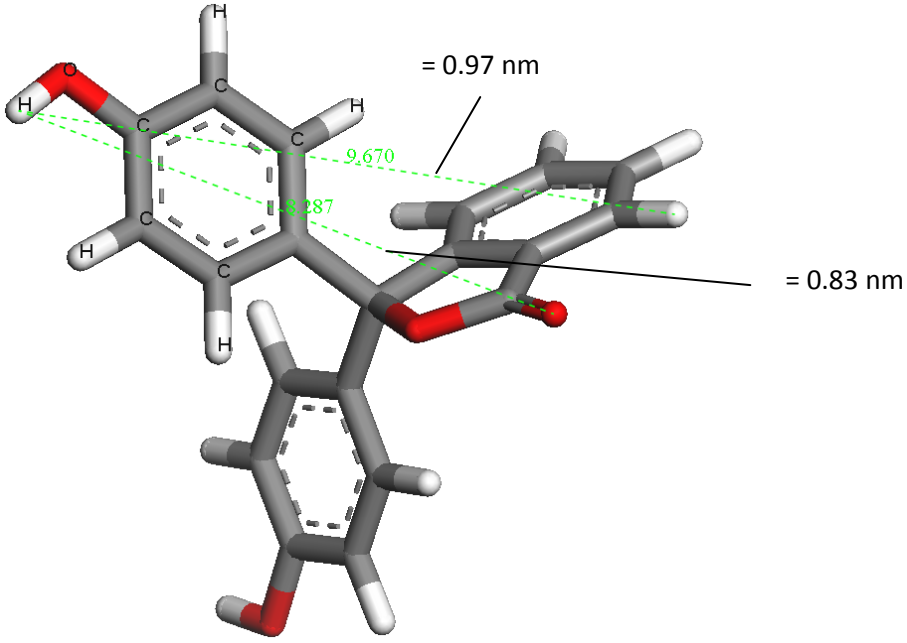

Figure 5.2.4: Molecular structure model of Coomassie blue, Methylene blue and Phenolphthalein; the light green dotted lines and the red one, respectively, represent the distances within the molecule in Angström [ACC05]; 1 Angström = 0.1 nm.

Discoloring experiments of lysozyme crystals are successful carried out and serve as another proof of existing diffusion processes. Completely colored and discolored lysozyme crystals are observed after 24 hours.

3) The water (crystal lattice)

The current section will focus on the total water content determination. When talking about the water content of lysozyme crystals (or in general protein crystals) a differentiation of two types has to be done. The two types of water are the “free” and the bonded water molecules. The “free” water is component of the enclosed solvent that is located in the crystal cavities (see dye experiments Tables 4.2.3 and 4.2.4). The bonded water molecules are understood as part of the crystal lattice as in “classical” hydrates.

Using the DSC and TGA techniques, it is possible to show and to measure the amount of both types of water, “free” and bonded. The coupled system of TG-DSC (STA), especially, is convenient because the changes in heat flow (evidences for structure alternations) and

weight (evidence for water loss and stability) are detected simultaneously. DSC and TG curves obtained match well if considering the observed heat flow changes and at the same time the occurring weight loss steps.
The DSC curves show first two endothermic peaks (melting – heat absorption) and then one strong exothermic peak (decomposition – heat release). The mentioned peaks appear for all three lysozyme crystal morphologies, but the intensity of the peaks of fresh and air-dried crystals vary. However, DSC data achieved from air-dried lysozyme crystals result in a more detailed curve. Overall, the two small endothermic peaks observed are related to dehydration. In the following, the strong exothermic effect correlates with the decomposition of the lysozyme crystals.
The described DSC peaks within the dynamic phase of the temperature profile start to occur likewise when loss of weight is detected by TGA. Two dehydration steps and one decomposition step are detected. The first step can be understood as the evaporation of “loose” or “free” water molecules (solvent). The second step which occurs at higher temperatures can be taken as the release of bonded water coming from the crystal lattice (“classical” water of a hydrate). A third step leads to decomposition which causes extra loss of weight. The decomposition, surprisingly, happens at very high temperatures around to 250 +/- 3 °C. It gives evidence for high lysozyme crystal stabilities which agrees with Drenth [DRE92]. Drenth concludes from his studies that ”protein molecules in the crystalline state are appreciably more stable and therefore denature less easily than in solution” [DRE92]. However, high stabilities don’t assured enzymatic activity demonstrated by the loss of activity during storage, e.g. HTO.
To measure the crystal lattice water more precisely, additional TGA measurements were carried out on air-dried lysozyme crystals. The same expected trend of obtained curves as seen for fresh lysozyme crystals is observed.
Summing up the total loss of water obtained from fresh lysozyme crystals (first and second dehydration step) differ in the water content for the different morphologies. In detail, the lowest water content which correlates well with the highest protein concentration is determined for HTO crystals. Tetragonal crystals show a lower water content than the HTO morphology. The opposite of HTO is noticed for the LTO crystals which means the highest water content and the lowest protein concentration. It seems that during crystallization the LTO morphology generates cavities / pores within the crystal lattice which are either larger in number or larger in volume, compared to Tetragonal and HTO crystals. This statement is supported by the TGA results obtained from air-dried lysozyme crystals, specifically the water loss of second dehydration step. As mentioned earlier, the second dehydration step refers to the loss of crystal lattice water. The crystal lattice water content is minor different for all three different morphologies. This does not confirm the results recorded by Matsuura [MAT03]. He analyzed and listed different amounts of water molecules attached to the lysozyme molecules within the Tetragonal and HTO crystals. These different notifications may be explained by different preciseness of the analytical methods or by the fact that the crystals in Matsuura’s studies are produced differently.
The existing differences in the water content among the Tetragonal, HTO and LTO crystals of the present work can be explained by the different morphologies which lead to different sizes (volume) or quantity of the crystal cavities / pores.

4) The salt, in present study sodium chloride (crystallizing agent)

For the detection of the fourth component, the crystallizing agent, here the sodium chloride, different methods are used. Hence, the sodium chloride concentration in the solution where crystallization takes place is expected to decrease while the crystallization proceeds. The sodium chloride is therefore expected to be a component of the lysozyme crystals.

One method to determine this sodium chloride concentration decrease takes advantage of the relation between the conductivity and the ionic strength of a solution. This relation is demonstrated by exemplary conductivity calculations (see chapter 4.2). A significant conductivity decrease of applied buffer solution is detectable after 24 hours of crystallization and indicates the reduced ion concentration. At this point, ions of the added salt including the ions of the buffer solution (solvent) have to be considered as incorporated in the lysozyme crystal.

Measuring the pH of lysozyme crystals dissolved in distilled water gives also interesting results. A pH close to 5 could be obtained when air-dried Tetragonal and/or HTO crystals are dissolved which is very close to the pH of the original crystallization buffer solution. A comparable trend is observed for the LTO crystals, too. It demonstrates that not only the sodium chloride is enclosed, but the acetate buffer and/or the glycine buffer, respectively, too. Obviously, the buffer salts are additional components of the lysozyme crystal. Here, it becomes clear that different buffers used for the crystallization of diverse lysozyme crystal morphologies cause different chemical compositions.

Previous conductivity measurements give evidence for the incorporation of sodium chloride within the lysozyme crystals during crystallization. An explicit poof of chloride is possible by the reaction with silver nitrate. Silver nitrate reacts in the presence of chloride to silver chloride which precipitates immediately into a white solid when mixed together, see equation 3.2.2.3. To prove the chloride as component of the lysozyme crystals, crystals are dissolved in distilled water and mixed with silver nitrate. All three morphologies show a white precipitate, meaning the Tetragonal, the HTO and the LTO crystals contain chloride. This allows and justifies the classification of lysozyme crystals in e.g. Tetragonal lysozyme chloride, but with respect of incompleteness / impreciseness.

In literature, a reaction of silver ions with acetate ions into a white solid is described as well [ULL64, ULL55]. This reaction is imaginable for the Tetragonal and the HTO morphology, because of their production in acidic acetate buffer. Comparing the solubilities of both possibly generated silver salts give answer which salt precipitates preferentially if acetate and chloride are present. Silver acetate has a solubility of 1 g/ 100 g water at 15 °C [ULL55]. In contrast, the solubility of silver chloride is extremely lower, 1.93 mg/ 1000 g water at 25 °C [ULL64, CHE11a]. The significant lower solubility of silver chloride and its solubility product of $pK_L=1.77*10^{-10}$ mol^2/L^2 [LID94] definitely confirm that silver chloride precipitates first. In case of excess silver ions, silver acetate formation cannot be totally excluded, but this is insignificant. The same reaction test carried out with LTO crystals, no acetate is available, also results in a white precipitate. On this account, the precipitation of silver chloride and the chloride ions as component of the lysozyme crystals are proven.

More detailed information on the crystal composition obtained by EDX support previous results. Main focus is on the sodium chloride incorporated in the Tetragonal crystal. EDX on Tetragonal crystals demonstrates the existence of sodium chloride and shows considerable differences in the crystal composition depending on where the crystal sample is taken from. The sample taken from the crystal surface contains less ionic sodium and chloride than the sample of the inner crystal. Consequently, the Tetragonal lysozyme crystal is inhomogeneous. The crystal cavities / pores give a plausible explanation. Crystal growth occurs consistent, as described earlier. The crystal lattice develops different forms of cavities. These cavities or pores are filled with solvent and dissolved sodium chloride which is demonstrated via dye experiments, conductivity, silver nitrate reaction and literature [BEN02, RET02, MAL11]. Resulting from this, only few chloride and/or sodium ions are expected to be incorporated in the lattice due to limited residues where attachment is possible [MAT03, VAN01]. However, sodium chloride enrichment in the pores coming from the enclosed solvent is feasible and explains the higher sodium chloride concentration inside the lysozyme crystals.

Further differences in the amount of enclosed sodium chloride among the different lysozyme crystal morphologies are detected by X-ray powder diffraction (XRPD). The differences are displayed through varied intensities of illustrated sodium chloride peaks (see Figure 4.2.9). Similar results were obtained by Bernardo [BER05]. The LTO morphology shows the highest peaks, estimating the highest sodium chloride fraction. Highest sodium chloride concentration is assumed to correlate with the highest solvent content which is already proven by TGA measurements (see Figure 4.2.7). Comparing the Tetragonal and HTO morphologies, the HTO morphology has higher peak intensities. Considering only the enclosed solvent content, which is lower for HTO than for Tetragonal crystals, then the peak intensities do not match. If considering the production conditions, specifically the buffer solution which has 6 wt% sodium chloride for HTO and 4 wt% for Tetragonal, the sodium chloride peaks are expected and shown to be higher for HTO than for Tetragonal crystals. Concluding, the sodium chloride fractions of the different lysozyme crystal morphologies match with the expectations in respect to their solvent content and production conditions. From EDX and X-ray data, the sodium chloride is assumed to be mainly incorporated in the crystal pores by the enclosed buffer solution. Only a small fraction of the sodium chloride can be expected to bind to the charged lysozyme molecule surfaces of the lysozyme crystal unit cell. Bernardo et al. [BER05] summarized his data and suggests: ”that the salt was in some way associated with the protein molecules and not only included in void spaces, or else the voids spaces could vary with processing conditions and accumulate different quantities of salt.” He also mentioned an interesting aspect of the “low crystallinity” which refers to the presence of amorphous protein. The same is observed for investigated Tetragonal, HTO and LTO lysozyme crystals. All three morphologies show a noticeable “hill” at the beginning of the X-ray pattern, usually coming from an amorphous material. It cannot be assured whether this “hill” represents amorphous lysozyme or an error due to limitations of the powder X-ray technique. In case of amorphous lysozyme being enclosed in the crystal, already small amorphous fractions would strongly impact the physical and chemical properties of the crystal like solubility, dissolution rate and chemical stability which are of great importance especially in pharmaceutical systems.

Described investigations and results can already describe the different lysozyme crystal morphologies very detailed. Working with two differently produced orthorhombic lysozyme crystals still asks for extra explicit distinction. Anyhow, it is still attractive to detect another significant disagreement, besides the composition, of the HTO and LTO morphology. XRD data from Aldabaibeh [ALD09a] already demonstrate varied space group parameters of the two, indicating different crystal lattices. Another attempt to achieve more detailed information on the differences, the means of fingerprints to identify the one or the other orthorhombic morphology, is carried out by Raman and Infrared (IR) spectroscopy. Raman pattern obtained for HTO and LTO considering the main peaks are generally in agreement with Liu [LIU10]. With regard to the whole wave number scan, from 500 to 3500 cm^{-1}, the Raman pattern of fresh lysozyme crystals could not give considerable evidences for further lysozyme crystal differentiations. After freeze-drying the HTO and LTO crystals and limiting the scan range to wave numbers 400 to 1800 cm^{-1}, the HTO morphology shows an additional outstanding peak at 1512 cm^{-1}. This peak is evidence for the incorporated chloride bondings and is significant because additional IR spectroscopy on fresh HTO crystals show the same peak at almost same wave number, 1520 cm-1. The small shift found is negligible and should be mostly due to the different technologies and crystal sample preparation. Concluding, the peak obtained at wave number 1512 to 1520 cm^{-1} can be used for explicit HTO identification.

Conclusion

Summarizing the results obtained by extensive analytic studies on lysozyme crystals of the present work leads to the final proof and conclusion that lysozyme crystals are multi-component systems, specifically solvates of the buffer and salt they are produced from. Presented analytics prove the four component composition of lysozyme crystals:

1) lysozyme content → analyzed by lysozyme concentration, specific activity
2) solvent - acetate or glycine buffer solution → analyzed by dye experiments using methylene blue and phenolphthalein, pH
3) water - “free” (enclosed solvent which contains water) and bonded water (crystal lattice) → analyzed by DSC and TGA
4) salt - in present study sodium chloride (crystallizing agent) → analyzed by conductivity, silver chloride precipitation, EDX and XRPD; EDX gives evidences that NaCl is enclosed in the crystal pores as well as captured between lysozyme crystal growth untis.

The composition of the solution (including temperature) in which crystallization takes place determines the composition of the lysozyme crystals. All solution components have to be expected being part of the crystal, either by incorporation in the crystal lattice through attachment to the lysozyme molecule or by embedding in the crystal cavities. At this point,

naming the lysozyme crystal according to its crystallization agent is justified, but incomplete e.g. Tetragonal lysozyme chloride. However, this classification does not represent the entire crystal composition required. Due to the fact that the crystal outcome is highly sensitive to the crystallization conditions a correct protein crystal classification also has to include the pH and the type of the buffer solution, the crystallizing agent and its concentration. An example for a complete lysozyme crystal name could be:

Table 5.2.1: classification of lysozyme crystals.

	Morpho-logy	**Pro-tein**	**pH**	**Mol-arity**	**Buffer**	**[5] Cryst. agent [wt%]**	**Type of [5] cryst. agent**	**Tempe-rature [°C]**
Tetragonal	[1] Tetra	[2] lys	5	0.1	[3] NaAc	4	[4] NaCl	4
Tetra-lys-5-0.1-NaAc-4-NaCl-4								
High Tempera-ture Ortho-rhombic	HTO	[2] lys	5	0.1	[3] NaAc	6	[4] NaCl	32
HTO-lys-5-0.1-NaAc-6-NaCl-32								
Low Tempera-ture Ortho-rhombic	LTO	[2] lys	9.6	0.05	Glycine	4	[4] NaCl	room tempe-rature ≈20
LTO-lys-9.6-0.5-glycine-4-20								

[1] Tetragonal
[2] lysozyme
[3] sodium acetate buffer
[4] sodium chloride
[5] crystallizing

The precise classification is important, because already minor changes e.g. in pH or salt concentration can cause noticeable changes in the crystal lattice, crystal composition and therefore in the crystal morphology.

5.3 Solubility and dissolution behavior of lysozyme crystals

The dissolution behavior caught special attention because an interesting dissolution phenomenon is observed which is not described in literature up to date.

5.3.1 Solubility

The protein solubility is originated by the primary structure of the lysozyme molecule. However, it is mainly controlled by the proteins electrostatic surface charges and the ever present interactions with the solvent. The electrostatic interactions with the environment (including the electrostatic double-layer and hydration layer) are assumed to take place equally at the lysozyme crystal surface (crystal / solvent interface) and the lysozyme molecule surface. If protein molecules approach each other, for example during salting-out, various kinds of bonds with varied strength, e.g. hydrogen bonds, salt bridges etc. can develop. The sum of these interactions / bonds is responsible for the protein crystal lattice, and thus for the solubility of lysozyme crystals, for more details (see chapter 2.2.1).
The solubility of the studied system describes the equilibrium concentration of dissolved lysozyme crystals in a sodium chloride buffer solution at different pH values and temperatures. Verifying the solubility parameters like the salt concentration, temperature or pH of the buffer solution (acidic acetate or phosphate buffer), the equilibrium state changes and has to balance again. The equilibrium (for used solubility “micro-apparatus” method) can be reached again via lysozyme crystal dissolution, which means by increasing the lysozyme concentration in the solvent. On an energetic level, the system always “wants” to attain the equilibrium state, because at this state the system has the lowest free-energy, ΔG. At certain conditions, if a “new” crystalline lysozyme morphology may exist with even lower free-energy, the “new” lysozyme morphology will nucleate and start to grow, simultaneously the “old” lysozyme morphology will dissolve and a transition into the “new” morphology can take place.

In this work, solubility investigations on different lysozyme crystal morphologies are carried out to add some new solubility data of the LTO morphology (which is already published by Aldabaibeh [ALD09a]) to the already partially existing phase diagram, and to support already known solubility behavior of the Tetragonal and/or HTO lysozyme crystals [ALD09a].
The phase diagram of present lysozyme crystals demonstrates a multi-component system. Within the range of investigation, solubility of Tetragonal, HTO and LTO lysozyme crystals clearly increases with temperature, but decreases with increasing pH and salt concentration. A strong dependency on the solution conditions (composition e.g. salt concentration, pH, and temperature) becomes obvious. Observed and presented solubility trends for Tetragonal and HTO lysozyme crystals (see Figures 4.3.1.1 to 4.3.1.3) are in good agreement with the data from literature e.g. [ALD09a, EWI94, FOR99, BEN02].
The question “Why the solvent environment / solution condition can strongly affect the lysozyme (globular) protein molecules and their properties such as solubility?” is already answered and discussed in detail by Aldabaibeh [ALD09a], can be studied in following references e.g. [MCP98, CHR83, SAL85, CAC91, BRI91, GUI92, EWI94, RET97, FOR99,

MCP99, NIN99, BOS01, LEG02, BEN02, RET02, VAL05, BAN06, RET07, VEK07, NAN08, PEK08], and is shortly explained in chapter 2.2.1.
Solubility data obtained for Tetragonal, HTO and LTO lysoyzme crystals were added to the same partially existing phase diagram as done in previous studies by Aldabaibeh [ALD09a]. On the base of this phase diagram, solubilities of the different morphologies were compared. Here, it has to be clearly pointed out that the solubilities of the Tetragonal, HTO and LTO crystals cannot be presented in the same phase diagram. Doing so is wrong!
Analytics carried out could explicit prove the multi-component character of lysozyme crystals, basically four main components such as the lysozyme, water in the crystal lattice, solvent (buffer and water) enclosed in crystal pores and salt(crystallizing agent). This proof and finding is crucial for the correctness of a phase diagram and has to be considered.
Comparing the solubilities of Tetragonal and HTO crystals is justified only by first sight because both morphologies crystallize in the same solvent (buffer solution). Tetragonal and HTO are solvates of the same buffer solution but their composition of the same components is different as demonstrated from the analytical studies. This means both are not the “classic” solvates, they are “pseudo” or “quasi” solvates. It is more obvious for the LTO morpholohy. The LTO morphology is crystallized at totally different conditions (different buffer and different pH, see chapter 3.2.1). Therefore, especially the LTO crystals have to be evaluated separately. It becomes obvious that the LTO morphology is not a different morphology from the same solvent (buffer) as the Tetragonal and HTO. Consequently, the LTO solubility also cannot be compared with Tetragonal and HTO crystals, and placing them in the same phase diagram, as illustrated in Figures 4.3.1.1 to 4.3.1.3, is wrong.

Furthermore, the transformation of the Tetragonal into the HTO morphology at high temperatures (above 25 °C) is well known and has been studied very detailed [ALD09a, VAS07, BUR01, BER74, COZ75]. The transformation occurs, because the lysozyme undergoes temperature induced conformational changes [COZ75, BUR01, SAL85]. According to this known transformation, an unknown transformation of the LTO crystals might take place at conditions shown in Figure 4.3.1.1 Another transformation of LTO crystals into a new high temperature Orthorhombic morphology which has not been described in literature obviously occurs, see Table 5.3.1. Considering the LTO solubility in Figure 4.3.1.1, however, an interesting observation is noted. The LTO solubility increases first, but in the range of 15 to 16 °C the solubility starts to decrease again. Here, the phase transformation could be the explanation. First, the solubility increases with temperature which is in agreement with the “normal” expected solubility trend. Above 16 °C, solubility with respect to the lysozyme concentration in the solvent deceases again which can be explained by nucleation of a new crystalline phase. Simultaneously, the dissolution of the LTO still proceeds. At a temperature above 20 °C, the solubility becomes constant, which means that dissolution of LTO occurs equally with the growth of the “new” crystalline phase. Unfortunately, checking the sample could not clearly show the formation of a new morphology. Only orthorhombic shaped crystals could be recognized, but they show differences in size. However, the very small orthorhombic crystals do indicate nucleation. The formation of a new solvate (polymorph?) can be still considered, because a new solvate (polymorph?) does not necessarily have to have a different habit / morphology [HIL06].

Table 5.3.1: Transformation of LTO lysozyme crystals into a new high temperature Orthorhombic morphology in a sodium phosphate buffer pH7 + 3 wt% NaCl + 25 mg/mL lysozyme at 40 °C.

Transformation of the LTO into a new high temperature Orthorhombic lysozyme crystal morphology			
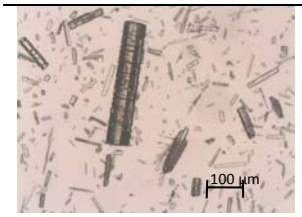	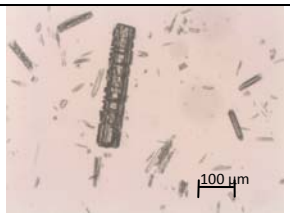	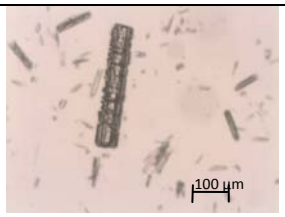	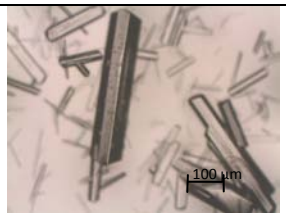
15 min	45 min	6 h 15 min	22 h 15 min

5.3.2 Dissolution behavior of lysozyme crystals

The same background as for the solubility (see chapter 2.2.1) helps to understand the dissolution phenomenon of Tetragonal, HTO and LTO lysozyme crystals. In the following discussion, approaches to explain the dissolution phenomena that were introduced in previous publications [MUE11a,b, MUE12] will be presented in more detail.

Tetragonal, HTO and LTO lysozyme crystals dissolve optically via the same dissolution mechanism. All morphologies show a comparable dissolution behavior, meaning the crystals become fragmented (skeleton-like) and fall apart in many smaller crystal particles which dissolve thereafter separately. Another interesting aspect is that a change in the conditions (e.g. pH, salt concentration) in which the lysozyme crystals dissolve can lead to a different dissolution behavior (HTO and LTO). When the dissolution behavior changes, the lysozyme crystals still fall apart in crystal fragments, but the orientation, the size and the shape of the generated crystal fragments varies. An exception is observed for the LTO lysozyme crystals. At basic pH values, the LTO crystals do not fall apart in fragments anymore. All crystal surfaces observed look smooth and edges become round, comparable with known dissolution observation of inorganic substances, e.g. sodium chloride.
The dissolution behavior observed for lysozyme crystals is not described as for inorganic substances and is not well-established as for organic crystals, and is only described for a few examples.
The dissolution of a sodium chloride crystal is used to illustrate expected and known dissolution behavior for inorganic crystals. The sodium chloride crystal is exposed to distilled water, Figure 4.3.2.1. Due to high undersaturation (solubility at 16 °C is approx. S = 360 g/L [MSD11, ULL60]), a very fast dissolution is expected and observed. Dissolution can be recognized immediately when sharp crystal edges become round [MYE01]. The crystal

becomes smaller and smaller and remain rounded while dissolution proceeds, until the crystal disappears.
Matsuoka [MAT86] demonstrates the melting behavior of crystalline m-chlornitrobezene (CNB) which looks optically very similar to the dissolution behavior of the lysozyme crystals. He explains the formation of a fragmented CNB crystal basically by an agglomeration process while forming of crystals. During dissolution the process will then be reversed.
The agglomeration approach to explain the dissolution phenomenon of lysozyme crystals as described for the CNB crystal would need certain frame condition: precipitation occurs only at extremely high supersaturation. If precipitation takes place, it happens extremely fast and generates numerous nuclei to decrease the supersaturation as fast as possible. Numerous small crystals (nuclei) could cause agglomerates to develop. Protein agglomerates could then behave as “single protein particles” that continue to grow until “pseudo”-single crystals are well developed. Their crystal surface might heal completely while growth proceeds. An agglomeration of very small lysozyme crystals directly after nucleation is imaginable. If agglomeration represents the basic mechanism of the lysozyme crystal growth, the same mechanism could be expected for the dissolution. Hence, crystal growth observation experiments should give first signs. Crystal growth studies of the Tetragonal lysozyme morphology by e.g. Buchfink [BUC08] did not show any evidences of a process just discussed. Furthermore, protein solutions are very complex systems, because many diverse interactions, as introduced in the solubility section, are present [LEU01]. Therefore, these interactions have to be considered for the dissolution process as well. Therefore, the option of an agglomeration process as a possible mechanism for the observed dissolution behavior is a very weak assumption.

Other options and thoughts existing in literature to explain the dissolution phenomenon of lysozyme crystals will be discussed in the following:

1) Crystal growth and dissolution follow the same basic model, just in different directions. The dissolution behavior of lysozyme crystals will therefore be discussed on the base of conventional crystallization aspects, according to Ulrich [KIR11].

1.1) Crystal defects are responsible for the unusual dissolution behavior. Such crystal defects can cause tensions in the crystal lattice at which dissolution is assumed to start and cause the crystal body to become fragmented, according to van der Hoek [HOE82] and Fabian [FAB93].

1.2) An additional “speculative thought” refers to mosaicity (mosaic structure), proposed by Rossiter [ROS90], possibly present in protein crystals that could also cause the lysozyme crystals to fall apart during dissolution.

1.3) Complex macrobonds of different strengths, that are assumed to exists in and determine the crystal lattice, are responsible for the dissolution behavior of lysozyme crystals, according to Matsuura [MAT03] and Oki [OKI99]. Under dissolution (undersaturation) conditions, the weakest macrobonds are supposed to break down first, stronger macrobonds thereafter.

1) Lysozyme crystal dissolution as the reverse process of crystal growth.

The main and fundamental dissolution model postulates that dissolution and crystal growth are the same, but in different directions. Therefore, the dissolution and the crystal growth have same mechanism just in reverse which was already introduced by several researches [FAB96, STA94, SAN88]. For example, Snyder [SNY07] assumed equal character of growth and dissolution and manipulated the crystal shape by a cycling mode of growing and dissolving. If assuming the same mechanism for both, the dissolution and the growth process of lysozyme crystals, the dissolution can be also limited by 1) the surface disintegration (formation of a fragmented lysozyme crystal body) and by 2) bulk diffusion. A third existing step considers the heat flow of the phase transfer [ULR89, ULR94, MUL01, KRU93, KIR11]. The step of heat flow / transfer has to proceed simultaneous with the detachment (surface reaction, step 1) and the transport (diffusion, step 2) step of the dissolution process. If the heat transfer step during crystallization / crystal growth is exothermic, the same step for the reverse process has to become endothermic. Here, it should be mentioned that an actual temperature decrease at the protein crystal interface through dissolution is expected, but it will be too little for detection, and thus it can be disregarded.

If crystal dissolution (or growth that is not part of current thesis) is observed under non-stirred conditions, which is the case in present study, the transport of protein molecules to the surface (growth) / away from the surface (dissolution) has to proceed through diffusion and natural convection. The required concentration gradient between interface crystal / solution and the bulk solution develops because of depletion (crystal growth) / enrichment (dissolution) of protein near the crystal surface [DUR96]. Again, similarities between growth and dissolution become obvious.

The protein (lysozyme) crystal growth occurs by incorporation of growth units which takes place according to a “layer by layer” or by a screw-dislocation” mechanism. Which incorporation mechanism happens is dependent on the supersaturation. This means both mechanisms are able to proceed [MCP98, DUR86, CHE03, ROS96]. As an example, Tetragonal lysozyme crystals at high supersaturation grow via “layer by layer” (2-D nucleation) and at low supersaturation via the screw-dislocation mechanism [NAD95]. Depending on the undersaturation and lysozyme crystal morphology, obviously the dissolution behavior can change as well, as observed for the HTO and LTO lysozyme crystal morphologies. An explanation might be a changing dissolution mechanism, as described for the crystal growth.

On the base of the basic model (1), additional speculative thoughts which explain the dissolution phenomenon of lysozyme crystals more detailed follow.

1.1) Crystal defects cause tensions in the crystal lattice which cause the lysozyme crystal to fall apart during dissolution.

Dissolution experiments in this work show fragmented lysozyme crystal bodies which look more like “etch-pits” formations [LAS01, LAS03]. The etching can be confirmed by several references [MCP98, MON93]. Monaco and Rosenberger observed and studied the etching on Tetragonal lysozyme crystals [MON93]. Their observations, the development of etch-pits over the lysozyme crystal surface in undersaturated solution, are comparable with own

studies. They suggest a theory that lattice defects leads to enhanced local lattice stress. At these “stress points” (strains) molecules will be promoted to leave the lattice. In other words, they describe a higher degree of undersaturation locally limited around the defect points. As a consequence, the dissolution should start at these crystal lattice defects. Other literature mentions same theory of etch-pits arising from lattice defects, point defects etc. [MUL01, SAN82].
The batch crystallization, which is used for lysozyme crystal production, represents a fast crystallization method (less than 24 h) and leads generally in present work to not “perfect” lysozyme crystals. Other crystallization methods e.g. the vapor diffusion method produces nearly “perfect” protein crystals. Not “perfect” lysozyme crystals are expected to have a high density of crystal defects which is assumed.
This speculation, which is still not totally proven, was introduced for inorganic crystals by van der Hoek [HOE82]. He postulates that crystal defects cause tensions within the crystal lattice. These tensions are assumed to lower the growth process, but activate and intensify the dissolution [HOE82, FAB93]. However, the detachment step during dissolution is generally much faster than the comparable attachment (incorporation) step during crystal growth (because dissolution does not require surface diffusion). This fact and the theory of crystal lattice tensions can plausible explain why dissolution generally occurs faster than growth at same driving forces and temperatures.
According to van der Hoek [HOE82], following “speculative guess” for lysozyme crystals could be expressed: If dissolution preferentially starts simultaneously at such widely spread out lattice defects, it seems possible that lysozyme crystals dissolve in a non-uniform way. The dissolution pictures of the dissolving lysozyme crystals, however, could be interpreted as follows: “Lysozyme crystal defects cause tensions in the crystal lattice. Due to these lattice tensions, it can be assumed that less energy is required to break the lattice bonds at these defect points. As a consequence, the lysozyme crystal starts to dissolve where crystal defects are located which could cause the crystal body to become first fragmented and then to fall apart. The crystal areas with less or no lattice defects could be responsible for the formation of crystal particles (fragments) seen during dissolution”.

1.2) Mosaicity (mosaic structure) as a reason for the falling apart of lysozyme crystals during dissolution.

With respect to the assumption of a high defect density in lysozyme crystals, another speculative thought, a concept of mosaicity, can arise. The theory of a mosaic structure (see chapter 2.2) in crystalline substances is not uncommon, and mentioned for some proteins, e.g. ferritin, apoferrtin and for lysozyme. Crystal images of mentioned proteins provide evidences for existing mosaicity because remarkable optical similarities are noticeable, still it is just speculative.
X-ray crystallography studies on lysozyme crystals were not continued because preliminary diffraction results were extremely bad. (Good diffraction results would indicate low mosaicity which means a good crystal “quality” with few lattice defects, see chapter 2.2.) Lysozyme crystals investigated showed extremely diffuse and non-evaluable diffraction results which is usually caused by highly disordered (theoretically) “mosaic blocks” and/or by crystals that contain a large number of lattice defects [ROS90].

An estimate of mosaicity of lysozyme crystals has been described in literature, too, but rare. However, one exemplary reference describes the mosaic structures for a lysozyme crystal (larger than 170 µm) and illustrates its dissolution (on page 187, [CAR03]) which looks identical with the dissolution observed in this study for Tetragonal crystals. Demonstrated dissolution is characterized by "fast" dissolution along the block boundaries which leads to a "hairy" morphology [CAR03]. Same reference also shows a lysozyme crystal of smaller size (less than 170 µm) that dissolves slowly and uniform which indicates a lack of block boundaries [CAR03], unfortunately no dissolution conditions are described. Again a correlation of size and crystal defects is postulated.
Nevertheless, one should consider whether used crystallization method delivers additional support for a theoretical mosaic structure to develop or not. Own lysozyme crystals produced by batch crystallization grew quite large. Crystal sizes (length and/or width) above 200 µm are very common. HTO and LTO crystals could reach sizes larger than 1 mm in length. According to above assumption that the larger the crystal the higher the density of crystal defects, lysozyme crystals should be highly disordered and/or draw through numerous defects. Actually, bad X-ray diffraction results of investigated lysozyme crystals support above mentioned. Furthermore, it also would strengthen the dissolution behavior on the base of etch-pits formation, described in the model (1.1). Regarding the screw-dislocation growth model, which is proved to exist, similarities can be recognized. Mosaicity and screw-dislocation, both develop either by incorporation of impurities and/or by lattice defects.
Indeed dissolution images show lysozyme crystal to fall apart in fragments, which might be interpreted as "mosaic blocks", but these generated crystal particles show a very irregular shape. From theoretically described mosaic blocks, one could understand a more uniform particle formation which is not observed. Nevertheless, the mosaic structure is a theoretical model mostly used in the field of crystallography science. [ROS90]. There are evidences for the existence of a mosaic structure which seem plausible, but explicit experimental data to confirm mentioned model are missing.

1.3) *Dissolution phenomenon of lysozyme crystals reasoned by the model of macrobonds.*
In the following, an additional model, the macrobond model, and reasons for the unusual dissolution behavior of lysozyme crystals on a microscopic level according to diverse existing interactions will be discussed. The solvent (water) – lysozyme, salt - lysozyme and the lysozyme – lysozyme interactions as well as the different types of bonds within the lysozyme molecules and the crystal have to be taken into account. The interactions and bonds that have an impact and control the crystal growth and the solubility, respectively, of protein crystals are assumed to reason the dissolution as well. Therefore, the model (1.3) involves complex macrobonds of different strengths which are believed to exists in and determine the crystal lattice, and thus the dissolution. The macrobond analysis was also used to examine the different crystal habits of cubic insulin crystals and their intermolecular interactions [OOT09]. Marcobonds vary in strength and hence varied energies are required for them to be broken. This fact is assumed to be base for the fourth model of the dissolution behavior of lysozyme crystals. Depending on the dissolution (solvent) condition, dissolution driving forces alter and the weakest macrobonds break down first which can explain the lysozyme crystal falling apart while dissolving. The assumed leftover macrobonds within generated lysozyme crystal fragments need additional "work" / energy to be broken.

The first step, the formation of a fragmented crystal body, seems to occur “faster” than the following dissolution of the crystal fragments. Obviously, the remaining undersaturation (after the first step) provides less strong driving forces for the “left-over” macrobonds to collapse. In this case, the slower dissolution of generated crystal particles can be explained.
With respect to the different macrobond strengths, the not changing dissolution behavior of Tetragonal lysozyme crystals can be explained. The macrobond D is by far the weakest bond, only 63 kJ/mol. The differences from D to the other macrobonds are quite large, from ΔE= 439 to 236 kJ/mol. Therefore, D should be always ruptured first which can result in a non-changing dissolution behavior. Taking a look to the macrobonds of HTO crystals, their strength does not vary as much as in Tetragonal crystals. In HTO, the macrobonds B (157 kJ/mol) and C (138 kJ/mol) [MAT03] are quite similar. The bond energy differences of B and C to A (271 kJ/mol) is far less if compared to Tetragonal crystals. Consequently, the solvent composition might direct which of the two bonds collapses first. Depending on which macrobond becomes preferentially attacked, certain particle shape formation should result. Literature does not give explicit macrobond data of the LTO morphology required for adequate comparison. Nevertheless, HTO and LTO are both orthorhombic. On account of this, comparable macrobonds for the LTO morphology might be assumed. This assumption can be supported by the fact that the dissolution behavior of LTO and HTO changes into the “bar”-formation by increased pH and salt concentration. On the other hand, the “bar”-formation for the LTO crystals occurs already at pH7 + 2 wt% whereas for HTO at a higher pH of 10 + 7 wt%. In addition, LTO does not develop the “bar”-like crystal particles at pH >8 anymore. At this point, existing macrobonds might be similar to some extent, but not the same. Another influence must exist, too. Influencing parameters suggested refer to the solubility (undersaturation), hydrophilicity of the lysozyme (interactions in the solvent), the solvent content and/or the pore size (additional surface area, crystal / solvent interface).

Last section in this discussion summarizes the effect of a) pH and sodium chloride, b) temperature and c) the undersaturation on the dissolution behavior (formation of fragmented crystal body) of lysozyme crystals.

a) effect of pH and sodium chloride (Figures 4.3.2.3 to 4.3.2.7)
All investigated lysozyme crystal morphologies generally dissolve by falling apart followed by a separate dissolution of the small crystalline parts. This behavior is observed in distilled water (pH5.75-6), pure buffer and buffer + salt solutions for all tested pH values (pH5.7 to 10), except for the LTO crystal morphology at pH8 and > 8. To distinguish between the effect of pH and salt concentration, the dissolution behavior is observed in pure buffer solutions with increasing pH from 5.7 to 8 and 10 (Figure 4.3.2.7).
No change in the dissolution behavior is observed for Tetragonal and HTO crystals. LTO at pH8 behaves exceptional and dissolves by rounding crystal edges, almost uniform. The pH can obviously influence the dissolution behavior of LTO crystals, but the particle formation during dissolution of Tetragonal and HTO is not affected in the same way.

An effect already of slightly increased pH and low salt concentration is noticeable for the LTO morphology. The dissolution fragmentation changes from needle like crystal particles to

“bar”-shape particles arranged width-wide. Here, which of the parameters, pH or salt concentration, has a stronger influence is not clear.
The effect of salt becomes obvious only for the HTO morphology. In pure buffer pH10, the HTO particles formed during dissolution look the same as in pure buffer at pH5.7 or 8 (see Figure 4.3.2.7). In contrast, in Figure 4.3.2.6 with 7 wt% NaCl, is shown a clear change in the particle formation. “Bar”-shape particles which contain many smaller particles develop.
Crystal fragments generated by dissolution can obviously change their orientation, size and shape, but this is dependent on the lysozyme morphology and the sensitivity to pH and salt concentration. Clear differences among the three morphologies by their different dissolution behaviors are demonstrated. Reasons are expected to be mainly related to the variations in the crystal lattice, macrobonds and the lysozyme structure which can alter during crystallization under different conditions. If dissolution is assumed to be the reverse of crystallization, given reasons are confirmed by the statement of Nanev. Nanev [NAN08] concluded that “along with the crystal composition the protein structure, especially at the crystal lattice contacts is the key to the crystallization behavior”.

Tetragonal, HTO and LTO have in common that in increase of pH and salt (pH > 7 to 8 and 10, 2 to 7 wt%) results in an outstanding slow dissolution process. The higher the pH and salt concentration the slower the dissolution seems to occur. Indeed, explicit dissolution rate studies are necessary, but generally a suppressed dissolution can be explained by:

- if pH (close to the pI) and salt concentration increases, see solubility data in the phase diagram of Figures 4.3.2.1 to 4.3.2.3, the undersaturation reduces (low undersaturation means weak driving force and dissolution has to become minimal), and/or

- if added salt itself is understood as an impurity (according to conventional crystallization: the influence of impurities on the crystal growth process is well known [NYV95] and already described for dissolution as well [FAB96, MUT77]), ions might block or hinder lysozyme crystals which alters or inhibits the interactions with water molecules. This can lead to suppressed as well as to an uniform dissolution in case for LTO.

b) effect of temperature (Figure 4.3.2.8)
Under constant solution conditions, a temperature increase can initiate phase transformation, e.g. Tetragonal to HTO. To study if the parameter temperature alone can change the dissolution behavior of lysozyme crystals with respect to the formation of crystal particles, dissolution observation at pH8 + 3 wt% NaCl and constant undersaturation, but at two different temperatures (16 and 32 °C) are tested. The LTO morphology is used for this kind of experiment, because its dissolution behavior seems to be more sensitive to environmental changes than of the HTO or Tetragonal morphology.
No change in the LTO dissolution behavior and no transformation for 16 or 32 °C are noticed. In this specific case, varied temperatures and same solution conditions (constant undersaturation) don’t influence the dissolution behavior regarding the formation of a fragmented crystal body. On the other hand, temperature changes which modify the undersaturation can change the dissolution behavior.

c) effect of undersaturation (Figure 4.3.2.9)

The Tetragonal, HTO and LTO lysozyme crystals have in common that the undersaturation e.g. in distilled water is very high. Therefore, the dissolution driving force is extremely strong and dissolution can occur extremely fast. As soon as the lysozyme crystals are exposed to distilled water, the crystals explosively fall apart and crystal fragment widely spread out. The fragments dissolve thereafter.

To evaluate the role of undersaturation on the dissolution behavior more specifically, dissolution experiments were set for Tetragonal crystals (pH8 + 3 wt% NaCl, constant temperature 16 °C) to three different undersaturations (0.5, 1.5 and 2), according their solubility data (Tetragonal crystals were used, because HTO and LTO crystals showed already varied dissolution pattern). Different undersaturation means that different dissolution driving forces exist. The driving force determines the dissolution rate, but the dissolution rate is not considered at this point. Nevertheless, it can be expected that increasing driving forces from very high (distilled water) to very low (S* = 0.5) may change the dissolution behavior of Tetragonal crystals, too, as observed for HTO and LTO crystals.

No change in the dissolution behavior in distilled water, at S*= 2 or S* = 0.5 is observed. Within the range of investigations, the undersaturation does not change the dissolution behavior regarding the crystals “falling-apart”.

An approach to explain this not changing dissolution behavior of Tetragonal crystals is related to described model of macrobonds (4), and that undersaturation causes the weakest macrobonds to collapse first. According to Matsuura [MAT03], it has to be the macrobond D (only 63 kJ/mol) for Tetragonal crystals, because the macrobonds A (345 kJ/mol), B (502 kJ/mol) and C (299 kJ/mol) are much stronger. The macrobond D is the weakest, because fewest bonds are involved. In addition, more water related bonds exist which are half as strong as non-water related bonds. Due to the big strength differences, the type D macrobonds should always collapse first, which means the dissolution behavior cannot change.

Summarizing all facts concerning the dissolution behavior:

- undersaturation is the driving force for the dissolution behavior of Tetragonal, HTO and LTO lysozyme crystals
- pH approaching the pI reduces the solubility and minimizes the undersaturation which reduces dissolution driving forces
- every pH which is different from the pI (isoelectric point) causes different surface charges of the protein (lysozyme) molecules
- changing pH and/or salt concentration of the solvent solution alters the surface charges (charge density) of the lysozyme and results in changed interactions (protein – protein, protein – solvent/salt)
- solvent / crystal interface interactions determine the dissolution
- lysozyme / crystal surface is selective and inhomogeneous due to different amino acid residues sticking out of the lysozyme molecule surface [NAV08]

- selective amino acids form different crystal contacts which leads to different macrobonds of various strength
- flexibility of amino acids varies and shows an impact; the shorter / smaller the amino acid, the less flexible amino acid becomes; the less flexible the amino acid group, the stronger the van der Waals forces [NAN08]
- crystal contact “position” (amino acid) controls crystallization behavior [NAN08] and in reverse it should direct the dissolution behavior
- different crystal morphologies have different crystal contacts [JAN95]
- sodium chloride ions can only bind to ionisable amino acid residues e.g. to arginine, lysine, glutamate or aspartate; amino acids that cannot be ionized are e.g. glutamine or asparagines
- crystallization always follows the aim to shorten the range of repulsive electrostatic interactions so that attraction becomes dominating; crystal lattice contacts form during crystallization only to reduce solubility and enhance lysozyme – lysozyme interactions; in reverse, dissolution needs strong repulsive electrostatic interaction to reduce the attractive forces; for lysozyme an optimal low pH and low salt concentration is required
- high temperatures (above 25 °C) can cause conformational changes in lysozyme, and thus transformation
- during transformation, temperature can activate / deactivate different patches (amino acid residues) for breaking existing and making new crystal lattice contacts; new / different crystal contacts result in altered interactions and modified crystal properties

Conclusion

Investigation on lysozyme crystals of different morphologies clearly demonstrate how complex and divers the dissolution is. First main difference to “classic” crystal dissolution (equally rounded crystal edges) is the fact that lysozyme crystals dissolve by the formation of skeleton-like crystal bodies which finally falls apart completely. The generated crystal fragments dissolve thereafter. The described dissolution becomes even more difficult to understand when studying different lysozyme crystal morphologies, which show different dissolution behavior, and when changing the dissolution conditions e.g. changing the pH, the temperature, the salt concentration etc. Changing the solvent composition and undersaturation modifies the lysozyme fragmentation during dissolution. The particles generated by dissolution can vary in size, shape and arrangement. The required time for lysozyme crystals to dissolve completely varies, too. Mentioned observations demonstrate how special and complicated dissolution can be and how many different factors / parameters have to be considered.

On the base of the lysozyme crystal dissolution studies, approaches to explain the dissolution phenomenon are introduced, but at current state no model of (1.1) to (1.3) can be totally assured.

The basic model introduced in 1) "*Lysozyme crystal dissolution as the reverse process of crystal growth.",* which includes the two step crystal growth model (the three step model, respectively, by Ulrich et al., [ULR89, KRU93]), is applicable for the dissolution process and provides a useful base for the understanding. The "diffusion layer model" with respect to Fick's law and the "interfacial barrier model" seem plausible, whereas the latter is more accurate due to consideration of the energy barrier. Introduced thoughts of (1.1), which explain the dissolution phenomenon on account on etch-pits formation, crystal defects and impurity incorporation, are considerable speculations because optical similarities between etch-pits and the fragmentation of lysozyme crystals might exist. Generally, etch-pit formation on crystal surfaces is a sign for "pseudo"-single crystals which develop by agglomeration and impurity incorporation / accumulation. As previously discussed, agglomeration as a model for observed dissolution behavior was excluded, that at the same time diminishes the relevance of the model (1.1).

Discussing the model (1.2) of existing mosaic structure brings out aspects which are plausible for the observed dissolution behavior. Even so, the mosaicity is just a theoretical model developed by crystallographers to explain a weak diffraction behavior of certain single crystals. The field of single-crystal lattice analysis by X-ray diffraction has a totally different focus, and thus a clear differentiation is required. Consequently, the mosaicity is not directly applicable for the dissolution phenomenon of lysozyme crystals.

The models (1.1) and (1.2) are imaginable explanations for the falling apart of the lysozyme crystals during dissolution. The main disadvantage of both models is, they cannot explain the change in the dissolution behavior of the HTO and LTO morphologies.

The third and in present study favored model (1.3) takes the various interactions and different bonds within the lysoyzme crystals into account. Starting from the crystallization of lysozyme, specific macrobonds of different strength (the sum of several amino acid –amino acid, amino acid – solvent (water, buffer) and amino acid – salt (e.g. Cl^-, buffer ions) interactions / forces) develop and stabilize the crystals lattice. Already small changes e.g. in pH, ionic strength, salt concentration etc. of the crystallization environment (solution) can affect the electrostatic field around the protein and the protein crystal. The dissolution is understood as the reverse process of the crystallization / crystal growth (basic model (1)). As a consequence, the model of macrobond formation just in opposite "direction" is most plausible to explain the dissolution behavior of lysozyme crystals. The macrobonds and their different strengths were precisely calculated for the Tetragonal and HTO morphology by e.g. Matsuura [MAT03] and Oki [OKI99]. These calculations enable a prediction of which macrobonds collapse first during dissolution. The weakest macrobonds determine the dissolution behavior of lysozyme crystals and therefore the way of "falling apart" in many fragments. In addition, the high sensitivity to the environmental solution conditions, as mentioned for the lysoyzme crystallization, explains the changes in the dissolution behavior when observed under modified dissolution conditions. One main disadvantage of present "macrobond"-model is that no macrobonds calculations that define the LTO morphology exist yet. Therefore, considering the same model for the LTO morphology as introduced for the Tetragonal and HTO lysozyme crystal morphology is completely speculative.

Outlook

Following Table 5.4.1 gives a short overview on the current crystallization research status of comparing conventional crystallization and protein crystallization. It is obvious that conventional crystallization is a very well studied field of science, whereas protein crystallization belongs to the "newer" research areas. An overview on protein crystallization history is given by McPherson [MCP91]. Protein crystallization still has many unanswered questions and asks for lot´s of future work.

Table 5.4.1: Overview of "classic"/conventional crystallization and protein crystallization.

[1] known, well studied.

[2] demand of research, missing understanding, optimization – control (future work).

[3] considered in present work for batch protein crystallization, already studied.

[4] focus in present work, investigation to give experimental proof, continuous work required.

Main characteristics	**"Classic" / Conventional crystallization**	**Protein crystallization**
optimization criteria	[1]solubility, purity, yield	[3]activity (enzymes), stability, [2]"purity", yield
composition	[1]pure substance (one component crystal)	[4]multi- component crystal (minimal 4 components)
admixtures	[1]variable	[3]common, e.g. salts, PEG
phase diagram	[1]basis	[4]partially defined
size distribution	[1]controlled	[2]not controlled
nucleation	[1]controlled (kinetics)	[2]not controlled
crystal growth	[1]controlled (kinetics)	[2]not controlled
dissolution	[2]controlled, but limited kinetics	[4]undefined, not controlled, kinetics?
crystal hardness	[1]defined, e.g. Vickers hardness	[2]undefined, too soft
seeding	[1]often	seldom
temperature	[1]variable, defined	[3]generally cool, partially defined
time	[1]variable, defined, controlled	[2]long duration
conclusion	**controlled**	**not controlled**

Generally, in protein crystallization, still much work has to be done for every protein (see Table 5.4.1). There are many tasks and challenges e.g. solubility measurements to develop complete phase diagrams which determine, describe and control crystallization as well as dissolution conditions and processes. Furthermore, studies on dissolution rates under controlled and defined conditions, studies of dissolution impact factors and the related mechanisms, investigations and calculation on dissolution enthalpy and entropy to extend the dissolution models, optimization studies for time efficient crystallization, activity preservation and enhancing the protein yield, research to control nucleation (seeding?), crystal growth and size distribution, as well as to predict crystal hardness, etc. should be in focus of future work.

In the specific case for lysozyme crystals, some information and data obtained for the Tetragonal, HTO and LTO morphology are summarized in Table 5.4.2. There are more interesting aspects and questions which need further attention. To mention a few, aspects of interests for industrial applications are for example “how to optimize the lysozyme batch crystallization to minimize activity loss?” and “how to optimize the crystal storage to avoid activity loss?”. With respect to improve the theoretical understanding, further crystal growth and dissolution observation studies e.g. by SEM under certain conditions would be of great value. Comparing the data (pictures and growth/dissolution rates) of both processes can lead to detailed evidences which again could prove the dissolution as reverse of crystal growth. In addition, investigations on the lysozyme crystal structures have to be continued of fresh in comparison to dried crystals, which also may proof assumed existing mosaicity. A possibly occurring phase transformation of LTO crystals into a “new” orthorhombic polymorph has to be studied more detailed by microscopy, solubility and by X-ray.

Table 5.4.2: Overview of lysozyme crystal investigation in present work.

Characteristic	Tetragonal	HTO	LTO	a few references, e.g.
[3]average: specific activity (U/mg)	53100	52000	54000	Tetragonal: [DIA10]
[3]stability	251 °C	251 °C	252.3 °C	-
[3]different salts	NaCl, KCl, $CaCl_2$*$2H_2O$, $BaCl_2$, Na_2CO_3	NaCl, KCl, $CaCl_2$*$2H_2O$	NaCl, KCl, $CaCl_2$*$2H_2O$, Na_2CO_3	[ALD46, MCP98, MCP09, VAN01, BRO96]
[3]different temperatures	4 °C	37 °C	room temperature	[ALD46, MCP98, ALD09a]
industrial applicability	yes, but optimization required	yes, but optimization required	yes, but optimization required	e.g. for insulin [KWO04]
[4]multi-component character	lysozyme NaAc buffer water NaCl	lysozyme NaAc buffer water NaCl	lysozyme glycine buffer water NaCl	[MCP91, MCP98]
[4]partially defined phase diagram	✓	✓	✓	[ALD09a, EWI94, FOR99, CAC91]
[4]undefined dissolution	no change in dissolution behavior	change in dissolution behavior at pH10+7 wt% NaCl	Change in dissolution behavior at pH7+2 wt% NaCl and pH8 /+2% NaCl	[CHE98,CAR03, FAB96]

However, just by taking a look at the dissolution behavior of lysozyme crystals, the complexity and diversity of the protein crystallization research becomes clear. Hence, it becomes obvious why protein crystallization is called to be still in the “baby-steps”, meaning at the beginning of complete understanding.

6. Summary

Protein crystals in therapeutic (e.g. insulin) as well as in industrial applications (e.g. detergents, natural food preservatives) are gaining great importance. Protein crystallization is also important as an industrial process step to purify proteins.
The understanding of protein crystals should be improved, because a wide and detailed fundamental knowledge on general protein crystallization (kinetics, thermodynamics) and the protein crystals are increasingly needed in industry.
The protein (lysozyme) batch crystallization was carried out successfully under varied conditions, but optimization is required to increase the yield and to minimize activity loss. “Simple” lab experiments were carried out on the Tetragonal, the HTO (high temperature orthorhombic) and the LTO (low temperature orthorhombic), and provided information to identify protein (lysozyme) crystals as multi-component systems. All three mentioned lysozyme crystal morphologies consist of four basic crystal components, but the mass fraction of each component varies. In general, the main components of protein (lysozyme) crystals are the protein (lysozyme analyzed e.g. by specific activity tests), bonded water in the crystal lattice (e.g. by TGA measurements), free water including the bulk solution (e.g. by diffusion – dyeing tests) and the crystallizing agent (e.g. by silver chloride precipitation or EDX).
It has to be “highlighted” that with respect to the Tetragonal and the HTO morphology, the LTO morphology is a totally different lysozyme crystal. It is proven that the crystal composition of either the LTO or the Tetragonal and HTO lysozyme crystals, which are produced in different buffer solution, is not the same. As a consequence, the LTO crystals cannot be compared with Tetragonal and HTO crystals by the mean of polymorphs or “classic” solvates. The Tetragonal and HTO morphologies can be understood as solvates, because they are produce at chemically the same buffer conditions. However, they are not “classic”solvates because the amount of the enclosed solvent content differs. This means, one has to differentiate among Tetragonal and HTO crystals as a “sub-type” of solvates or “quasi” / “pseudo” - solvates, too. At this point, obviously merging solubility data of LTO, Tetragonal and HTO crystals in the same phase diagram is wrong.
It becomes clear how complex the protein crystallization is, and that crystallization conditions are of great importance. From this, a suggestion of how to precisely classify and name protein crystal is useful. An example which includes all important protein crystal parameters for Tetragonal crystals in this study could be: Tetra – lys – 5 - 0.1NaAc – 4 – NaCl - 4.
The solubility and dissolution are major physical properties and play a key role in their applicability. The determination of the solubility and the control of the dissolution to optimize the beneficial effect (e.g. therapeutic effect, preservation or cleaning effect) become crucial and fundamental.
The solubility measurements of lysozyme crystals showed various impact factors e.g. temperature, pH, salt concentration etc. The same is observed for the dissolution of lysozyme crystals. At the same time, a very strange dissolution behavior is recognized. The dissolution occurs via the formation of a fragmented, skeleton-like crystal body. This dissolution phenomenon has not been precisely described in literature, but with respect to its complex crystal structure it is not surprisingly. Approaches to explain the dissolution

phenomenon are introduced. The fundamental hypothesis postulates the dissolution process as the reverse of the crystal growth. On this base, it is assumed that the dissolution behavior is mainly controlled by numerous and diverse electrostatic interactions and/or van der Waals forces. Different arguments finally lead to the conclusion that the model, which takes the existence of complex macrobonds of different strength into account, explains the observed dissolution behavior the best. Under dissolution (undersaturation) conditions, the weakest macrobonds are supposed to break down first, stronger macrobonds thereafter. Two additional models that explain the unusual dissolution behavior by crystal defects and mosaicity are also introduced, but evaluated as inadequate.

Mentioned aspects improve the current understanding of protein crystals and protein crystallization, which helps to develop more efficient crystallization processes and to optimize the applicability of crystalline products.

7. Zusammenfassung

Proteinkristalle gewinnen bei therapeutischen (z.B. Insulin) sowie bei industriellen Anwendungen (Medikamente, Lebensmittelzusatzstoffe, Konservierungsmittel, Waschmittelzusätze etc.) immer mehr an Bedeutung. Zudem stellt die Proteinkristallisation auch einen wichtigen Prozessschritt bei der Proteinaufreinigung dar.
Es soll ein Beitrag zum besseren Protein- bzw. Proteinkristall-Verständnis erbracht werden, da ein umfangreiches Basiswissen zur Protein-Kristallisation (Kinetik, Thermodynamik) und den Proteinkristallen für die Auslegung industrieller Anlagen notwendig ist.
Die Kristallisation wurde unter verschiedenen Bedingungen erfolgreich durchgeführt. Dennoch bedarf es bei der Batch-Proteinkristallisation einer Optimierung, um die Ausbeute zu erhöhen und den Aktivitätsverlust des Lysozyms zu minimieren. Proteinkristalle konnten als „Multi-Komponenten"-Systeme anhand von „einfachen" Laborexperimenten identifiziert werden. Hierzu sind die Tetragonalen, die HTO (high temperature orthorhombic) und die LTO (low temperature orthorhombic) Kristalle des Lysozyms genauer untersucht worden. Alle drei Lysozymkristall-Morphologien haben vier Hauptbestandteile, jedoch variieren sie in ihren Massenanteilen. Im Allgemeinen bestehen Proteinkristalle (Lysozymkristalle) aus dem Protein (Lysozym, nachgewiesen z.B. mittels Aktivitätstests), dem im Kristallgitter gebundenen Wasser (gemessen z.B. mittels TGA), freiem diffusionsfähigen Wasser einschließlich der Pufferlösung (d.h. dem Puffer aus dem sie kristallisiert wurden, visualisiert durch z.B. Färbeversuche) aus einem Kristallisationshilfsmittel wie z.B. Salz (hier NaCl, nachgewiesen mittels Fällungsreaktion als Silberchlorid oder durch EDX).
Hervorzuheben ist, dass im Vergleich zur Tetragonalen und/oder HTO- Morphologie es sich bei der LTO-Morphologie um ein anderes Lysozymkristall handelt, da gezeigt werden konnte, dass Tetragonal- und HTO-Kristalle eine unterschiedliche Kristallzusammensetzung aufweisen als die LTO-Kristalle. Sie weisen den Einschluss einer unterschiedlichen (aus der sie kristallisiert wurden) Pufferlösung auf. Aufgrund dessen dürfen LTO-Kristalle nicht im Sinne von Polymorphen oder „klassischen" Solvaten mit den Tetragonalen oder HTO-Kristallen verglichen werden. Die Tetragonalen und HTO Kristalle sind Solvate, da sie unter chemisch gleichen Bedingungen, d.h. aus derselben Pufferlösung, hergestellt werden. Dennoch können sie trotzdem nicht als „klassische" Solvate bezeichnet werden, da sie einen unterschiedlichen Wassergehalt aufweisen und die in den Kristallporen eingeschlossenen Puffermengen variieren. Somit muss man erneut differenzieren zwischen den „klassischen" Solvaten und sogenannten „Quasi"- oder „Pseudo"-Solvaten (Tetragonal, HTO). Demzufolge ist es falsch, Löslichkeiten der Tetragonalen, der HTO zusammen oder mit den Löslichkeiten der LTO-Morphologie in einem Phasendiagram darzustellen.
Die Komplexität der Proteinkristallisation sowie die Bedeutung und der Einfluss der Kristallisationsbedingungen auf die Lysozymkristalle sind deutlich, woraufhin ein mögliches Benennungsschema zur eindeutigen Klassifizierung der Proteinkristalle, das alle Kristallisationsbedingungen berücksichtigt, u.a. am Beispiel von Tetragonalen Lysozym-kristallen vorgestellt wird: Tetra – lys -5 - 0.1 - NaAc – 4 – NaCl - 4.
Die Löslichkeit und auch die Auflösung sind wichtige physikalische Eigenschaften, die die industrielle Anwendung bzw. Anwendbarkeit bestimmen. Die Messung von Löslichkeitsdaten und auch die Kontrolle der Auflösung sind Grundlage für die optimale Nutzung der

Proteineigenschaften (z.B. in der Therapie von Erkrankungen, als Konservierungsmittel oder Reinigungsmittel). Anhand von durchgeführten Löslichkeitsmessungen konnten bereits viele Einflussfaktoren festgestellt werden, welche auch bei der Auflösung eine wichtige Rolle spielen. Zudem wurde ein ungewöhnliches Auflöseverhalten beobachtet, was aufgrund der komplexen Proteinkristallzusammensetzung nicht überraschend ist. Das Auflösen von Lysozymkristallen erfolgt durch die Bildung eines „skelettartigen“ Kristallkörpers, der in einzelne Kristallfragmente zerfällt, die sich anschließend auflösen. Solch ein Auflöseverhalten wurde bisher in der Literatur noch nicht beschrieben. Erklärungsansätze zum Auflösephänomen von Lysozymkristallen, welches sich je nach Bedingungen auch verändern kann, werden diskutiert. Grundlegend wird behauptet, dass die Auflösung der umgekehrte Prozess zum Kristallwachstum ist. Zusätzlich wird davon ausgegangen, dass die Auflösung bzw. das Auflöseverhalten von zahlreichen Wechselwirkungen wie z.B. den elektrostatischen Wechselwirkungen und den van der Waals-Kräften bestimmt wird. Diesbezüglich liefert das Model, welches auf „Macro-Bindungen“ basiert, die sich aus der Summe vieler unterschiedlicher Wechselwirkungen zusammensetzen, die plausibelste Erklärung für das besondere Auflösemuster. Diese „Macro-Bindungen“ sind je nach Zusammensetzung unterschiedlich stark und können somit das Auflöseverhalten unterschiedlich beeinflussen. Bei entsprechenden Auflösebedingungen, d.h. in untersättigten Lösungen, werden die schwächsten “Macro-Bindungen” zuerst gespalten, die stärkeren demzufolge im Anschluss. Zwei weitere Modelle, die Kristallgitterdefekte und Mosaik-Strukturen als Ursache für das ungewöhnliche Auflöseverhalten in Betracht ziehen, werden vorgestellt, aber als unzureichend bewertet.
Genannte Aspekte haben die Wissensbasis der Proteinkristalle bzw. der Kristallisation und Auflösung erweitert, sodass die Prozesse und Produkte (Kristalle) gezielter und effektiver genutzt werden können.

8. List of abbreviations and symbols

Abbreviations:

Ag	silver
Al	aluminum
AgCl	Silver chloride
C	carbon
Ca	calcium
- COOH	carboxyl group
- CH_3COO^-	acetate ion
CNB	m-chlornitrobezene
DSC	Differential Scanning Calorimetry
EDX	Energy-Dispersive-X-Ray Spectroscopy
F	fluoric
GRD	growth rate dispersion
H	hydrogen
HTO	high temperature orthorhombic lysozyme crystal
IR	Infra-red
lys	lysozyme
Mg	magnesium
N	nitrogen
Na^+	sodium ion
- NH_2	amino group
NO_3^-	nitrate ion
P	phosphor
O	oxygen

R	residue
RNS	RNA; Ribose-nucleic acid
S	sulfur
SEM	Scanning Electron microscopy
TGA	Thermogravimetric Analysis
UV / Vis	Ultraviolet / Visible
vdW	van der Waals forces
XRPD	Powder X-Ray Diffraction

Symbols:

A	surface area [cm^2]
c	concentration [mg/mL]
c_b	concentration of the substance at the surface of the bulk solution (b = bulk) [mg/mL]
$c_{crystallizing\ agent}$	concentration of crystallizing agent
$c_{protein}$	protein concentration of lysozyme sample solution [mg/mL]
c_s	concentrations of the substance at the crystal surface (s = surface) [mg/mL]
d	constant distance / spacing between the planes in the atomic lattice
δ	angle between the incident ray and the scattering planes
D	diffusion coefficient of the substance [cm^2 / s]
D_f	diffusion coefficient [m^2 /s]
dc / dx	concentration gradient [mol /m^3]
DF	dilution factor [-]
E	extinction at 450 nm [-]
E	extinction (absorbance) at 280 nm [-]
ε_λ	extinction coefficient [2,64 mL/mg*cm]

ΔG^0	Gibbs free energy
$\Delta G^0_{L\text{-}L}$	energy of a dense liquid
ΔG^0_c	energy of a mesoscopic cluster
ΔG^*_1	energy of the barrier to form a cluster
ΔG^*_2	energy of the barrier to form a nucleus in the dense liquid
h	thickness of the stagnant liquid layer [cm]
J	amount of solid molecules through a unit surface area per time [mol / m^2*s]
λ	wave length (nm)
L	path length of the cuvette [cm]
M	mass of substance dissolved [mg or mmol]
M	molecular weight [g/mol]
n	integer
T	time [s]
V_{enzyme}	volume of enzyme sample solution [mL]

9. References

[ACC05] Accelrys Software Inc., MaterialsStudio 4.0, San Diego, USA, 2005

[AJE11] http://www.msscien.com/aj/Fund_UV/web/lambert-beer-law.188+m52087573ab0.0.html; Analytics Jena, Fundamentals, quantitative analysis, UV Vis Spectroscopy, Lambert-Beer law, 28.10.2011, 11 Uhr

[ALD09a] Aldabaibeh N.
Towards an improved understanding of the variables controlling crystal modification and phase transition in protein crystals, dissertation 2009, IIT, university of Illinois, USA

[ALD09] Aldabaibeh N., Jones M. J., Myerson A. S., Ulrich J.
The solubility of orthorhombic lysozyme crystals obtained at high ph;Crystal Growth & Design 9 (2009) 7 3313-3317

[ALD46] Alderton G., Fevold H. L.
Direct crystallization of Lysozyme from egg white and some crystalline salts of Lysozyme; Journal of Biological Chemistry, 164 (1946) 1-5

[AND87] Andrews S. J., Hails J. E., Harding M. M.
The mosaic spread of very small crystals deduced from Laue Diffraction patterns; Acta Cryst. A43 (1987) 70-73

[ANN08] Annunziata O., Payne A., Wang Y.
Solubility of lysozyme in the presence of aqueous chloride salts: Common-ion effect and its role on solubility and crystal thermodynamics; J. Am. Chem. Soc. 130 (2008) 40, 13347-13352

[APG08] Apgar M. C.
The influence of pH on nucleation, solubility and structure of lysozyme protein crystals; Master thesis 2008, University of Florida

[ASH04] Asherie N.
Protein crystallization and phase diagrams 1; Methods 34 (2004) 266-272

[ATA95] Ataka M.
Nucleation and growth kinetics of hen egg-white lysozyme crystals; Prog. Crystal Growth and Charact. 30 (1995), 109-128

[ATA93] Ataka M.
Protein crystal growth: an approach based on phase diagram determination; Phase Transitions 45 (1993) 205-219

[ATK90] Atkins P.W.
Physikalische Chemie; VCH, Weinheim 1990, ISBN: 3-527-25913-9

[BAN06] Banga A.K.
Therapeutic peptides and proteins - formulation, processing, and delivery systems; second edition, CRC Press 2006

[BAS10] Basavaraj K., Nanjwade M.
PowerPoint Presentation, Department of Pharmaceutics, KLE University's College of Pharmacy, Cell No: 0091 9742431000, E-mail: bknanjwade@yahoo.co. in 19. Nov. 2010, KLECOP, Nipani

[BEN02] Bènas P., Legrand L., Riès-Kautt M. M.
Strong and specific effects of cations on lysozyme chloride solubility; conference paper, Acta crystallographica D58 (2002) 1582-1587

[BER05] Bernardo A., Calmanovici C. E., Miranda E. A.
Oberservance of polymorphic behaviour during dissolution of insulin and lysozyme; Brazilian Journal of Chemical Engineering 22 (2005) 3, 331-339

[BER73] Berthou J., Jolles P.
The influence of urea on crystallization and polymorphism of hen lysozyme;North-Holland Publishing Company – Amsterdam 31 (1973) 2, 189-192

[BER74] Berthou J., Jolles P.
A phase transition in a protein crystal: the example of hen lysozyme; Biochimica et Biophysica Acta 336 (1974) 222-227

[BIO09] Biopraktikum (2009) am Biozentrum der Martin-Luther Universität Halle-Wittenberg, Arbeitsgruppe Pietzsch, Pharmazie

[BOS01] Boström M., Williams D. R. M., Ninham B. W.
Specific ion effects: why DLVO theory fails for biology and colloid systems; Physical review letters 87 (2001)16

[BOS03] Boström M., Williams D.R.M., Ninham B.W.
Specific ion effects: why the properties of lysozyme in salt solution follows a Hofmeister series; Biophys J. 85 (2003) 2, 686-694

[BRA99] Branden C., Tooze J.
Introduction to protein structure; second edition., Garland, New York 1999

[BRI91] Bringe N.A., Kinsella J. E.
Effects of cations and anions on the rate of the acidic coagulation of casein micelles: the possible role of different forces; Journal of Diary Research 58 (1991) 195-209

[BRO96] Broide M. L., Tomic T.M., Saxowsky M. D.
Using phase transition to investigate the effect of salts on protein interactions; American Physical Society, physical review E 53 (1996) 6, 6325-6335

[BUC90] Buckton G.
The role of compensation analysis in the study of wettability, solubility, disintegration and dissolution; International Journal of Pharmaceutics 66 (1990) 175-182

[BUC08] Buchfink R.
Messung der Flächen- und Massenwachstumsgeschwindigkeiten tetragonaler

Lysozymkristalle bei tiefer Temperatur und Vergleich mit Literaturdaten; Diplomarbeit 2008, Martin-Luther-Universität Halle-Wittenberg, Halle

[BUR01] Burke M. W., Judge R. A., Pusey M. L.
The effect of solution thermal history on chicken hen egg white lysozyme nucleation; Journal of Crystal Growth 232 (2001) 301-307

[BUR51] Burton W. K., Cabrera N., Frank F. C.
The Growth of crystals and the equilibrium structure of their surfaces; Phil. Trans. R. Soc. Lond. A243 (1951) 866, 299-358

[CAC91] Cacioppo E., Pusey M. L.
The solubility of the tetragonal form of hen egg white lysozyme from ph 4.0 to 5.4; J. Cryst. Growth.114(1991) 286-292

[CAR03] Carter C. W., Sweet R. M.
Macromolecular Crystallography; Vol. 368, Part 3, Elsevier Inc., ISBN: 0-12-182271-0

[CHA12] Chaplin M.
http://www.lsbu.ac.uk/water/hofmeist.html; latest update 2.02.2012

[CHE84] Chernov A. A.
Modern Crystallography III; Crystal Growth, Springer, Berlin 1984

[CHE98] Chernov A. A.
Crystal Growth and Crystallography; Acta Crystallographica A54 (1998), 859-872

[CHE03] Chernov A. A.
Protein crystals and their growth; Journal of Structural Biology 142 (2003) 3-21

[CHE11] http://chemistrytable.webs.com/enthalpyentropyandgibbs.htm

[CHE11a] www.chemexper.com

[CHR83] Christenson H. K.
DLVO - Theory and salvation forces between mica surfaces in polar and hydrogen- bondingliquids; 1983
http://puns.rsc.orgIdoi:10.1039/F19848001933

[COZ75] Cozzone P. J., Opella S. J., Jardetzky O., Berthou J., Jolles P.
Detection of new temperature-dependent conformational transition in lysozyme by carbon-12 nuclear magnatic resonance spectroscopy; Proc. Nat. Acad. Sci. USA 72 (1975) 5, 2095-2098

[CRE93] Creighton, T. E.
Proteins: structures and molecular properties; second edition, W. H. Freeman and Company, New York 1993

[CUI06] Cui H. L., Yu Y., Chen W. C., Kang Q.
Study of growth mechanism of lysozyme crystal by batch crystallization method; Chinese Chemical Letters 17 (2006) 1, 101-104

[DAI04] Dai G. L., Yu Y., Kang Q., Hu W. R.
Studying aggregate in lysozyme solution by atomic force microscope;Chinese Chemical Letters 15 (2004) 10, 1237-1240

[DAV96] Davidson V. L., Sittman D. B., Hyde R. M.
Intensivkurs: Biochemie; Übersetzerin: S. Grässel, Wiener Verlag GmbH Urban und Schwarzenberg 1996, ISBN: 3-541-18251-2

[DER06] Derewenda Z. S., Vekilov P.
Entropy and surface engineering in protein crystallization; Acta crystallographica D62 (2006) 116-124

[DIA10] Diaz-Borbon V. P., Ulrich J.
Advances toward optimization of a novel freeze out protein crystallization

technology, 17th international workshop on industrial crystallization, BIWIC 2010, Sept.8-10., Martin-Luther-University Halle-Wittenberg, Halle, Germany, Eds: Torsten Stelzer and J.Ulrich, Cuvillier Verlag Göttingen, 232-240

[DOK06] Dokoumetzidis A., Macheras P.
Historical Perspectives - A century of dissolution research: From Noyes and Whitney to the Biopharmaceutics Classification System; International Journal of Pharmaceutics 321 (2006) 1-11

[DOW09] Down D. R., Lehr J. H.
Environmental instrumentation and analysis handbook; Wiley-Interscience 2009, John Wiley & Sons, Inc.

[DRE92] Drenth J., Haas C.
Protein crystals and their stability; Journal of Crystal Growth, 122 (1992) 107-109

[DRE98] Drenth J., Haas C.
Nucleation in protein crystallization; Acta Cryst. D54 (1998), 867-872

[DUC92] Ducruix A. F., Giege R.
Crystallization of nucleic acids and proteins; a practical approach, second edition, Oxford University Press, Oxford 1992

[DUM08] Dumetz A. C., Chockla A. M., Kaler E. W., Lenhoff A. M.
Protein phase behavior in aqueous solutions: crystallization, liquid-liquid phase separation, gels, and aggregates; Biophysical Journal 94 (2008) 2, 570-583

[DUR86] Durbin S. D., Feher G.
Crystal growth studies of lysozyme as a model for protein crystallization; Journal of Crystal Growth 76 (1986) 583-592

[DUR96] Durbin S. D., Feher G.
Protein crystallization; Annu. Rev. Phys. Chem. 47 (1996) 171-204

[EVA76] Evans R. C.
Einführung in die Kristallchemie; Walter de Gryter, Berlin 1976

[EWI94] Ewing F., Forsythe E. L., Pusey M. L.
Orthorhombic lysozyme solubility; Acta Cryst. D50 (1994) 424-428

[FAB96] Fabian J.
Untersuchungen zur Auflösekinetik in der Lösungskristallisation; Dissertation 1996, Universität Bremen

[FAD11] http://www.fad.gov/ohrms/dockets/ac/02/briefing/3900B1_04_Polymorphism.htm 12.12.2011, 10Uhr

[FAZ62] Fazekas De St Groth S., Webster R. G., Datyner A.
Two new staining procedures for quantitative estimation of proteins on electrophoretic strips; Biochimica et Biophysica Acta 37 (1962) 377-391

[FEH85] Feher G., Kam Z.
Nucleation and growth of protein crystals: general principles and essays; Method. Enzymol. 114 (1985) 77-204

[FEH86] Feher G.
Mechanisms of nucleation and growth of protein crystals; Journal of Crystal Growth 76 (1986) 545-546

[FLE22] Fleming A.
On a remarkable bacteriolytic element found in tissues and secretions; Proc. R. Soc. Lond. B93 (1922) 306

[FOR94] Forsythe E., Ewing F., Pusey M.
Studies on tetragonal lysozyme crystal growth rates; Acta Cryst. D50 (1994) 614-619

[FOR99] Forsythe E. L., Judge R. A., Pusey M. L.
Tetragonal chicken egg white lysozyme solubility in sodium chloride solutions; J. Chem. Eng. Data 44 (1999) 637-640

[FRA58] Frank F. C.
On the kinematic theory of crystal growth and dissolution processes; in: Growth and Perfection of Crystals; R. H. Doremus, B. W. Roberts, D. Turnbull (Eds), J. Wileys, New York 1958, 411-420

[FRE94] Frey M.
Water structure associated with proteins and its role in crystallization; Acta Cryst. D50 (1994) 663-666

[GAR71] Garside J.
The concept of effectiveness factors in crystal growth; Chem. Eng. Sci. 26 (1971) 14251-1431

[GAR81] Garside J., Tavare N. S.
Non-isothermal effectiveness factors for crystal growth; Chem. Eng. Sci. 36 (1981) 863-866

[GAR89] Gardiner D. J.
Practical Raman spectroscopy, Springer-Verlag (1989), ISBN 978-0387502540

[GIL02] Gilliland G. L., Tung M., Ladner J. E.
The biological macromolecule crystallization database: crystallization procedures and strategies; Acta Cryst. Biol. Cryst. D 58 (2002), 916-920http://wwwbmcd.nist.gov:8080/bmcd/bmcd/html

[GÖB98] Göbel R.
Volk und Wissen Verlag, Wissensspeicher Physik, 1.Auflage, 1998, ISBN 3-06-021717-3

[GOL03] Goldstein J.
Scanning electron microscopy and x-ray microanalysis; Vol. 1, third edition, Springer Verlag, 2003, ISBN 0-306-47292-9

[GOR71] Gorin G., Wang S. F., Papapavlou L.
Assay of lysozyme by its lytic action on M. lysodeikficus cells; Analytical Biochemistry 39 (1971)

[GRA99] Grant J. W.
Theory and origin of polymorphism; in: Polymorphism in Pharmaceutical Solids, H.G. Brittain (ed.), Marcel Dekker, Inc., New York 1999, 1-34

[GUI92] Guilloteau J.P., Riès-Kautt M., Ducruix A. F.
Variations of lysozyme solubility as a function of temperature in the presence of organic and inorganic salts; Journal of Crystal Growth 122 (1992) 223-230

[HEI75] Heimann R. B.
Auflösung von Kristallen; in: Applied Mineralogy; V.D. Frechette, et al. (Eds), Springer Verlag, Wien, New York 1975

[HEI99] Heizmann W. R., Döller P. C., Kropp S., Bleich S.
Kurzlehrbuch Medizinische Mikrobiologie und Immunologie; 2. überarbeitete Auflage, Schattauer Verlag Stuttgart, New York 1999, ISBN: 3-7945-1961-2

[HIL06] Hilfiker R.
Polymorphism; Wiley-VCH, Weinheim 2006, ISBN-10: 3-527-31146-0

[HOE82] van der Hoek B., van der Eerden J. P., Bennema P.
The influence of stress on spiral growth; J.Crystal Growth 58 (1982) 365-380

[HOF04] Hofmann G.
Kristallisation in der industriellen Praxis; WILEY-VCH Verlag GmbH & Co. KGaA, Weinheim 2004, ISBN: 3-527-30995-0

[HOF88] Hofmeister F.
Zur Lehre von der Wirkung der Salze; Arch. Exp. Pathol. Pharmakol. 24 (1888) 247-260

[HÖH10] Höhne G., Hemminger W. F., Flammersheim H. J.
Differential Scanning Calorimetry, second edition, Springer Verlag 2010, ISBN: 978-3-642-05593-5

[HÖR01] Hörter D., Dressman J. B.
Influence of physicochemical properties on dissolution of drugs in the gastrointestinal tract; Advanced Drug Delivery Reviews 46 (2001) 75-87

[HOW88] Howard S. B., Twigg P. J., Baird J. K., Meehan E. J.
The solubility of hen egg white lysozyme; Journal of Crystal Growth 90 (1988) 94-104

[HYP11] http://www. Hyperphysics.phy-astr.gsu.edu/hbase/tables/therprop.html

[ISR11] Isrealachvili J. N.
Intermolecular and surface forces; third edition, Academic Press (Elsevier) 2011, ISBN: 978-0-12-391927-4

[IVE60] Ives M. B., Hirth J. P.
Dissolution kinetics at dislocation etch pitch in single crystal of lithium fluoride; Journal of Chemical Physics 33 (1960) 517-525

[IVE63] Ives M. B.
On kink kinetics of crystal dissolution; J.Phys.Chem. Solids 24 (1963) 275-281

[JAN95] Janin J.
Principles of protein – protein recognition from structure to thermodynamics; Biochimie 77 (1995) 497 – 505

[JUD95] Judge R., Johns M., White E.

Protein purification by bulk crystallization: The recovery of ovalbumin; Biotech.& Bioeng. 48 (1995) 316

[PHI05] Philibert J.
One and a half century of diffusion: Fick, Einstein, before and beyond; Diff.Fund. 2, 2005, 1-10

[JUD99] Judge R. A., Jacobs R. S., Frazier T., Snell E. H., Pusey M. L.
The effect of temperature and solution pH on the nucleation of tetragonal lysozyme crystals; Biophysical Journal 77 (1999) 1585-1593

[KIR11] Kirk-Othmer
Encyclopedia of Chemical technology; fifth edition, Processes & Process Engineering, Crystallization by Ulrich J., Stelzer T, Wiley-online library 2011
http://onlinelibrary.wiley.com/book/10.1002/0471238961/topics

[KOO98] Koolman J., Röhm K. H.
Taschenatlas der Biochemie, 2. überarbeitete und erweiterte Auflage, Thieme Verlag Stuttgart 1998, ISBN: 3-13-759402-2

[KRU93] Kruse M., Ulrich J.
Kristallwachstum in der Lösungskristallisation als Drei-Stufen-Model; Chem. Ing. Tech. 65 (1993) 1, 60-63

[KWO04] Kwon J. H., Lee B. H., Lee J. J., Kim C. W.
Insulin microcrystal suspension as a long-acting formulation for pulmonary delivery; European Journal of pharmaceutical science 22 (2004) 2-3, 107-116

[LAC74] Lacmann R., Franke W., Heimann R.
The dissolution forms of single crystals spheres, I: Theory for the molecular-kinetics interpretation; Journal of Crystal Growth 26 (1974) 107-116

[LAS01] Lasaga A. C., Luttge A.
Variations of crystal dissolution rate based on a dissolution stepwave model;

Science 291 (2001) 5512, 2400-2404

[LAS03] Lasaga A. C., Luttge A.
A model for crystal dissolution; European Journal of Mineralogy 15 (2003) 603-615

[LEC01] Leckband D., Israelachvili J.
Intermolecular forces in biology; Quarterly Reviews of Biophysics 34 (2001) 2, 105-267

[LEG02] Legrand L., Riès-Kautt M., Robert M. C.
Two polymorphs of lysozyme nitrate: temperature dependence of their solubility; Acta Cryst. D58 (2002) 1564-1567

[LID94] Lide D. R.
Handbook of chemistry and physics; 75th edition (special student edition), CRC press 1994, 8-58

[LIM98] Lim K., Nadarajah A., Forsy E. L., Pusey M. L.
Locations of bromide ions in tetragonal lysozyme crystals; Acta Crystal. D54 (1998) 899-904

[LIU10] Liu Y., Wang X., Ching C. B.
Toward further understanding of lysozyme crystallization: phase diagram, protein-protein interaction, Nucleation Kinetics, and Growth Kinetics; Crystal Growth and Design10 (2010) 548-558

[LU02] Lu J., Wang X. J., Ching C. B.
Batch crystallization of soluble proteins: effect of precipitant, temperature and additive; Progress in crystal growth and characterization of materials 45 (2002), 201-217

[LYS10] http://lysozyme.co.uk/, 16.12.2010, 9:00Uhr

[MAL07] Malek K.
Solute transport in orthorhombic lysozyme crystals: a molecular simulation study; Biotechnol. 29 (2007) 1865-1873

[MAL11] http://www.nt.ntnu.no/users/skoge/prost/proceedings/aiche-2004/pdffiles/papers/251h.pdf

[MAT03] Matsuura Y., Chernov A. A.
Morphology and the strength of intermolecular contacts in protein crystals; Acta Cryst. D59 (2003) 1347-1356

[MCB97] McBridge M. B.
A critique of diffuse double layer models applied to colloid and surface chemistry; Clays and Clay minerals 45 (1997) 4, 598-608

[MCP90] McPherson A.
Current approaches to macromolecular crystallization; Eur. J. Biochem. 189 (1990) 1-23

[MCP91] McPherson A.
A brief history of protein crystal growth; J. Cryst. Growth 110 (1991) 1

[MCP98] McPherson A.
Crystallization of biological macromolecules; Cold Spring Harbor Laboratory Press, Cold Spring 1998

[MCP09] McPherson A.
Introduction to macromolecular crystallography; second edition, Wiley-Blackwell 2009, ISBN: 978-0-470-18590-2

[MCQ76] McQuarrie D. A.
Statistical Mechanics, Harper Collins, New York 1976

[MEL11] http://www.melvynbecerra.cl/images/KFTitrationBasics.pdf

[MEN09] Menczel D. J., Prime R. B.
Thermal Analysis of Polymers; Fundamentals and Applications , Wiley 2009, ISBN: 978-0-471-76917-0

[MET91] Mettler; Bedienungsanleitung, Karl-Fischer-Titrator DL35 Mettler- Toledo AG, 1991

[MIC99] Michinomae M., Mochizuki M., Ataka M.
Electron microscopic studies on the initial process of lysozyme crystal growth; Journal of Crystal Growth 197 (1999) 257-262

[MOL01] Mollet H., Grubenmann A.
Formulation Technology; Wiley-VCH, Weinheim 2001, ISBN: 3-527-30201-8

[MON93] Monaco L. A., Rosenberger F.
Growth and etching kinetics of tetragonal lysozyme; Journal of Crystal Growth 129 (1993) 465-484

[MOR95] Morozov V. N., Kachalova G.S., Ectodienko V. U., Lanina N.F., Morozova T. Y.
Permeability of lysozyme tetragonal crystals to water, Eur. Biophys. J. 24 (1995) 93-98

[MSD11] Material Safety Data Sheet of sodium chloride
http://www.sciencelab.com/msds.php?msdsId=9927593

[MUL01] Mullin J. W.
Crystallization; 4th edition, Buttworth Heinemann 2001, ISBN: 0-7506-4833-3

[MUE11a] Müller C., Ulrich J.
A more clear insight of the lysozyme crystal composition; Crystal Research & Technology 46 (2011) 7, 646-650

[MUE11b] Müller C., Ulrich J.
Dissolution phenomenon of lysozyme crystals; in proceedings, ISIC 18, edited

by B. Biscans, M. Mazzotti, Zürich (Schweiz) 2011, 494-495

[MUE12] Müller C., Ulrich J.
The dissolution phenomenon of lysozyme crystals; Crystal Research & Technology 47 (2012) 2, 169-174

[MUR01] Murphy D. B.
Fundamentals of light microscopy and electronic imaging; Wiley (2001), ISBN: 0-471-25391-X

[MUS97] Muschol M., Rosenberger F.
Liquid-liquid phase separation in supersaturated lysozyme solutions and associated precipitate formation/crystallization; J.Chem. Phys. 107 (1997) 6, 1953

[MUT77] Mutaftschiev B.
Adsorption and crystal growth; in: R. Vauselow, S.J Jong (Eds): Chemistry and Physics of Solid Surfaces, CRC Press 1977, 74-86

[MYE01] Myerson S. A.
Handbook of Industrial Crystallization Edited; Elsevier Science & Technology Books 2001, ISBN: 0-7506-7012-6

[NAD95] Nadarajah A., Forsythe E. L., Pusey M. L.
The averaged face growth rates of lysozyme crystals: the effect of temperature; Journal of Crystal Growth 151 (1995) 163-172

[NAD96] Nadarajah A., Pusey M. L.
Growth Mechanism and Morphology of Tetragonal Lysozyme Crystals; Acta Cryst. D52 (1996), 983-996

[NAD97] Nadarajah A., Meirongli T., Pusey M. L.
Growth Mechanishe E.L.m of the (110) Face of Tetragonal Lysozyme Crystals; Acta Cryst. D53 (1997), 524-534

[NAN08] Nanev C. N.
How do crystal lattice contacts reveal protein crystallization mechanism?; Crystal Research & Technology 43 (2008) 9, 914-920

[NCB11] http://bcbi.nlm.gov/Class/MLACourse/Modules/MolBioReview/iupacaa abbreviations.html; latest update 2.02.2012

[NEU53] Neurath H., Bailey K.
The proteins - chemistry, biological activity, and methods; Part A, Academic Press Inc., New York 1953

[NIN99] Ninham B. W.
On the progress in forces since the DLVO theory; Advances in colloid and Interface science 83 (1999) 1-17

[NYV95] Nyvlt J., Ulrich J.
Admixtures in crystallization;VCH Weinheim (1995), ISBN: 3-527-28739-6

[OHA73] Ohara M., Reid R. C.
Modeling Crystal Growth Rates from Solution, Prentice-Hall, New Jersey 1973

[OKI99] Oki H., Matsuura Y., Komatsu H., Chernov A. A.
Refined structure of orthorhombic lysozyme crystallized at high temperature: correlation between morphology and intermolecular contacts; Acta Cryst. D55 (1999) 144-121

[OOT09[Ootaki M., Endo S., Sugawara Y., Takahashi T.
Crystal habits of cubic insulin from porcine pancreas and evaluation of intermolecular interactions by macrobond and EET analyses; Journal of Crystal Growth 311 (2009) 4226-4234

[PAN11] http://www.panalytical.com/index.cfm?pid=314
30.08.2011, 9:22 Uhr

[PDB10] http://www.rcsb.org/pdb/home

[PDB10a] http://www.pdb.org/pdb/explore/explore.do?structureId=193L;16.12.2010, 10:10 Uhr

[PDB11b] http://www.rcsb.org/pdb/explore/explore.do?structureId=1BGI; 7.02.2011, 10 Uhr

[PDB11c] http://www.pdb.org/pdb/explore/explore.do?structureId=1JPO; 7.02.2011, 10:15Uhr

[PDB11 d] http://www.rcsb.org/pdb/explore/remediatedSequence.do?structureId=193L; 7.02.2011, 10 Uhr

[PEK08] Peker S. M., Helvaci S. S.
Solid-Liquid Two Phase Flow; first edition, Elsevier, Netherlands 2008, ISBN: 978-0-444-52237-5

[PET07] Petrova E. V., Smirnov V. A., Rashkovich L. N.
Some properties of the solvent on monoclinic lysozyme crystals; Crystallography Reports 52 (2007) 275-279 Crystallogr. Rep. 52 (2007) 275

[PHA11] http://www.pharmainfo.net/tablet-evaluation-test/dissolution/theories-dissolution; latest update 2.02.2012

[PHI05] Philibert J.
One and a Half Century of Diffusion: Fick, Einstein, before and beyond, Diff.Fund. 2, 2005, 1-10

[PUS88] Pusey M., Gernert K.
A method for rapid liquid-solid phase solubility measurements using the protein lysozyme; Journal of Crystal Growth 88 (1988) 419-424

[PUS91] Pusey M. L., Munson S.

Micro-apparatus for rapid determinations of protein solubilities; Journal of Crystal Growth 113 (1991) 385-389

[PUS02] Pusey M. L., Nadarjajah A.
A model for tetragonal lysozyme crystal nucleation and growth; Crystal Growth and Design 2 (2002) 6, 475-483

[QU06] Qu H., Louhi-Kultanen M., Rantanen J., Kallas J.
Solvent-mediated phase transformation kinetics of an anhydrate/hydrate system; Crystal Growth & Design 6 (2006) 9, 2053-2060

[RAM11] Dippel B.
http://www.raman.de; 2011

[RET97] Retailleau P., Riès-Kautt M. M., Ducruix A. F.
No Salting-in of Lysozyme Chloride observed at low ionic strength over a large range of pH; Biophysical Journal 73 (1997) 2156 – 2163

[RET02] Retailleau P., Ducruix A. F., Riès-Kautt M. M.
Importance of the nature of anions in lysozyme crystallization correlated with protein net charge variation; conference paper, Acta crystallographica D58 (2002) 1576 - 1581

[RIE89] Ries-Kautt M.M., Ducruix A. F.
Relative effectiveness of various ions on the solubility and crystal growth of lysozyme; Journal of biological chemistry 264 (1989) 2, 745-748

[RÖM12] http://www.roempp.com/prod/roempp.php; 2012

[ROS96a] Rosenberger F., Vekilov P., Muschol M., Thomas B. R.
Nucleation and crystallization of globular proteins - what we know and what is missing; J. Cryst. Growth 168 (1996) 1

[ROS96] Rosenberger F.
Protein crystallization; Journal of Crystal Growth 166 (1996) 40-54

[ROS90] Rossiter B. W., Hamilton J. F.
Physical Methods of Chemistry, Determination of structural features of crystalline and amorphous solids; second edition, Vol.V, John Wiley & Son Inc., Wiley-Interscience Publication, New York 1990, ISBN: 0-471-52509-X

[RYU09] Ryu B. H.
Protein crystallization by freeze-out technology; dissertation 2009, Martin-Luther Universität Halle-Wittenberg

[SAK68] Sakakibara R., Hamaguchi K.
Structure of lysozyme; Journal of Biochemistry 64 (1968) 5, 613-618

[SAL85] Salunke D. M., Veerapandian B., Kodandapani R., Vijayan M.
Water-mediated transformations in protein crystals; Acta Cryst. B41 (1985), 431-436

[SAN82] Sangwal K., Szurgot M., Karniewicz J., Kolasinski W.
On the selective etching of KDP crystals; Journal of Crystal Growth 58 (1982) 261-266

[SAN88] Sangwal K.
Etching of crystals. Theory, experiments, and application; North-Holland, Amsterdam 1987

[SAN07] Sangwal K.
Additives and crystallization processes: from fundamentals to applications; John Wiley & Sons 2007, ISBN: 978-0-470-06153-4

[SAZ96] Sazaki G., Kurihara K., Nakada T., Miyashita S., Komatsu H.
A novel approach to the solubility measurement of protein crystals by two-beam interferometry; Journal of Crystal Growth 169 (1996) 355-360

[SCH89] Schellenberger A.
Enzymkatalyse; VBB Gustav Fischer Verlag Jena (1989)

[SER11] http://serc.carleton.edu/research_education/geochemsheets/techniques/XRD.html, 30.08.2011, 10 Uhr

[SHU52] Shugar D.
The measurement of lysozyme activity and ultra violet inactivation of lysozyme; Biochimica et Biophysica Acta 8 (1952) 302-309

[SIG11] http://www.sigmaaldrich.com/etc/medialib/docs/Fluka/General_Information/hydranal_overview_e.Par.0001.File.tmp/hydranal_overview_e.pdf

[SNY07] Snyder R. C., Doherty M. F.
Faceted crystal shape evolution during dissolution or growth; AIChE Journal 53 (2007) 5, 1337-1348

[SMO52] Smolelis A. N., Hartsell S. E.
Factors affecting the lytic activity of lysozyme; Laboratories of Bacteriology 63 (1952) 665-674

[SMO52] Smolelis A. N., Hartsell S. E.
Factors affecting the lytic activity of lysozyme; Laboratories of Bacteriology 63 (1952) 665-674

[SOP62] Sophianopoulos A., Holcomb D., Vanholde K., Rhodes C.
Physical Studies of Lysozyme. I. Characterization; J. Biol. Chem. 237 (1962) 1107

[STA94] Stavek J., Ulrich J.
Interpretation of crystal growth and dissolution by reaction fractal dimensions; Cryst. Research & Technology 29 (1994) 6, 763-785

[STR07] Stryer L., Berg J. M., Tymoczko J. L.

Stryer Biochemie; 6. Auflage, Elsevier Spektrum Akademischer Verlag 2007, 36-37, ISBN: 978-3-8274-1800-5

[SUM26] Sumner J. B.
The isolation and crystallization of the enzyme urease, J. Biol. Chem. 69 (1926) 435-441

[TES07] Teslyuk Y., Vasylkiv Y., Nastishin Y.
Structural phase transition in lysozyme crystals; Ferroelectrics 346 (2007) 1, 49-55

[THO04] Thompson C.
Dissolution equation, Calculations and Relationships- A brief survey, Pharmaceutics Part I (2004) 31-33

[TUL83] Tuladhar M. D., Carless J. E., Summers M. P.
Thermal behaviour and dissolution properties of phenylbutazone polymorphs; J. Pharm. Pharmacology 35 (1983) 208-214

[ULL55] Foerst W.
Ullmann's Encyclopädie der technischen Chemie; 3. Völlig neu gestaltete Auflage, 6. Band, Urban & Schwarzenberg, München-Berlin 1955

[ULL60] Foerst W.
Ullmann's Encyclopädie der technischen Chemie; 3. Völlig neu gestaltete Auflage, 12. Band, Urban & Schwarzenberg, München-Berlin 1960

[ULL64] Foerst W.
Ullmann's Encyclopädie der technischen Chemie; 3. Völlig neu gestaltete Auflage, 15. Band, Urban & Schwarzenberg, München-Berlin 1964

[ULR81] Ulrich J.
Zur Kristallisation durch thermischen Abrieb; Dissertation 1981, Fakultät für Machinenwesen der RWTH Aachen

[ULR89] Ulrich J.
Growth rate dispersion - A review; Crystal Research and Technology 24 (1989) 3, 249-257

[ULR94] Ulrich J.
Entwicklungen bei der Lösungskristallisation in den letzten Jahren; Chem. Ing. Tech. 66 (1994) 10, 1341-1345

[ULR03] Ulrich J., Glade H.
Melt crystallization: Fundamentals, Equipment and Applications; Shaker Verlag 2003, ISBN-10: 3832215336

[VEK96] Vekilov P. G., Monaco L. A., Thomas B. R., Stojanoff V., Rosenberger F.
Repartitioning of NaCl and protein impurities in lysozyme crystallization; Acta Cryst. D52 (1996) 785-798

[VEK04] Vekilov P. G.
Dense liquid precursor for the nucleation of ordered solid phases from solution; Cryst. Growth and Design 4 (2004) 671-685

[VEK07] Vekilov P. G.
What is the molecular level role of the solution components in protein crystallization; Crystal Growth and Design 7 (2007) 11, 2239-2246

[VAL24] Valeton J. J. P.
Wachstum und Auflösung der Kristalle; Teil 1-3, Z. Kristllogr. 59 (1923) Teil 1,135-169 und Teil 2, 335-365; Z. Kristllogr. 60 (1924) Teil 3, 1-38

[VAL80] Valvani S. C., Yalkowsky S. H.
Solubility and portioning in drug design; in S.H. Yalkowsky, A.A. Sinkula and S.C. Valvani (Eds): Physical Chemical Properties of Drugs, Dekker, New York 1980, 201-230

[VAN01] Vaney M. C., Broutin I., Retailleau P., Douangamath A., Lafont S., Hamiaux C.,

Prange T., Ducruix A. F., Ries-Kautt M.
Structural effects of monovalent anions on polymorphic lysozyme crystals; Acta Cryst. D57 (2001) 929-940

[VAS07] Vasylkiv Y., Nastishin Y., Vlokh R.
On the problem of phase transitions in lysozyme crystals; www.http://wenku.baidu.com (2007)

[VEE11] Veesler S., Hammadi Z., Candoni N., Grossier R., Ildefondo M., Ferté N., Roger M.
Practical aspects of crystallization from solution; Centre Interdisciplinaire de Nanoscience de Marseille (2011), Aix Marseille university

[VER87] Vere A. W.
Crystal growth, Principles and Progress; Plenum Press, New York 1987

[WAN06] Wanka J., Peukert W.
Die Bedeutung des zweiten osmotischen Viralkoeffizienten für die Proteinkristallisation; Chemie Ingenieur Technik 78 (2006) 3, 273-278

[WEB97] Weber P. C.
Overview of protein crystallization methods; Methods in Enzymology 276 (1997) 13-22

[WEB08] Weber M.
Industrial purification of the enzyme urease from jack beans using crystallization; Dissertation 2008, Martin-Luther Universität Halle-Wittenberg

[WEI05] Weissborn R.
Dynamik in Proteinkristallen: Unelastische Lichtstreuung und Röntgenstrukturanalyse während Mikrowellenbestrahlung; Dissertation 2005, Universität Konstanz

[WIE99] Wiencek J. M.
New Strategies for protein crystal growth; Annu. Rev. Biomed. Eng. 1 (1999) 505-534

[WOR10] http://www.worthington-biochem.com/LY/default.html; 16.12.2010, 9:20Uhr

[ZIM46] Zimm B. H.
Applications of the methods of molecular distribution to solutions of large molecules; J. Chem. Phys. 14 (1946) 164-179

Appendix

A.1 Lysozyme activity test

1. test buffer solution
   - 11.7 mL of 0.2 M KH_2PO_4
   - add 18.3 mL of 0.2 M K_2HPO_4
   - add 425 µL of 4 M NaCl solution
   - add 50 mL distilled H_2O
   - check pH value, if needed adjust pH to 7

3. substrate solution
   - eppendorf tube of 2 mL volume
   - 30 mg Micrococcus luteus
   - add 1 mL test buffer solution
   - mix well by vortex
   - take 50 µL of Micrococcus solution in 20 mL test buffer solution = substrate solution and mix well by vortex
   - check at wavelength 450 nm → 0.8 (take 950 µL in a disposable cuvette + 50 µL test buffer sol. and mix)

10. lysozyme sample solution
    - dissolve 10 mg lyophilized lysozyme pure or air-dried lysozyme crystals (HTO, LTO, Tetragonal) in 1mL test buffer solultion
    - dilute to 1 mg/mL (900 µL test buffer solution + 100 µL lysozyme solution

11. activity determination
    - set thermostat which is connected to the spectrophotometer to constant 25 °C
    - keep substrate solution at all times in water bath at 25C, mix well before each measurement
    - pipetting and measuring at 450 nm

A.2 Solubility of lysozyme crystals

solubility at pH5.7 + 3 wt% NaCl

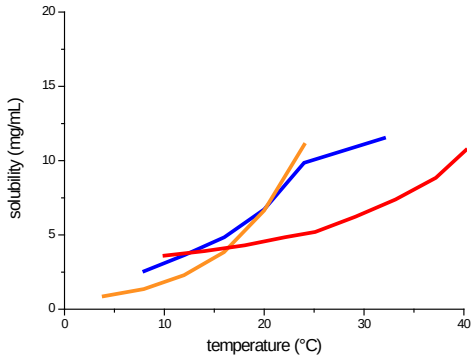

solubility at pH5.7 + 5 wt% NaCl

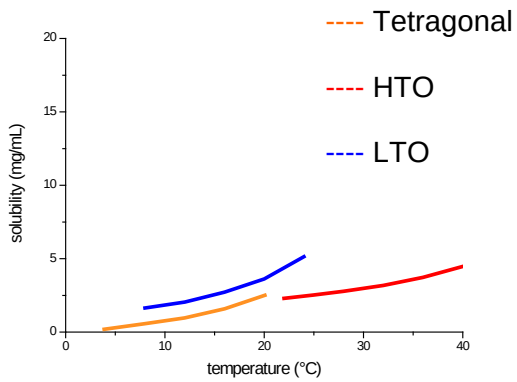

Figure A.2.1: Solubility of lysozyme crystals at pH7 + 3 wt% (left) and 5 wt% (right) NaCl.

solubility at pH7 + 3 wt% NaCl

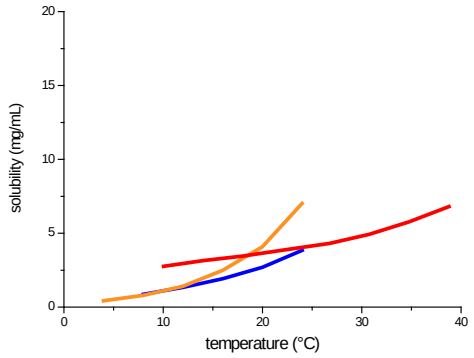

solubility at pH7 + 5 wt% NaCl

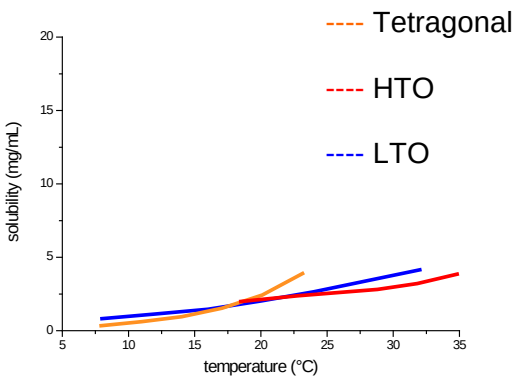

Figure A.2.2: Solubility of lysozyme crystals at pH7 + 2 wt% (left) and 7 wt% (right) NaCl.

solubility at pH8 + 3 wt% NaCl

solubility at pH8 + 5 wt% NaCl

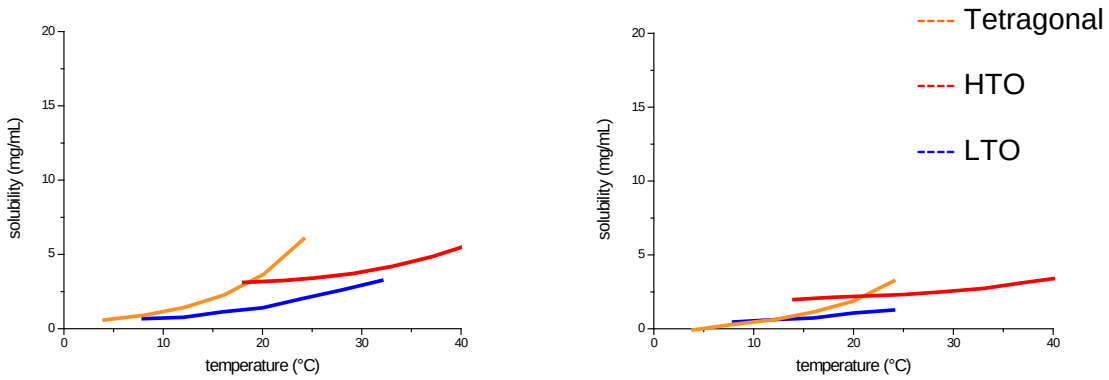

Figure A.2.3: Solubility of lysozyme crystals at pH8 + 3 wt% (left) and 5 wt% (right) NaCl.

CURRICULUM VITAE

Claudia Müller

Surname:	Müller
Given name:	Claudia
Email:	claudia.mueller@iw.uni-halle.de
Date of Birth:	12.03.1982
Place of Birth:	Anklam Germany

Education

June 2007 – April 2012	PhD position at the Martin-Luther University of Halle-Wittenberg (MLU): Center of Engineering / Thermal Separation Processes Supervisor: Prof. Ulrich PhD in Engineering (18th April 2012)
October 2002 - May 2007	Martin-Luther-University of Halle-Wittenberg (MLU): Studies in Nutritional Science Specifications: nutritional medicine, food technology Final degree: Diploma in Nutritional Science
August 2000 - June 2002	AuPair in California, USA Mira Costa College: Human Biology (part time student) UCSD (University of California, San Diego): Molecular Biology (part time student)
June 2000	General qualification for university entrance

Vocational experiences: PhD position

- PhD thesis in the field of protein crystallization:
  How to describe protein crystals correctly? -case study of lysozyme crystals-
  Field of research:
  - production / crystallization conditions of different lysozyme crystal morphologies
  - studies of the lysozyme crystal composition
  - solubility / phase diagram of different lysozyme crystal morphologies
  - dissolution of different lysozyme crystal morphologies (bioavailability of the protein)

  Diagnostics required: microscopy, DSC, TGA, photometer, enzymatic activity test (micrococcus luteus), BCA-test or Bradford test, powder X-ray diffraction, Raman-spectroscopy, IR-spectroscopy, EDX, conductivity

- Cooperation projects:
  - Prof. Dr. Markus Pietzsch, Martin-Luther-Universität Halle Wittenberg, Faculty of Natural Sciences I - Biosciences Institute of Pharmacy c/o Biozentrum Weinbergweg 22, D-06120 Halle (Saale) Germany
    Phone: ++49 (0) 345 / 55 25 949, fax: ++49 (0) 345 / 55 27 260
    Email: markus.pietzsch@pharmazie.uni-halle.de
    Field of research:
    - purification by crystallization of an API- protein out of the biomass (protein: new recombinant L- Asparaginase II used in leukemia therapy)

    Analytics required: SDS-Page, chromatography, centrifugation, filtration, dialysis, microscopy, crystallization screening

  - Summer School in South-Korea (20. - 29. September 2009): Hanbat National University (HNU in Deajeon/ Department of Crystallization Technology, South-Korea) and Busan National University (BNU in Busan, South-Korea)
    Responsibilities: organization, teaching, supervision - coaching

- Industry projects:
  Crystallization of inorganic materials
  Field of research:
  - investigation of product quality, product purity, crystal morphology and hardness
  - further investigation related to the crystallization conditions and downstream-processes (filtration, drying), influence of additives / impurities, influence of stirring, mass and energy balances of the process

  Diagnostics required: microscopy (polar microscopy), SEM (REM), ultra-sound, DSC, TGA, ICP, refractometer, photometer
  Aim: definition of major error source, potential solutions and future perspectives

- Mentoring of students (Diploma and/or Master thesis)

- Organization:
  - Conferences e.g. BIWIC 2010 in Halle
  - Summer School in South-Korea (20. - 29. September 2009)

Internship / Practical training

August 2005 – September 2005	Martin-Luther University Halle-Wittenberg, Institute of Toxicology
February 2005 – March 2005	Diakonie – Hospital Elbingerode Diabetes consultation, assistance and support

Personal awards / Scholarships

April 2011	Scholarship – by Martin-Luther University Halle - Wittenberg
May 2011	Traveling Scholarship concerning the ISIC Conference in 2011 – by DECHEMA, Society of Chemical Technology and Bio-Technology

May 19.-20. 2011	„HAUS DER TECHNIK“ (Crystallization Workshop, Berlin)
May 11.-15. 2009	„ACHEMA“ 29th (International Exhibition-Congress on Chemical Engineering, Environmental Protection and Biotechnology, Frankfurt)
September 10.-12. 2008	„BIWIC“ 15th (International Workshop on Industrial Crystallization, Magdeburg)

Languages

English	excellent (speaking and writing)
French	well (speaking and writing)
Spanish	basic

Publications

- Müller, C., Ulrich, J., The dissolution phenomenon of lysozyme crystals, Crystal Research & Technology 47 (2012) 2, 169 – 174.
- Müller, C., Ulrich, J., Dissolution Phenomenon of Lysozyme Crystals, in proceedings, ISIC 18, edited by B. Biscans, M. Mazzotti, Zürich (Schweiz) 2011, 494 – 495.
- Müller, C., Ulrich, J., A more clear insight of the lysozyme crystal composition, Crystal Research & Technology, 46 (2011) 7, 646 – 650.
- Müller, C., Liu, Y., Migge, A., Pietzsch, M., Ulrich, J., Recombinant *L*-Asparaginase B and its Crystallization - What is the Nature of Protein Crystals?, Chemical & Engineering Technology, 34 (2011) 4, 571 – 577.
- Müller, C., Migge, A., Pietzsch, M., Ulrich, J., Recombinant L-Asparaginase II - purification by crystallization and membrane separation, BIWIC' 10, Halle, edited by Stelzer, T., Ulrich, J., Cuvillier Verlag Göttingen, 2010, 375 – 385.

- Müller, C., Ulrich, J., The effect of additives on the crystal shape of ammonium sulphate, in proceedings, ISIC 17, Vol. 3, edited by J. P. Jansens, J. Ulrich, Maastricht (Netherlands) 2008, 1367 – 1676.

Presentations

- Seminar at the University of Szeged, Hungary, Department of Pharmaceutical Technology (http://www2.pharm.u-szeged.hu/phtech/index-en.html), October 10.-14. 2011

- Seminar at Orion Pharma Finland company (http://www.orion.fi/en/), December 2010

- „Fachausschuss der Kristallisation“ of Processnet, March 11.-12. 2010

Conferences participated, Poster presented

- ISIC 18 (International Symposium of Industrial Crystallization), September 13.-16. 2011

- BIWIC 17th (International Workshop on Industrial Crystallization), September 8.-10. 2010

- ISIC 17 (International Symposium of Industrial Crystallization), September 14.-17. 2008

Additional training

October 2008 – February 2012	Fitness Trainer at the Martin-Luther-University
August 1998	DLRG Life-Guard